Ice Formation in the Gulf of St. Lawrence

by

Graydon D. Lally

A thesis submitted to the Faculty of Graduate Studies
in partial fulfillment of the requirements for the
degree of Master of Science.

Department of Meteorology
McGill University
Montréal, Québec

July 1973

Abstract

Twice-daily meteorological data are used for the calculation of a surface energy budget over the Gulf of Saint Lawrence. This budget provides a forcing function for certain water body processes and results in the formation and growth of an annual ice cover.

A diagnostic computer simulation of the water processes and their reaction to the meteorological processes is explained and tested in this thesis. The results indicate that ice formation and growth can be simulated with quite reasonable accuracy.

Résumé

Les données météorologiques, journelières, prises aux douze heures furent utilisées afin de déterminer le bilan énergétique superficiel du Golfe Saint-Laurent. Ce balin initient certains processus d'eau lesquels causent la formation et la croissance d'un champ de glace annuel.

Cette thèse décrit un modèle de ces processus marine et leurs inter-actions aux conditions atmosphérique ambientes. Les résultats démontrent que la formation et la croissance de glace peuvent être raisonablement réproduites.

Aknowledgements

I wish to express my gratitude to Dr. E. Vowinckel without whose patience interest and stimulating discussion this work would have been much more difficult and far less enjoyable. Also I thank my wife Susan for her encouragement, patience and interest in this work.

My thanks to Mrs. C. Chouinard for typing this manuscript and again to Susan who typed all the Flow Charts.

I am indebted to the Atmospheric Environment Service of the Department of the Environment for their financial assistance.

TABLE OF CONTENTS

LIST OF FIGURES

LIST OF TABLES

LIST OF FLOW CHARTS

LIST OF SYMBOLS

AEIS - Area of ice as a fraction of one grid square area

ALB - Albedo of a solid surface (ice or snow)

DFL - Flux of long wave radiation down from the atmosphere

FG - Flux of heat to the surface from below

GT - Water temperatures

HEAT - The heat which goes into forming ice over open water

HTL - The heat which goes into adding ice to an existing layer of ice

QE - Flux of latent heat of evaporation or sublimation

QS - Flux of sensible heat

RB - The residual of the energy budget terms

RESHT - Heat stored in the water which makes its way to the surface to meet existing ice

RLU - Flux of long wave radiation up from the earth's surface

SGA - The solar radiation which reaches the surface before the albedo is accounted for

STIE - The snow layer which turns to ice due to the ice flooding

THAW - The heat which goes into thawing ice from above

CHAPTER 1

INTRODUCTION

The object of this thesis is to produce an accurate daily picture of the formation, growth and drift of ice in the ice field of the Gulf of St. Lawrence for the winter season 1971/72.

Work on the ice fields of this area has been carried out by Coombs (Co62) and Matheson (Ma67). Coombs work consisted of using two week average meteorological conditions in the Gulf area for the period mid-November 1961 to mid-February 1962. From these average meteorological values he calculated the terms of the surface energy budget and related these results to ice formation in the Gulf. His greatest difficulties came in trying to estimate fluxes of latent and sensible heat at a distance from the shore reporting stations. His time period of study was limited by the dates at which oceanographic data were available. Matheson's work was a correlation of synoptic weather conditions with periods of heavy ice growth. He found that certain values for the energy fluxes, with given synoptic weather conditions, substantiated the heavy or light ice buildup periods. As in the case of Coombs, lack of data was a major problem in Matheson's work.

In a model of high resolution and short time step this data problem must be overcome. In short, the oceanographic data are discontinuous in time and the meteorological data are not representative over the water surface at distances greater than 50 km from the shore.

The model discussed in the present work is that of a water body containing many of the real physical processes which are simulated by a computer. The water body, once initialized with temperature and salinity, requires no further real data input, but instead reacts solely to the surface energy budget. This then overcomes the lack of oceanographic data. The model is run on a computer in conjunction with an air mass modification model by Morin (Mo73). Morin's model takes land meteorological parameters and carries them out over the water body via the air streams present for that time period. The air mass is then modified by latent and sensible heat

fluxes. Thus, over the water body there are representative surface air and dew point temperatures from which a surface energy budget may be calculated.

The model of the water body, using Morin's model to alter the meteorological parameters, is then run to give ice field pictures every twelve hours. The author feels that this will assist in understanding how the ice field reacts to the water and atmospheric phenomena.

CHAPTER 2

THE MODEL

This chapter includes a discussion of the surface energy budget, its various terms and the water processes which respond to the budget. The sections which follow are divided into subsections: (a) theoretical aspects, (b) computer simulation and, where applicable, (c) results of tests for each phenomenon or process considered in the model

2.1 The Surface Energy Budget

(a) It is the summation of all heat energy arriving at or leaving the surface. In equation form:

$$Q_{SO}(1-\alpha) + Q_{LD} - Q_{LU} - Q_L - Q_H + Q_G = 0 \qquad 2.1(1)$$

where: Q_{SO} - is the solar radiation reaching the surface
α - is the albedo or reflectivity of the surface
Q_{LD} - is the long wave radiation down from the atmosphere
Q_{LU} - is the long wave radiation up from the surface
Q_L - is the flux of latent heat of vaporization from the surface
Q_H - is the flux of sensible heat from the surface
Q_G - is the flux of heat from below the surface

Table 2.1.1 shows other sources of heat energy not considered in equation 2.1(1). They are compared to the first term of that equation only, as all terms are of the same magnitude, on the average.

(b) The basic energy budget equation in the model is:

$$SGA(1-ALB) + DFL + RLU - QE - QS - FG = RB \qquad 2.1(2)$$

where, term for term, the definitions of the symbols in 2.1(1) apply to this equation, except for RB. Because each term of 2.1(2) may not be calculated correctly, RB is not zero. Thus RB is the residual of the

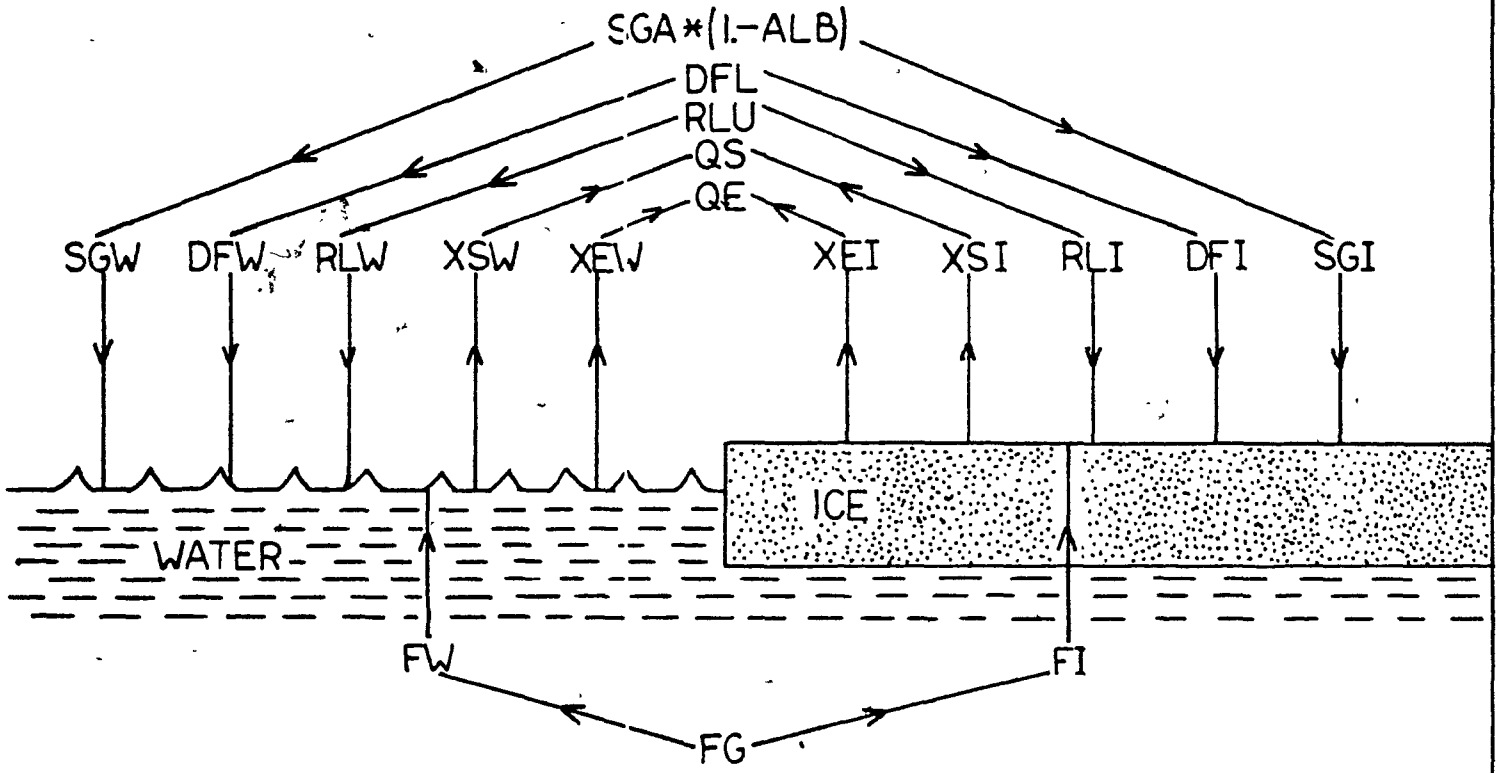

ALL ARROWS POINT IN THE DIRECTION OF DEFINED POSITIVE FLUX WITH RESPECT TO THE SURFACE

BREAKDOWN OF SURFACE FLUXES

FIGURE 2.1-1

balance of the other terms. The terms of 2.1(2) are shown in Figure 2.1-1, where the arrows show the positive direction of the flux of heat.

In the case of a water surface, all terms on the left hand side of equation 2.1(2) may be calculated with the exception of FG, thus FG is taken over to the right hand side to replace RB and thus the equation

$$FG = SGA(1-ALB) + DFL + RLU - QE - QS \qquad 2.1(3)$$

The solar radiation which remains after reflection due to the albedo is not totally absorbed at the surface as some of the solar beam penetrates the water. Therefore, this term is dealt with separately (see section 2.11), but prior to the calculation of FG and the equation used in the model is:

$$FG = DFL + RLU - QE - QS \qquad 2.1(4)$$

The effects of incorporating SGA enter FG via the surface water temperature as RLU, QE and QS are all dependent upon it.

For an ice surface (with or without snow cover), FG may be calculated directly from a formula (section 2.8) and thus it is necessary to calculate RB. The residual heat must then be reduced to a minimum and redistributed among the other terms of equation 2.1(2). This is done by altering the ice or snow surface temperature as discussed in section 2.9. It should also be pointed out that in the case of ice and snow all solar radiation is assumed to be absorbed at the surface, for reasons which will become clear in section 2.8.

When the budgets over ice and water are calculated, it is done assuming that the entire grid area is covered by ice and/or water. Thus the results are weighted according to the area occupied by each. The order of operations for calculating the surface energy budget is shown in FLOW CHART 2-1.

2.2 The Solar Radiation Arriving at the Surface

(a) As the solar beam passes through the atmosphere, its intensity is reduced by absorption, scattering and reflection from clouds. The depletion

Source of Heat	Average Magnitude cal cm^{-2} min^{-1}	Percent of total
Absorption of solar radiation	0.2000	96.0
Energy from the viscous dissipation of the tides	0.0020	1.0
Mechanical energy of the wind transformed to heat energy	0.0002	.7
Heat energy conducted up from the earth's interior	0.0001	.3
Radioactive disintegration of sea water	0.0040	2.0

Sources of heat energy in a water body with a comparison to the absorption of Solar Radiation. Based on figures from Defant, (De61)

TABLE 2.1.1

Source of Depletion	Percent Depletion
Reflection by clouds	24 %
Scattering by water vapour Scattering by air molecules Scattering by dust	6
Absorption by dust	5
Absorption by ozone	2
Absorption by clouds	3
Absorption by water vapour Absorption by carbon dioxide	9
TOTAL DEPLETION	49%

Average depletion of the solar beam as it passes through the atmosphere.

TABLE 2.2.1

FLOW CHART OF BUDGET CALCULATION
FOR ANY SINGLE GRID POINT

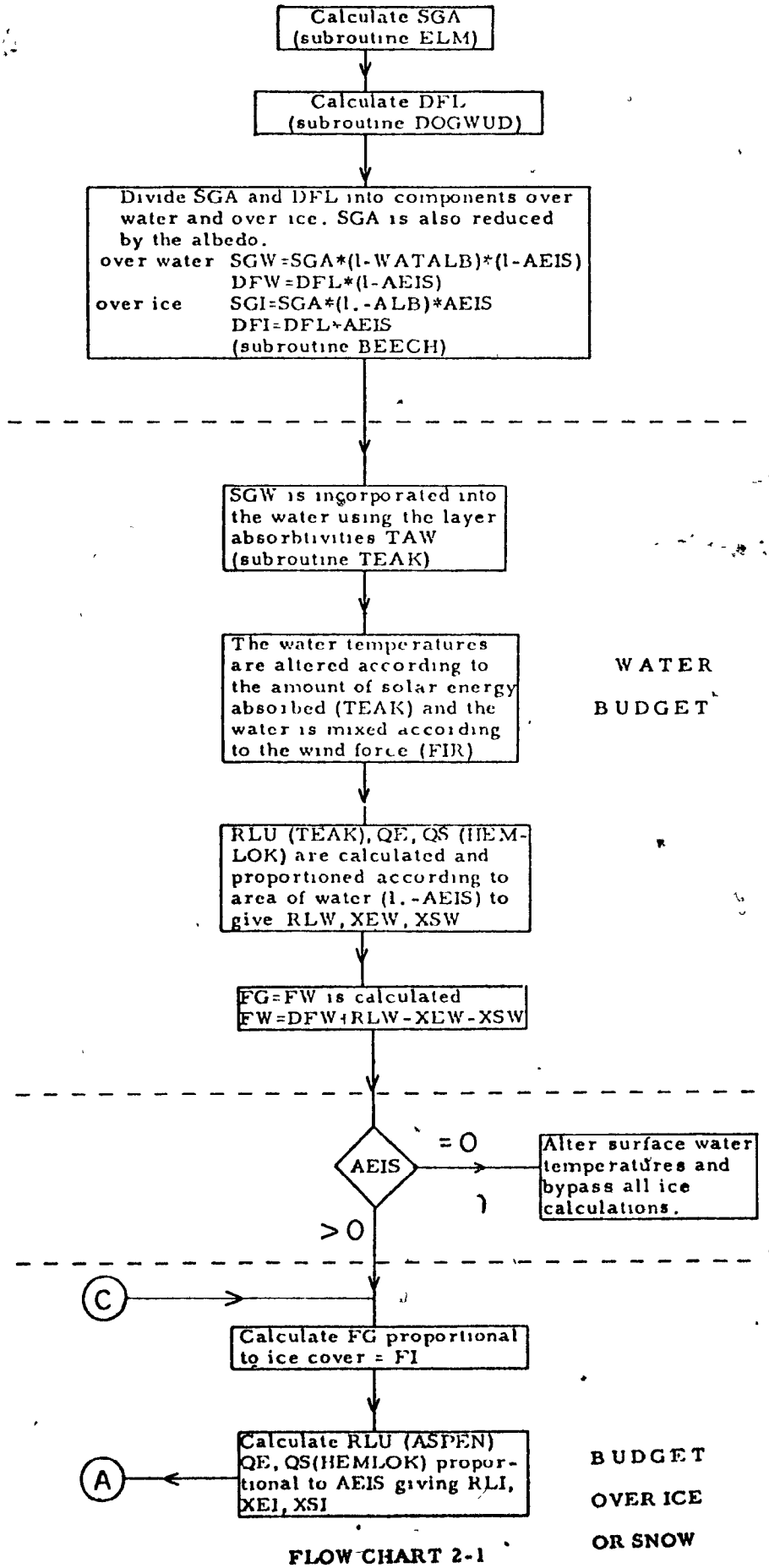

FLOW CHART 2-1

FLOW CHART 2-1 (cont.)

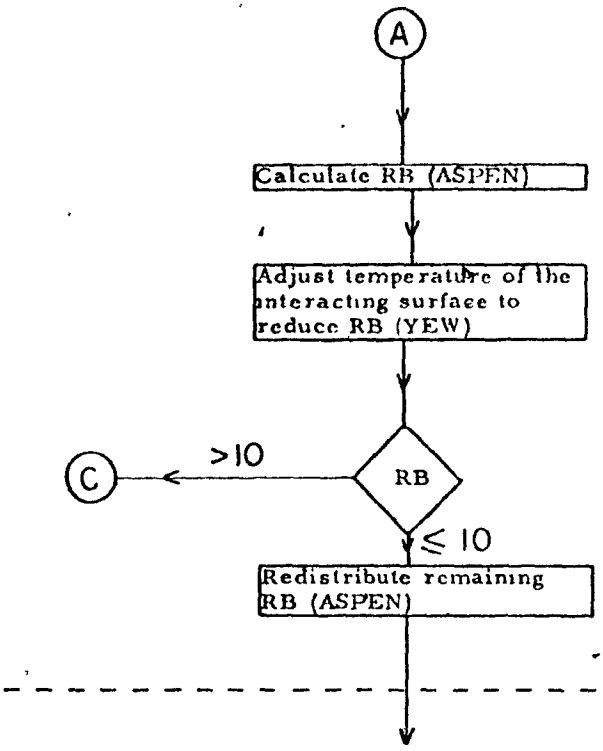

of this heat flux depends upon the concentration of absorber mass, scattering particles and the path length of the solar beam. The relative importance of the sources of depletion are shown in Table 2.2.1. The energy which remains after all the depletion processes in the atmosphere take place is Q_{SO}.

(b) The calculation of short wave radiation reaching the surface (SGA) is done in subroutine"ELM"in the model. The astronomical constants which give the radiation at the top of the atmosphere are calculated in subroutine "HELENA". The subroutine "ELM" corresponds exactly to "ULRIKE", where both "ULRIKE" and "HELENA" are routines developed by Vowinckel and Orvig, (VO72). The methods used to find the atmospheric sounding necessary in "ELM" are found in work by Morin, included in Appendix A. The reader is referred to these two publications for details on "ELM" and its requirements.

2.3 The Surface Albedo

(a) Some of the solar radiation reaching the surface is immediately reflected back into the atmosphere. The amount of energy reflected is proportional to the albedo (α) of the surface under consideration. The albedo is dependent upon three things

(i) The angle of incidence of the solar radiation
(ii) The wave length of the radiation
(iii) The nature of the underlying surface

The angle of incidence dependency is most easily shown for radiation impinging on a water surface. The effect of the hour angle is shown in Table 2.3.1 after Zillman (Zi72). The albedo as seen in that table is highest at dawn and dusk and lowest at noon, local time. Noting, however, that at times of highest albedo (most reflection of energy), there is the least energy reaching the surface and vice versa, the effective daily average albedo is little influenced by the dawn and dusk values.

The effect of declination angle are shown in Table 2.3.2 which contains values of albedo over a year for various latitudes, after Budyko (Bu64). The seasonal fluctuations of albedo again do not affect the annual average albedo linearly. The annual average albedo is much closer to the

TIME	Hours after midnight Local Australian Time, (L.A.T.)												
	6	7	8	9	10	11	12	13	14	15	16	17	18
Albedo of the water varies from 0. to 1.	26	.22	10	.07	.05	05	04	.05	.05	.07	10	.21	25
Incoming solar radiation in cal $cm^{-2} hr^{-1}$	1.9	15.8	35.3	50 8	65.5	73.8	76.0	74.9	68.1	41 3	38.6	15.3	1.4
Reflected solar radiation in cal $cm^{-2} hr^{-1}$	0.5	3.5	3.5	3.6	3 3	3.7	3.0	3.7	3.4	2.9	3.9	3.2	0.4

Total incoming solar radiation = 558.7 cal cm day

Total reflected solar radiation = 38.6 cal cm day

Linearly averaged daily albedo = 0.127

Daily effective albedo = 0.069 where ·

"Daily Effective Albedo" = $\frac{\text{Total reflected solar radiation}}{\text{Total incoming solar radiation}}$

The change of albedo as a function of the sun's hour angle and the "Daily effective albedo"

TABLE 2.3.1

	MONTH	Jan.	Feb.	Mar.	Apr.	May	June	July	Aug.	Sept	Oct.	Nov	Dec.
50 NORTH	Clear Sky Solar Radiation	4 8	8 2	13 3	18 5	22 2	23.7	22 6	19 1	14 4	9 7	5 8	3 9
	Reflected Solar Radiation	.77	.98	1 2	1 3	1.5	1 4	1 6	1 3	1 2	1 1	81	62
	Albedo	16	12	09	.07	07	06	07	07	08	11	14	16
40 NORTH	Clear Sky Solar Radiation	8.8	12 2	16 4	20 3	23 0	24 0	23 4	20 9	17.0	13.2	9 7	7 7
	Reflected Solar Radiation	97	1 1	1 3	1.4	1 4	1 4	1 4	1 3	1.2	1.1	1 1	.92
	Albedo	11	09	08	.07	06	06	.06	06	.07	.08	.11	12

(all radiation values are in units of Kcal cm^{-2} $month^{-1}$)

LATITUDE

Yearly Effective Albedo for 50 degrees North latitude is 0.082

November - April Effective Albedo for 50 North is 0.104

Yearly Effective Albedo for 40 degrees North latitude is 0.074

November - April Effective Albedo for 40 North is 0.090

where the Effective Albedo for a given time period is $\frac{\text{sum of the reflected radiation}}{\text{sum of clear sky radiation}}$

The effect of the Sun's declination angle on a water albedo

TABLE 2.3.2

summer minimum than to the winter maximum due to the large values of solar radiation coming in during the summer months.

The wavelength dependence and underlying surface are both more complex, as the former is somewhat dependent on the latter. In general, single wave length components are not considered separately but rather the radiation at all wavelengths is taken together as has been done in both tables 2.3.1 and 2.3.2.

The nature of the underlying surface is very effective in altering the albedo, as is seen when snow and ice exist above the water. This is best illustrated in the following summary which has been paraphrased from Langleben (La68):

> For a fresh snow cover the albedo was measured as being very close to 1. (on a scale 0 to 1). As soon as some melting of this snow occurred the value dropped sharply and when some loose snow was blown away to expose the ice, the albedo dropped to 0.6. For five days the existing surface underwent normal deterioration and albedo dropped to 0.5. There was extensive melting then, and the formation of melt ponds gave an average albedo of 0.3.

The above change in albedo from a high of 1 to a low of 0.3 took place over a ten day period. This is 700% of the seasonal variation in water albedo due to the declination angle and occurred over a surface whose nature varied drastically and rapidly. These large fluctuations necessitate a comprehensive look at snow and ice albedos, in the model.

(b) In the model the albedo of the water surface, (WATALB), was given a constant value of 0.095, after Table 2.3.2. The running period was only expected to be from November to April, thus the value should be a reasonable approximation.

A more detailed procedure, in the form of subroutine "LARCH", is used to find the snow and ice albedo. Portions of subroutine "LARCH" are based on Langleben's findings (La68) and other portions use criteria described by Vowinckel and Orvig (VO72) in their subroutine "LORE". The range of albedo values possible in "LARCH" are from 0.3 to 0.9, the former for ice with melt ponds, the latter for freshly fallen snow. Any surface unaltered by fresh snow fall or melting will still deteriorate, with a subsequent

drop in albedo. This deterioration is probably due to snow recrystalization and fallout of particulate matter from the atmosphere. Thus the albedo from a previous time step is lowered by 4% in the next later time period. This reduction is based on Langleben's measurements. Vowinckel and Orvig use a surface temperature dependence of albedo in their "LORE" and this has been included in "LARCH". Further in "LORE" if snow exists in a sufficiently thin layer, then the surface below influences the albedo. The influence is found using the matrix ETA, which gives the percent influence for up to five inches of snow after which the underlying surface is assumed to have no influence. Finally, if the wind force is sufficient (10 $msec^{-1}$ in the model), some ice will be cleared and there will be two surface albedos to consider. These two albedos are calculated and considered to represent half the surface area each; so they are averaged.

The subroutine "LARCH" therefore makes use of several albedo determining criteria to allow a rapid day-to-day change in albedo, It is hoped that this detailed approach will prove more effective in giving a short period picture of the energy budget than would average climatological values. This should be most readily seen when melting occurs in the spring.

2.4 Longwave Radiation from the Atmosphere

(a) The water vapour, carbon dioxide, ozone and clouds in the atmosphere absorb and emit longwave radiation at their respective temperature, (T). The quantitative amount of heat energy is found using a form of the Stephan-Boltzmann Law:

$$Q = e\sigma T \qquad 2.4(1)$$

where: Q is the heat flux, e is the emissivity of the given property and σ is the Boltzmann constant. The first three constituents mentioned are selective emitters over small wavelength bands. Cloud, however, emits energy at all wavelengths. Further, as shown in Table 2.4.1, most of the longwave radiation reaching the surface originates in the lowest 150 millibars of the atmosphere.

(b) The calculation of the flux of longwave radiation reaching the surface (DFL) takes place in subroutine "DOGWUD", which is equivalent to Vowinckel and Orvig's subroutine "DORIS", (V072). These subroutines consider the mass

Percentage of Longwave back-radiation which:	Originates below the following levels, (in meters)
9.3	0.1
15.9	0.4
20.3	0.8
25.8	2.0
35.0	6.0
44.6	20.0
58.9	100.0
74.6	400.0
84.8	1000.0
94.5	4000.0

The percentage of backradiation down to the surface from the atmosphere, which originates below certain levels.

TABLE 2.4.1

Type of Surface	Emissivity of the Surface
Water	0.92 - 0.96
Freshly fallen snow	0.82 - 0.995
Granular snow	0.89
Ice	0.92

Types of surfaces and their respective emissivity ranges.

TABLE 2.5.1

of water vapour and carbon dioxide, as well as the cloud cover, for any given grid point. The method used is outlined in Vowinckel and Orvig's papper and the methods used to determine the appropriate values for the radiosonde ascent are given in Morin (Mo73), a portion of which is shown in appendix A.

2.5 Longwave radiation emitted by the Surface

(a) This radiation is calculated using equation 2.4(1) from the previous section, where T is the representative surface temperature of snow, ice or water. The emissivities of these three surfaces are not exactly equal to 1 as is shown by Table 2.5.1. The emissivity is somewhat wavelength dependent and differs for each surface.

(b) In the model all emissivities are taken to be equal to 1. This will tend to overestimate the energy flux from the ground to a varying extent but, in general, on the order of 4%. The actual formulae used vary only in that different temperatures are employed. The Boltzmann constant has been multiplied so that it gives a value for a 24 hour period. Thus it must be multiplied by the desired time step, (SUE). The general formula used is then:

$$RLU = -(1.1707E07*("T" + 273.16)**4/24.)*SUE \qquad 2.5(1)$$

The term RLU differs over water and ice due to their differing temperatures. For a water surface RLU is calculated by replacing "T" in 2.5(1) by the surface water temperature, GT(8). For an ice surface "T" is replaced by TG, the ice or snow surface temperature. The RLU term over a water surface is calculated in subroutine "TEAK", while RLU for an ice surface is calculated in subroutine "ASPEN"

2.6 The Flux of Latent Heat

(a) This flux is a result of molecular diffusion and turbulent transport in the lowest two metres of the atmosphere above the moisture source. According to Roll (Ro65); since there is little accumulation of moisture in the two metre layer compared to the flux through it, it may be assumed that the flux is constant with height. This then allows the flux of heat to be represented in the following form:

$$Q_L = -\rho K_E \frac{\partial \bar{q}}{\partial z} \qquad 2.6(1)$$

where: K_E is the coefficient of eddy transport
ρ is the density of the air in the lowest two metres
$\bar{q}$ is the time averaged value of the specific humidity

The theoretical methods of calculating K_E require measurements of a number of micrometeorological parameters. These are not generally available and even if they were there is no proof that the values of K_E so obtained are representative for large areas especially where the air mass is being rapidly transformed.

(b) The latent heat flux term (QE) is calculated in subroutine "HEMLOK" which corresponds to Vowinckel and Orvig's "VERA". The equation in these two subroutines used to calculate QE is:

$$QE = 0.4176*EVPLTH*CDF*(\overline{TXSH} - TDSH)*U*SUE \qquad 2.6(2)$$

where EVPLTH is the latent heat of either sublimation or evaporation, depending on the underlying surface.

CDF is a measure of the turbulence and its value depends on the wind force and drag coefficient or on the air-sea temperature gradient, whichever is causing the turbulence.

TXSH is the specific humidity of the air very close to the surface

TDSH is the specific humidity of the air approximately two metres above the surface.

and U is the portion of the area considered which is either an evaporating or sublimating surface.

SUE is the time, as mentioned before.

The origins of this equation, and the details of how the CDF term is found, appear in Vowinckel and Orvig (VO72).

2.7 The Flux of Sensible Heat

(a) The same argument as that of 2.6(a) results in an equation for the sensible heat flux similar to 2.6(1), that is:

$$Q_H = -\rho c_p K_S \frac{\partial \bar{T}}{\partial Z} \qquad 2.7(1)$$

where c_p is the specific heat at constant pressure

$\bar{T}$ is the time averaged temperature

and K_S is the coefficient of eddy transfer for heat. Again the coefficient K_S is difficult to find theoretically and is thus determined empirically.

(b) The calculation of the flux of sensible heat is carried out in subroutine "HEMLOK", which uses the following equation for QS.

$$QS = 103.68*CDF*GR*1.25*SUE \qquad 2.7(2)$$

where GR is the air-sea temperature gradient, and other terms are either defined previously or are described in Vowinckel and Orvig (VO72), under the discussion of subroutine "VERA".

2.8 The Flux of Heat from Below the Surface

The flow of heat to, or away from, a surface is dependent on the temperature gradients found in the substance below. The flow is governed by the thermal diffusion equation:

$$\rho c_p \frac{\partial T}{\partial t} = \nabla\cdot(k\nabla T) \qquad 2.8(1)$$

where ρ is the density of the substance below the surface

c_p is specific heat of that substance

and k is the thermal conductivity of the substance.

The actual heat flow through the surface is given by:

$$Q_H = k \frac{\partial T}{\partial Z} \qquad 2.8(2)$$

where $\frac{\partial T}{\partial Z}$ is the temperature gradient across the surface.

In the case of a water body the transfer of heat due to thermal diffusion is often masked by other more rapid processes which change the thermal structure of the body. Rather than go into these here the reader should refer to section 2.10, where these processes will be outlined. The main concern of the present discussion is the flux of heat through an ice or ice and snow layer. For these types of solid substances, equations 2.8(1) and 2.8(2) may be utilized to calculate the flux from below. For homogeneous substances the equations are quite straightforward, it is only when substances of a heterogeneous nature are considered that problems are created. Both snow and sea ice fall into this latter category. The problems with sea ice

are probably best documented. Such ice contains varying concentrations of air bubbles, varying salinity and varying concentrations of brine cells. These variations mean that, ρ, c and k all change from one area of the ice to another. Thus, to apply the equation 2.8(1) adequately, the structure of the ice should be known in some detail. Hudson Bay ice is documented by Schwerdtfeger (Sc62), and for Arctic sea ice, Maykut and Unterstiener (MU69).

(b) In the model the flux of heat into or out of the water body is linked directly to a surplus or deficit of heat at the water surface in the manner described in section 2.1.

The treatment of ice and snow layers is more difficult. Aside from the variability of ρ, c and k there is the problem of actual computation for a multilayered system. The equation 2.8(1) requires such a system for grid point calculation, and the appropriate finite difference form of the equation is:

$$\Delta T_n = \frac{k}{\rho c} \{\frac{T_{n+1} - 2T_n + T_{n-1}}{(\Delta Z)^2}\} \Delta t \qquad 2.8(3)$$

where ΔT_n is the temperature change for layer n

Δt is the time over which the calculation takes place

ΔZ is the layer thickness.

As stated by Gagnon (Ga72) it is necessary for equation 2.8(3) to be computationally stable for the program to be executable. The criterion for computational stability of the above equation from Dingle and Young (DY65) is that:

$$\frac{2(k\Delta t)}{\rho c(\Delta Z)} = 1 \qquad 2.8(4)$$

choosing reasonable values for ΔZ, k and (c), say that

$$\Delta Z = 10 \text{ cm}, \quad k = .0055 \text{ cal cm}^{-1} \text{ K}^{-1} \text{ sec}^{-1}$$

and $(\rho c) = 0.47 \text{ cal cm}^{-3} \text{ K}^{-1}$

Then the time step required to give computational stability is on the order of 10^2 seconds, but the desired time step is twelve hours or 10^4 seconds. In order to use this latter time step, the layer thickness would have to be raised to 100 cm. The ice in the Gulf of St. Lawrence has been reported

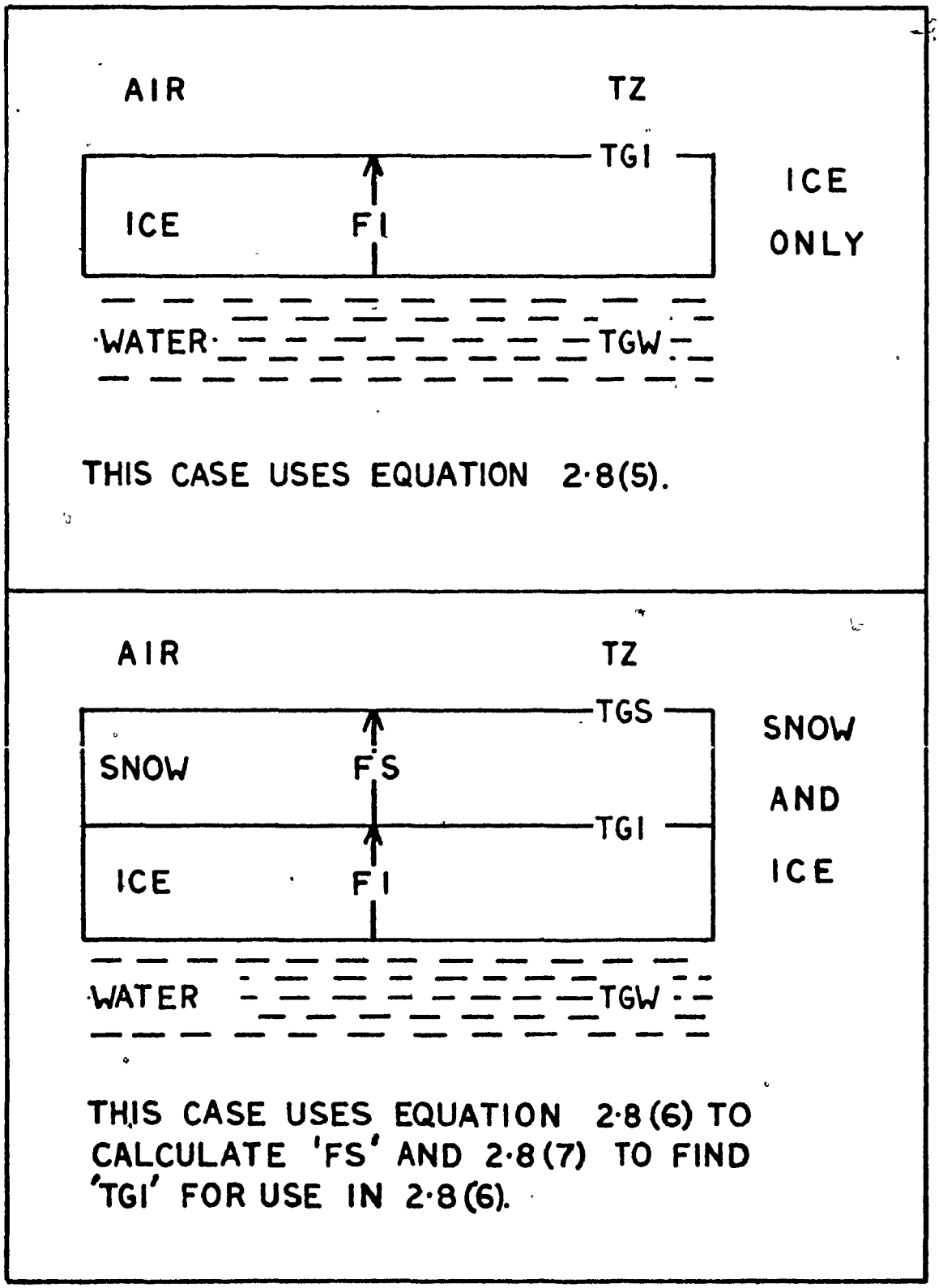

METHODS OF GROUND FLUX CALCULATION FOR ICE AND SNOW SURFACES.

FIGURE 2·8-1

to vary from 15 to 75 cm, except in area of rafting and shore pile-up, (Pounder, lecture given to Canadian Meteorological Society meeting, Montreal group), thus this is not practical. The model then makes use only of equation 2.8(2) and takes the temperature of the top of the ice and the bottom of the ice as being the gradient which determines the heat flux.

With reference to Figure 2.8-1, the equation used to calculate the heat flux for an ice layer is:

$$FI = -(TGI - TGW)*CONE/EIS*SUE \qquad 2.8(5)$$

where FI is the value of FG for an ice layer and is positive if the flux is upward to the surface

CONE is the heat conductivity of ice (a constant)

EIS is the thickness of the ice layer

TGI is the temperature of the ice surface

and TGW is the temperature of water below the ice.

For the case of a snow layer covering the ice surface layer, a two layer system is used. The snow is formed in subroutine "SPRUCE" and is considered to be evenly distributed over the surface at all times for this particular calculation. As will be seen in section 2.9, the ice temperature TGI is known only once during the balancing scheme, namely the first time through, as it is saved from time step to time step. Thus there must be some method by which TGI may be calculated for balance purposes. Just as the flux through the ice layer was calculated so too can the flux through the snow layer be accomplished by an equation of the same form:

$$FI = -(TGS - TGI)*CONS/SSN*SUE \qquad 2.8(6)$$

where TGS is the temperature of the top surface of snow

CONS is the conductivity of heat for snow

and SSN is the thickness of the snow layer.

Using the assumption that no heat is allowed to buildup at the ice surface then clearly 2.8(5) and 2.8(6) are equal and they may be solved for TGI.

FLOW CHART OF GROUND FLUX (FG) CALCULATIONS

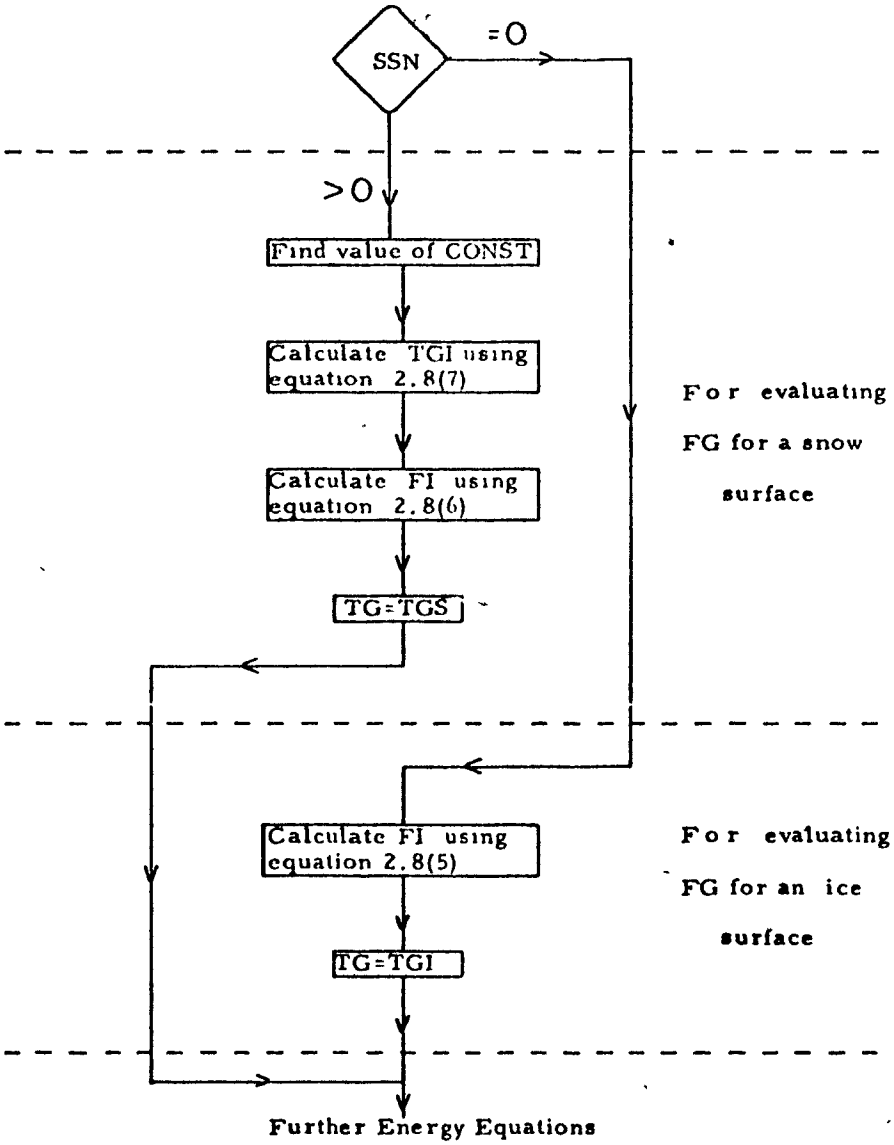

FLOW CHART 2-8

Then TGI = (TGS + (CONST*TGW))/(CONST + 1) 2.8(7)

where CONST = (SSN/EIS)*(CONE/CONS)

Then TGI is used in 2.8(6) to calculate FI. These calculations take place in subroutine "ASPEN" as shown in FLOW CHART 2-8. As can be seen by equations used to calculate the flux of heat through the surface, the system used is simple and thus cannot hope to represent adequately the true picture of heat flow through ice and snow covers. The errors in this system again are difficult to evaluate, as the temperature structure of the real ice for which the calculations are made is not known. Larger errors will probably occur due to CONE and CONS being constant values. The magnitudes of these errors again depend upon the actual structure of the ice and snow, but in general one may say that the values of FI as determined by "ASPEN" will be too low, as the conductivities chosen are at the low end of the scale.

2.9 The Balancing of the Surface Energy Budget

Ideally, equation 2.1(1) holds true and the terms of the equation give no residual heat, but in actual fact the equations used to calculate the energy budget terms are not exact. In general, the term RB of equation 2.1(2) is non-zero and the remaining energy must be redistributed.

For a water surface the balance at the surface is considered to result in a gain or loss of water heat storage, depending upon whether there is a surplus or deficit of heat at the surface.

The balance over an ice or snow surface is more complex. One parameter, however, affects four of the six basic energy budget terms, namely the surface temperature of ice or snow. It affects Q_{LU}, Q_H, Q_L and Q_G when it is altered and therefore it can be utilized to accomplish the balance of equation 2.1(2). During this balancing Q_{SO} and Q_{LD} are unaffected.

(b) The radiation balance of the budget over an ice or snow surface is carried out in subroutine "YEW", which is equivalent to Vowinckel and Orvig's "LEDA", (V072). It is an iterative process which requires a recalculation of RLI, FI, XEI and XSI each time one iteration is finished. The value of RB is used to alter TG in the appropriate direction until RB becomes

BALANCING OF THE SURFACE ENERGY BUDGET

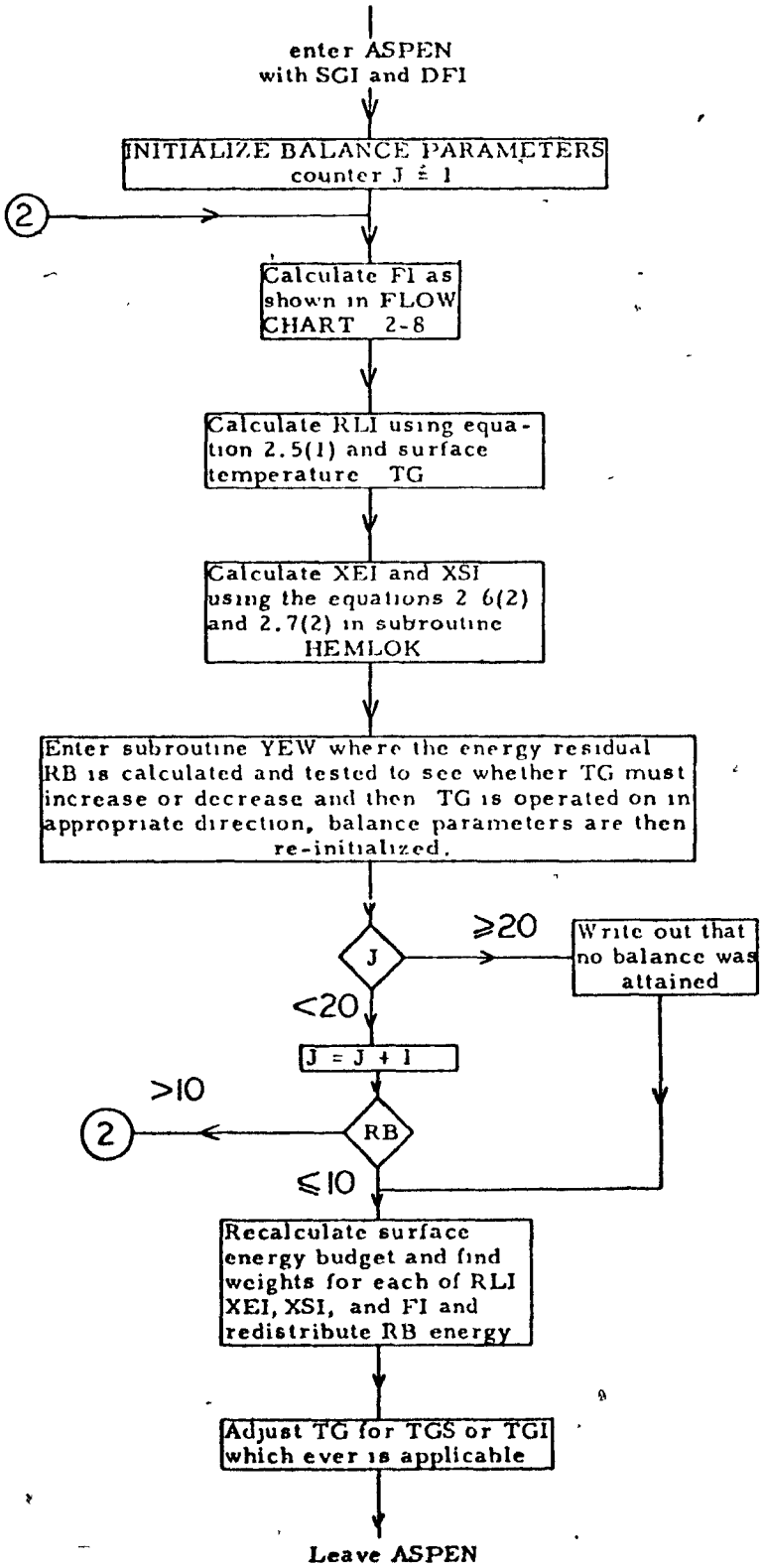

FLOW CHART 2-9

sufficiently small, (RB must be $\leq$ 10 cal cm^{-2}). When this condition is accomplished the remaining heat in RB is redistributed among the four above terms in proportion to their magnitudes. The actual equation used in YEW to calculate RB is:

$$RB = SGI + DFI + RLI - XEI - XSI + FI \qquad 2.9(1)$$

where SGI is solar radiation reaching the surface after the albedo has been accounted for

XEI is the latent heat flux from the ice

and XSI is the sensible heat flux from the ice.

All the terms of 2.9(1) have been proportioned by the amount of ice cover present at the grid square. A practical limit has been set on the number of times an attempt at balance can be made. Thus, if there is still no balance after 20 iterations the remaining energy in RB is distributed proportionately among the four terms, as mentioned before.

The entire heat budget calculation and balance is done within subroutine "ASPEN", which calls subroutine "YEW" as shown in FLOW CHART 2-9. Only the two constant terms SGI and DFI are calculated outside this budget subroutine.

2.10 The Water Processes and Their Reaction to the Surface Energy Budget

(a) A body of water is constantly reacting to the surface energy balance. If there is a deficit of heat at the surface the water must give up heat, which it contains in storage, in order to balance this deficit. The processes by which this heat may be brought to the surface are thermohaline convection in reaction to a density gradient rendered unstable by the surface cooling. Secondly, if the water experiences turbulent motion due to wind stress heat is also transported. In the absence of these two phenomena, molecular heat conduction must serve. In the case of a surplus of heat at the surface, the amount of heat in storage in the water may be augmented if processes exist to transport that heat downward. Turbulent motion and molecular heat conduction are two obvious processes which could accomplish the downward transport of heat. Thermohaline convection, on the other hand,

would require a similtaneous rise in salinity to give a downward transport as this would help overcome the increased stability of the density structure due to surface warming. Finally, a second reaction results from a heat deficit at the surface, that is the formation of ice. Ice will form if the heat deficit is sufficiently large to lower the surface temperature below its freezing point and no heat is available from below to rectify this deficit.

For the time being, only vertical processes will be considered, leaving the horizontal processes to section 2.17. The processes thus far mentioned which transport heat are:

(i) Molecular heat conduction

(ii) Thermohaline convection

and (iii) Dynamic convection (turbulent mixing).

The time scale of these processes must be examined to ascertain which are significant. Considering molecular conduction first, Defant (De61) shows that the time for one half the magnitude of a surface temperature change to reach 1 m is on the order of $\frac{1}{4}$ of a year and to reach 10 m, 27 years. This means that the other two processes are orders of magnitude faster in transporting surface heat anomalies. Thermohaline convection is on the order of hours and dynamic convection if not quite as fast is only slightly slower, possibly on the order of days. Thus, with negligible error molecular conduction may be neglected as a significant water body process.

Other vertical processes which will be considered besides (ii) and (iii) are ice formation and build-up, absorption of solar radiation, brine migration, and flooding of the ice when the snow cover becomes thick.

2.11 Absorption of Solar (Shortwave) Radiation

(a) Solar radiation reaching the surface of a water body experiences reflection back to the atmosphere and the remaining radiation penetrates the water where it is absorbed. The transmission of solar energy through water is dependent upon the turbidity of the water and the wavelength of the light. The turbidity or optical mass of the water is a function of the concentration of organic and inorganic matter present. In a body of water

Water Mass Type	Description of the Water Mass	Percent of Radiation absorbed in the layer									
Oceanic (clear)	Old clear oceanic water in low productivity areas (low latitude)	71.4	6.8	7.2	6.6	3.0	1.3	0.9	1.1	0.6	1.1
Oceanic (normal)	Medium productive oceanic water in low & medium latitudes	78.2	9.1	7.3	3.7	0.9	0.5	0.2	0.1	-	-
Oceanic (turbid)	Highly productive oceanic areas especially during plankton bloom (tropical waters)	84.4	8.1	4.7	2.0	0.3	0.1	-	-	-	-
Coastal (normal)	Medium productive coastal or shelf water	89.6	6.5	3.2	0.6	0.1	-	-	-	-	-
Coastal (turbid)	Estuarian & coastal waters during intensive plankton bloom or waters near the coast where sediment is brought up due to wave action.	95.1	4.0	0.9	-	-	-	-	-	-	-
Layer Number		1	2	3	4	5	6	7	8	9	10
Layer Thicknesses in meters	from:	0	2.5	5.0	10	20	30	40	50	75	100
	to :	2.5	5.0	10	20	30	40	50	75	100	150

Laevastu's water mass types and their corresponding percentage absorptions.

TABLE 2.11.1

such as the Gulf of St. Lawrence the turbidity will probably differ from one region to another since there are several sources of inorganic particulate matter. Laevastu (La60) describes various water mass types and for these gives absorptivities of solar radiation with depth. These are shown in Table 2.11.1.

Solar radiation penetrates snow and ice to a lesser extent than for water, but the depth of penetration is still wave length dependent. Table 2.11.2, from Sellers (Se65), shows the percentage of radiation transmitted for given depths. Though it does not show values for sea ice explicitly, it should help to give some estimate of the penetration depth of solar radiation.

(b) The model does not allow the absorption of solar radiation to be selective. To do so would require a detailed knowledge of the energy spectrum at the ground. And this is not available from the solar radiation calculations. Instead, a bulk value of heat is derived from subroutine "ELM". This allows the use of bulk absorption values for radiation in the water body. To this end the values of Laevastu are used.

The Gulf of St. Lawrence water varies in turbidity and there are three distinct areas, according to T. Platt of the Bedford Institue of Oceanography (personel communication). Their individual characteristics are the result of sediment inflow and the sea life present. The three areas are shown in Figure 2.11-1. A description of the area and the accompaning absorptivities are shown in Table 2.11.3. The values correspond to Laevastu's Coastal turbid and Coastal normal water mass regions, with values from Area III lying halfway between the two. Rather than use up computer storage space to hold the different values for each point, a scheme was devised whereby the absorptivities are chosen on the basis of the real depth of water over any one point. The depth regimes in the Gulf correspond quite well to the areas delineated in Figure 2.11-1.

The selection of absorptivities is done in the main program using an indicator matrix called LDMX, of which the last three numbers give the grid point depth in metres. The absorption values are carried in to subroutine "BEECH", where the value of SGW is found and thence to subroutine

DEPTH	Wet Snow	Dry Snow	Glacier Ice
2.5 cm	—	—	86.7
5.0	8.0	—	75.2
10.0	2.4	18.5	56.6
15.0	1.1	5.5	42.5
20.0	0	3.2	32.0
25.0		2.2	24.1
40.0		1.2	10.2
60.0		0.6	3.0

Percentage of solar radiation which is transmitted through given depths of certain solid substances.

TABLE 2.11.2

Region	Description and Depth	Absorptivities (TAW)							
I	Magdelan Shallows 100m	.951	.040	.009	0	0	0	0	0
II	Laurentian and Esquiman Channels 200m	.896	.065	.032	.006	.001	0	0	0
III	Northern Shore of the Gulf 100 200	.934	.053	.012	.001	0	0	0	0
Layer Number		8	7	6	5	4	3	2	1
Layer Thickness (TAH) in centimeters		250	250	500	1000	1000	2000	3000	4000

Absorptivities of Solar Radiation used for various regions of the Gulf of St. Lawrence.

TABLE 2.11.3

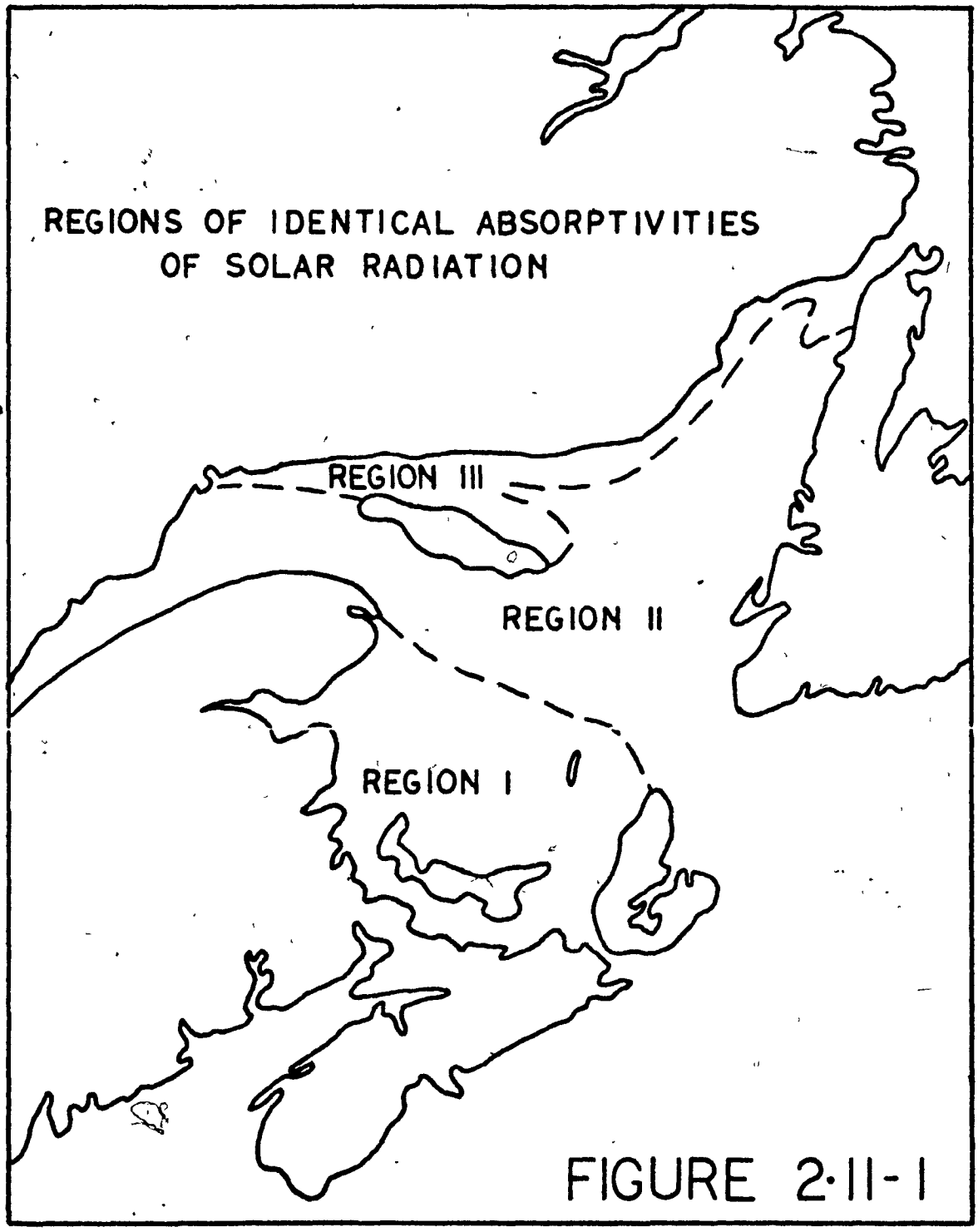
REGIONS OF IDENTICAL ABSORPTIVITIES
OF SOLAR RADIATION
REGION III
REGION II
REGION I

FIGURE 2·11-1

"TEAK" where the heat is distributed amongst the layers. The procedure used is shown in FLOW CHART 2-11.

In the case of an ice or snow surface no penetration is allowed; all radiation is said to be absorbed at the surface. This will prove a better approximation in the case of a snow surface than with ice. A primary reason for its omission is the fact that neither ice nor snow are multilayered (section 2.8), making incorporation quite difficult. The result of absorbing all radiation at the surface will be to make values of RLU, QE and QS too large, but possibly more important it will not allow the water below the ice to warm as the radiation penetrates.

(c) In light of the variability of absorption in different areas of the Gulf of St. Lawrence, tests were carried out to check the effect of different absorptivities on a grid point. The two indicators used to compare the results are:

(i) Date upon which ice forms (no advection is included)

(ii) The graph of the heat content of the water body.

The tests were carried out using radiosonde and surface data from Sept Isles Quebec (72811) for the years 1967 and 1968. The water body was eight layers thick, or 120 metres, and all other processes were kept constant. The resultant freezing dates are shown in Table 2.11.4 along with the absorptivities used, and the graphs of heat content versus time appear in Figure 2.11-2. Rather than use a smaller range of absorptivities as seen in Table 2.11.3, a wide range was chosen in order to approximate the extremes. The differences recorded in the Freezing dates are extremely small and the maximum difference is only 36 hours. This should allow a wide choice of absorptivities with negligible error. The graphs of heat content would indicate that, in the case of largest penetration depth, there is more heat given off at later dates which will slightly affect the atmospheric heat budget.

2.12 Dynamic Convection (turbulent mixing)

(a) Dynamic convection is a turbulent process caused by the stresses set up in the water body as wind blows across the surface. The resultant

INCORPORATION OF SHORT WAVE RADIATION
INTO WATER BODY

FLOW CHART 2-11

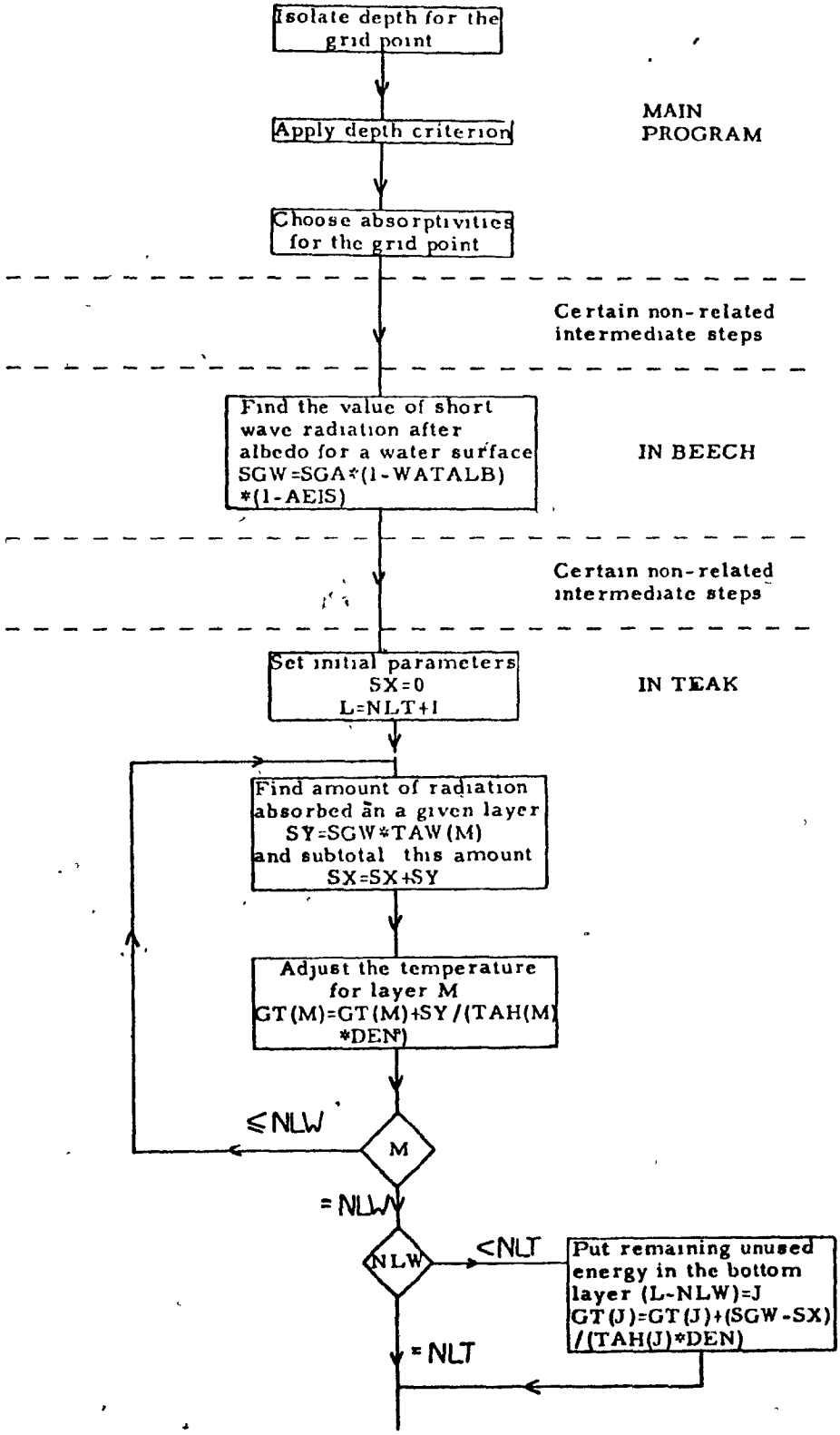

Go on to calculate energy Budget of water body.

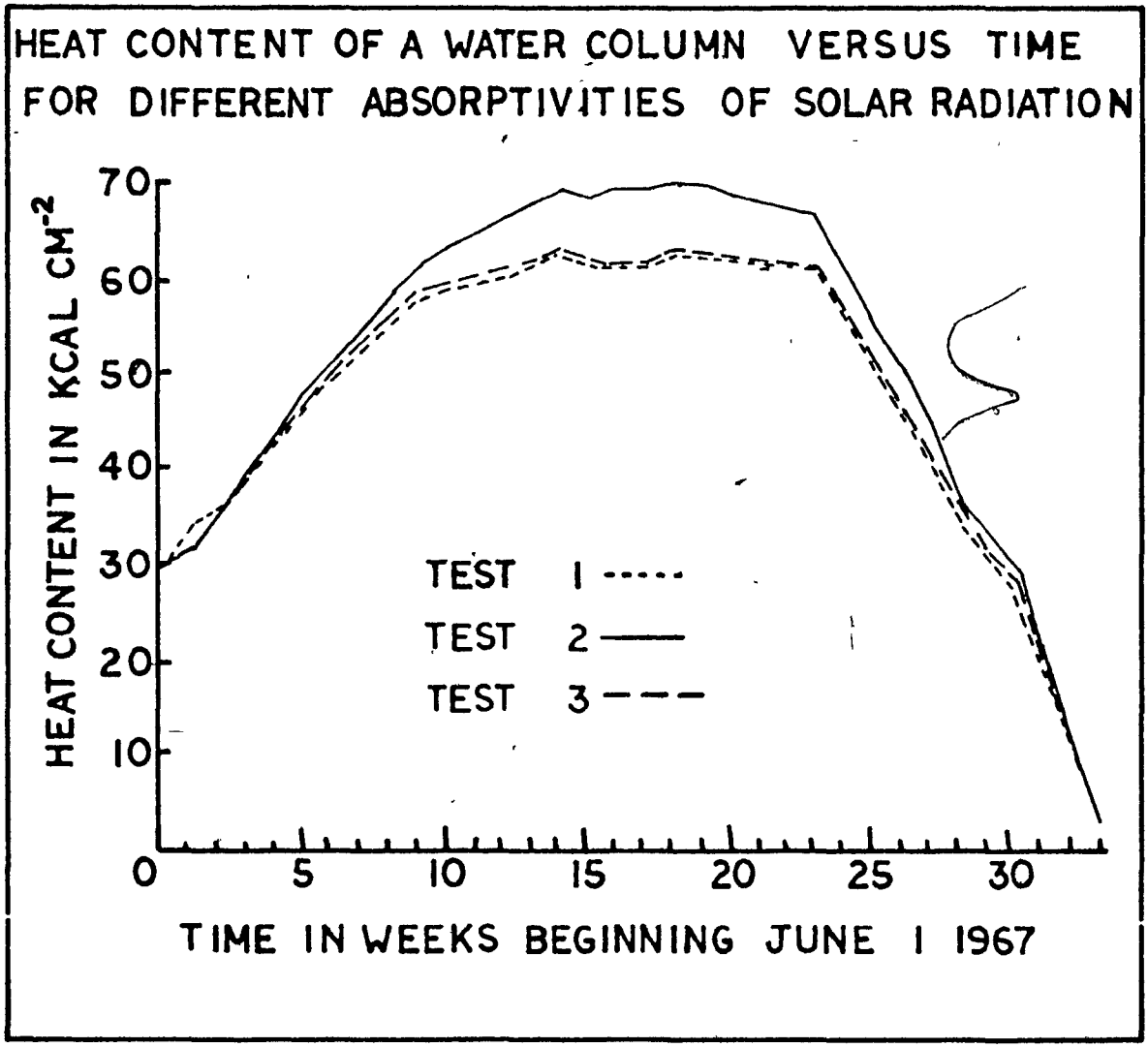

FIGURE 2·11-2

Test No.	Absorptivities								Freeze-up Date
1	.999	.001	0	0	0	0	0	0	Jan 12/68 day
2	.714	.068	.072	.066	.030	.022	.011	.017	Jan 13/68 day
3	.934	.053	.012	.001	0	0	0	0	Jan 12/68 night
Layer No.	8	7	6	5	4	3	2	1	

Test Absorptivities and Freeze-up dates for a single point

TABLE 2.11.4

disordered eddying causes quanta of water to move and thence become mixed. Turbulence is a dissipative phenomenon, the dissipation being caused by work being done against the viscous forces in the fluid. The dissipative effects of the fluid are larger if the fluid is stably stratified in its density structure.

In a stably stratified fluid the regimes of turbulent and non-turbulent motion are separated by a sharp interface, which is gradually broken down as entrainment of non-turbulent water takes place. In this case the turbulence does work to overcome the buoyancy created by the stability of the fluid. If sufficient energy is available for the creation of turbulent motion, then a mixed layer of water forms. It is this mixed layer which creates a heat storage facility in the water body. Finally, the depth of the mixed layer is dependent upon two things: First the amount of negative buoyancy force available for mixing and, second, the magnitude of the buoyancy forces that must be overcome. The amount of negative buoyancy force is a function of the wind force and the duration of that wind. The buoyancy forces are a function of the density gradient and thus depend upon water temperature and salinity.

(b) The simulation of dynamic convection considers both the turbulent energy made available to the water and the stability structure. The latter however, does not consider the density explicitly as in fact the temperature only is used to determine the stratification of the water body.

The scheme used is derived from empirically derived curves of the Royal Navy (Anon 68). These curves were derived from three years of observations at the weather ships 4YI and 4YJ in the Northeast Atlantic ocean. Two sets of curves are used, the first set shown in Figure 2.12-1 relates the wind force and duration of that wind to give an indicator of the available turbulent energy. This number is called the Wind Mixing factor (WMF). The second set of curves is used to find the dissipative forces in the water, Figure 2.12-2. These curves relate the wind mixing factor and the buoyancy forces to give the depth to which the mixed layer will extend.

As mentioned before, the salinity is not explicitly accounted for and

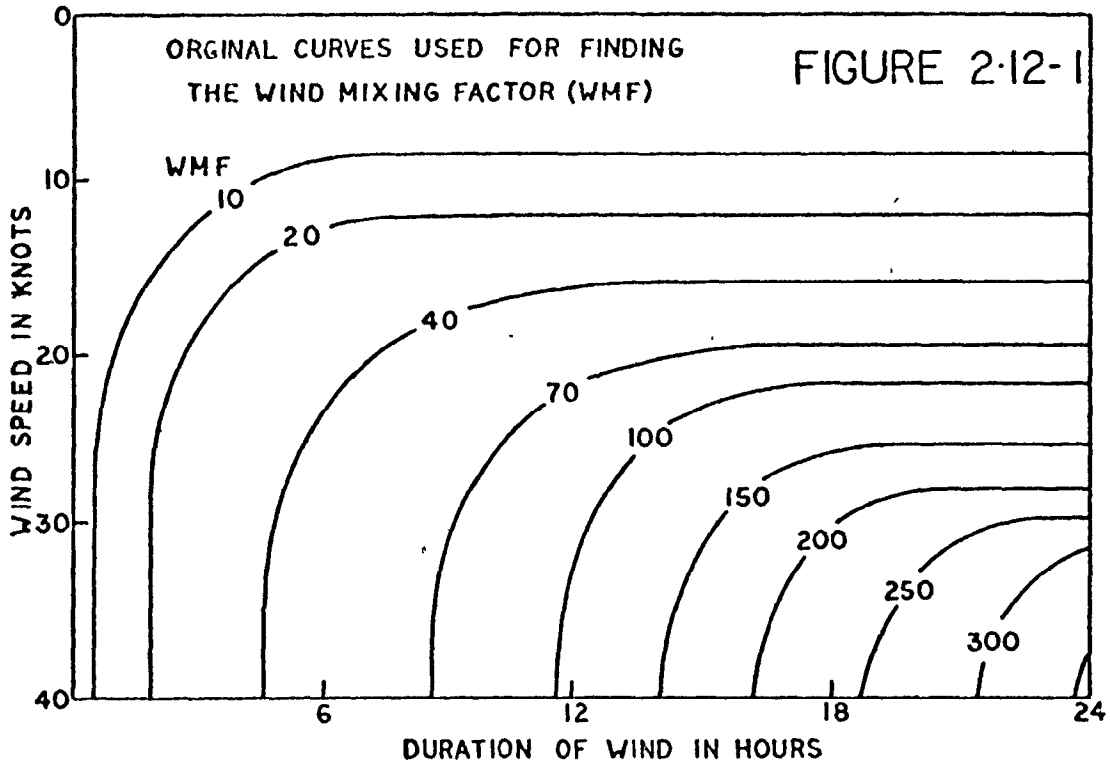

FIGURE 2·12-1

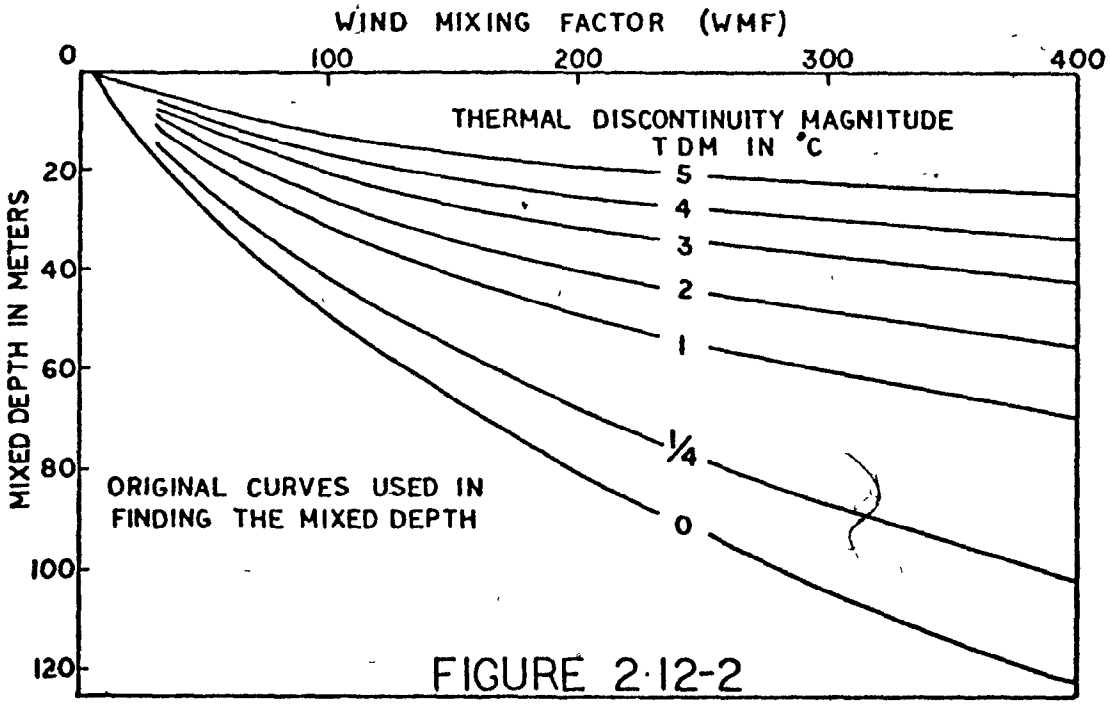

FIGURE 2·12-2

must be considered a constant throughout. In the case of the Gulf of St. Lawrence, the salinity of the water is assumed known for all points and thus could be considered if an adequate scheme were available to do so. As the salinity is not known for the water near the ships where the observational data were obtained for the curves, only qualitative statements may be made about the probable errors. In the Gulf the salinity structure is such that it enhances the stability of the temperature derived density curves. Thus, if the Northeast Atlantic in the region of 4YI and 4YJ is neutral, or if it is more saline at the surface than below, these curves will overestimate the mixed depth. If, on the other hand, the structure is more saline below and less saline above than is the Gulf, these curves will underestimate the mixed depth. As the Gulf has large sources of fresh water flowing into it, and more saline Atlantic water below, the former condition will probably exist and the derived mixed depths will be an overestimate.

The procedure of transforming the curves of Figure 2.12-1 and 2.12-2 into a form more amenable to computer calculation necessitated the redrawing of the curves in Figure 2.12-2. These new curves appear in Figure 2.12-3, where only the 12- and 24-hour curves are important as these times are multiples of the time step used. These two new curves resulted in four equations which gave a best fit to the curves. These equations are found in subroutine "FIR". The curves of 2.12-2 were broken up in to families of curves which were given equations of best fit and these equations are found in subroutine "LINDEN".

The major difficulty in implementing the Royal Navy scheme was in the identification in the computer program of the thermal discontinuity magnitude (TDM). The method used to overcome this problem in the model uses the assumption that any change in density from a more to a less stable condition will dissipate turbulent energy. The second problem encountered was how to remove the bias imposed on the system by having finite layer thickness. This second difficulty was overcome by assuming that the curves of Figure 2.12-2 give a potential mixed depth and show the rate at which energy is dissipated if a given thermal discontinuity magnitude exists. This then allows the use of the following scheme. Given any two layers of water,

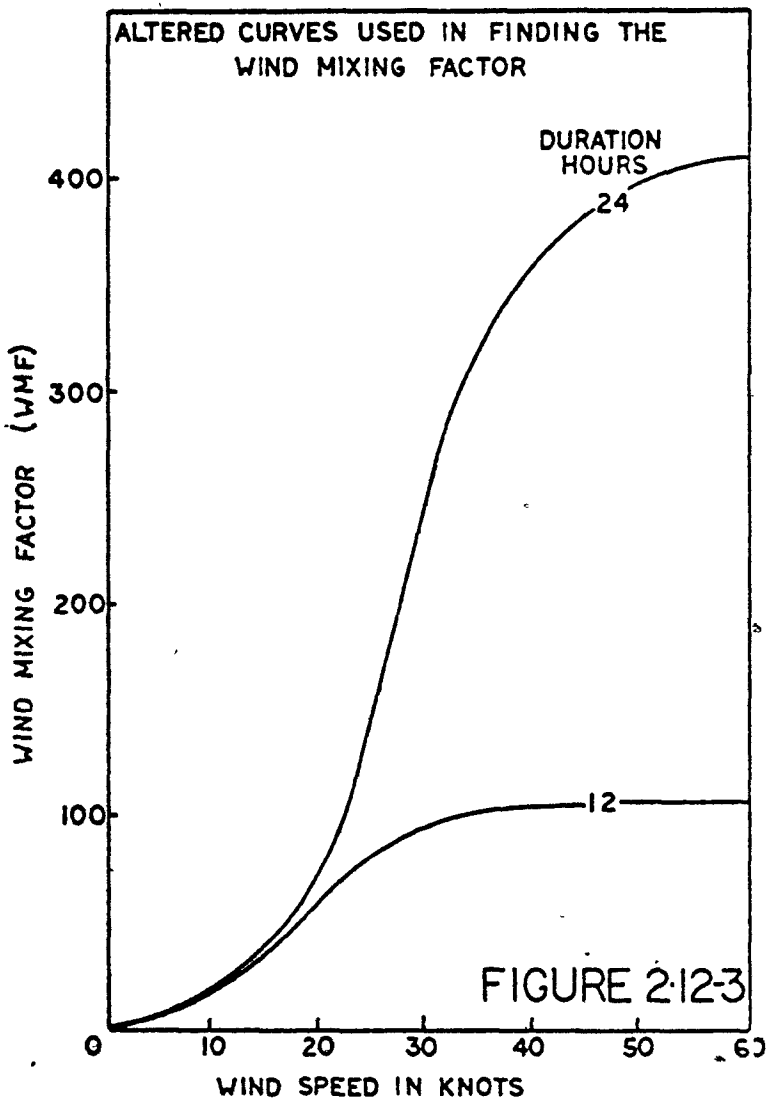

FIGURE 2·12-3

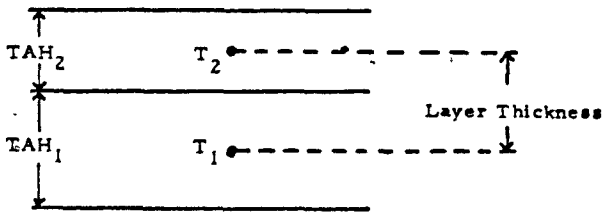

1. Layer Thickness = $\frac{TAH_2 + TAH_1}{2} = THICK$

2. Thermal Discontinuity Magnitude TDM = $T_2 - T_1$

3. Potential mixed depth for a given value of TDM is found in subroutine "LINDEN" and is called DWZ

4. The energy (DELENG) used in mixing the layer is then:

$$DELENG = \frac{THICK}{DWZ}$$

5. The total energy (ENG) used in mixing up to this point is :

$$ENG = ENG + DELENG$$

The energy of mixing which is expended in the dynamic mixing of one or more layers of water

FIGURE 2·12-4

there is a TDM value and this in conjunction with subroutine "LINDEN" will give a value for the mixed depth (DWZ). Now, to find the amount of energy lost in mixing the water for which TDM has been measured, the thickness of that layer is divided by DWZ to give a fraction of the total energy used. This is illustrated in figure 2.12-4 and the FLOW CHART 2-12 will also assist in understanding the procedure used.

(c) In order to estimate the errors caused by either an overestimate or underestimate of the mixed depth, tests were run to find sensitivity of the system to varying mixed depth evaluations. The method used was to calculate the mixed depth DW in the normal manner and then multiply this figure by different factors. The results which were checked were the dates of ice formation and the graphs of water body heat content. Again the atmospheric data used were those of Sept Isle, Québec. The factors and resultant freezing dates appear in Table 2.12.1 and graphs of the heat content of the water body versus time appear in Figure 2.12-5.

The results show that the heat storage in the water body reacts strongly with the calculated mixed depth, and as a result so do the freezing dates. The freezing dates show, however, that if the present scheme is an overestimate of reality, it creates less error than if it is an underestimate. In terms of salinity enhancement Table 2.12.1 may be interpreted as follows. If the multiplicative factor 1 assumes some salinity profile then the factor 2 shows the effect of a more isohaline structure and hence less stability. The multiplicative factors less than 1 show the effect of a more stable salinity structure than that which has been assumed. These possible errors must be considered when the results are evaluated, if it is at all possible to isolate their effect.

2.13 Thermohaline Convection

(a) Thermohaline convection is simply the reaction of the water to an unstable density gradient. It can be triggered in two ways (i) the surface water becomes colder and hence more dense (in sea water with Salinity > $24.7^{o}/oo$) and (ii) the surface water becomes more saline. This is true of lower layers as well and, of course, any combination of (i) and (ii) may

THE DYNAMIC CONVECTION PROCESS

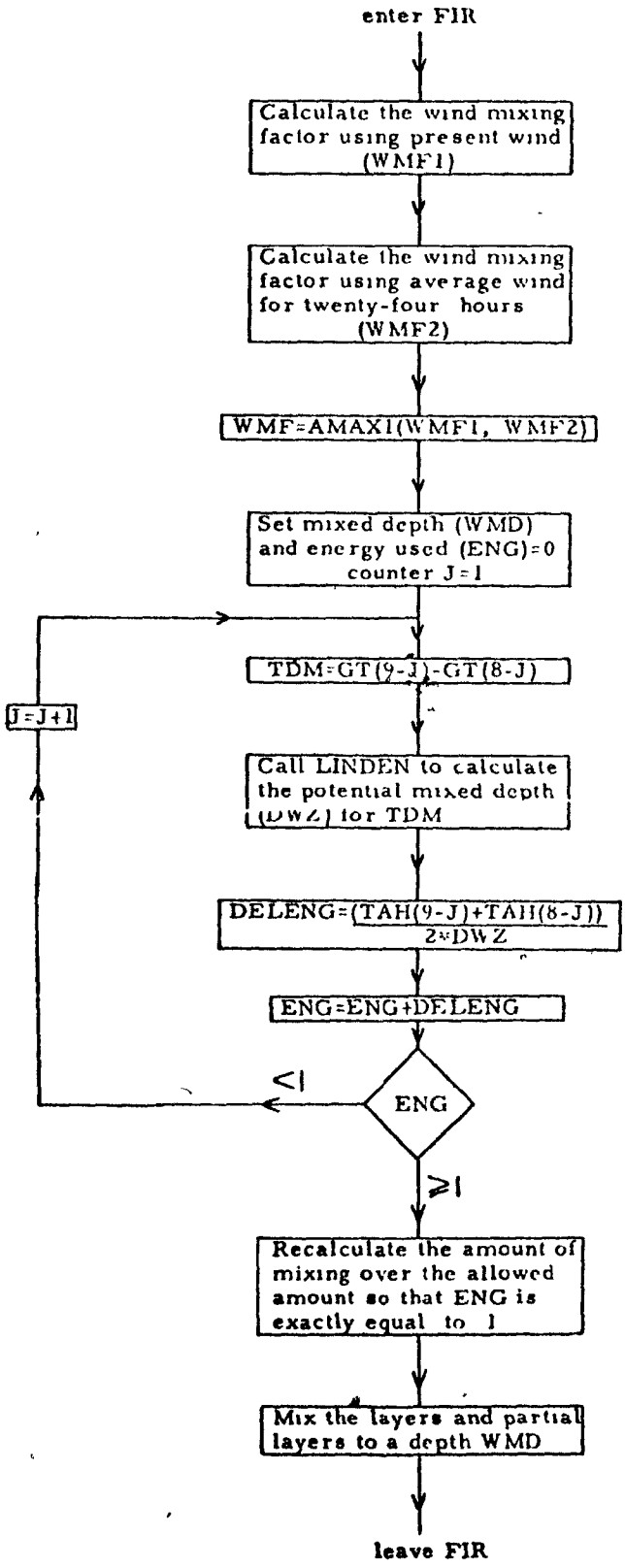

FLOW CHART 2-12

HEAT CONTENT OF A WATER COLUMN VERSUS TIME FOR VARYING MIXING DEPTH FACTORS

FIGURE 2·12-5

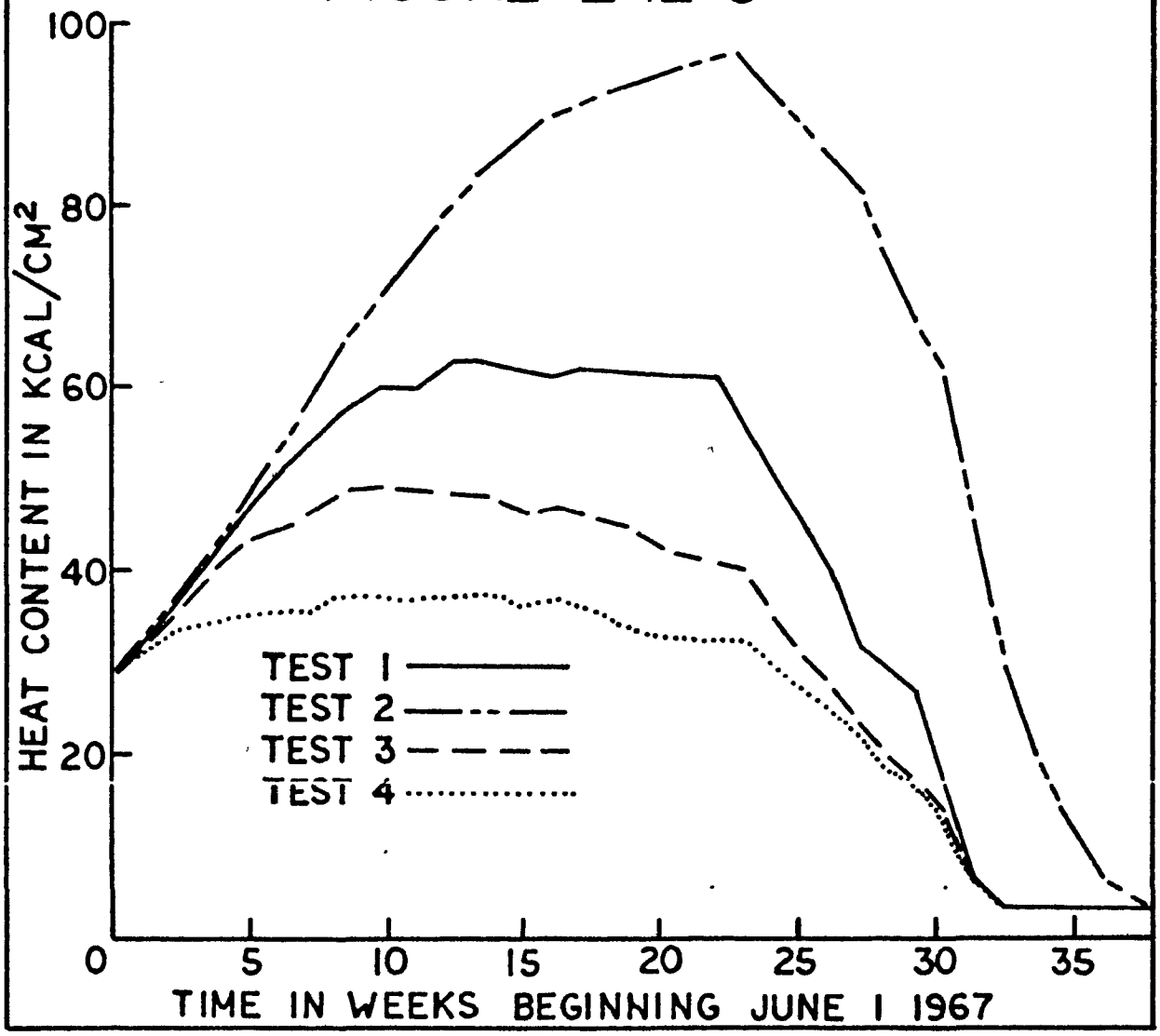

TEST NO.	MULTIPLICATIVE FACTOR	FREEZE-UP DATE
1	1.00	Jan. 11, 1968 daytime
2	2.00	Feb. 15, 1968 daytime
3	0.50	Jan. 4, 1968 night-time
4	0.05	Jan. 3, 1968 night-time

Freeze-up dates with several different wind mixing factors

TABLE 2.12.1

have similar effect.

Cooling of the surface layer occurs most often in the fall when colder air begins to pass over the water, reducing the heat storage there. An increase in salinity readily occurs when ice forms on the water, dropping out brine into the water and making it more dense. There are two additional processes which affect the surface density, namely precipitation and evaporation. Both these processes act through the salinity, making the surface layer either less or more saline.

(b) This process is easily simulated given temperature and salinity profiles. It amounts to comparing the density of any lower layer with the layer above. If there is instability the layers will be mixed, if not no mixing occurs. Only surface cooling and salinity increase due to ice formation are considered in the program. Precipitation and evaporation are considered to be too small to affect the system significantly. This is easily seen if a centimeter of water is evaporated and that water's original salinity is $30.00^{o}/oo$, then the top layer of water in the model, being 250 cm, undergoes a salinity increase of $0.03^{o}/oo$. When these salinities are initially put into the model they are accurate to only $0.10^{o}/oo$, so the increase of $0.03^{o}/oo$ is below the allowable error. The process takes place in subroutine "OAK".

2.14 Ice Formation and Build-up

(a) The constant removal of heat from the water body experienced in the fall months eventually results in the depletion of available heat for surface layer warming. At some point the heat supply becomes insufficient to keep the water open and the result is the formation of an ice sheet. After ice forms, heat is conducted through it causing more ice to form on the underside of the existing sheet. With the onset of warmer spring weather the ice will melt from above and eventually disappear. During the winter, heat may have been trapped in the water below but remained unavailable for surface warming due to a stable density structure. Then, as the salt from ice formation is dropped in the water the density structure becomes unstable and the overturning causes the heat to rise and thus melts

the ice from below. In these ways the ice will form, grow and decay.

(b) All these processes are allowed for in the model. The initial formation of ice takes place in subroutine "ASH". This routine is called when the temperature of open water falls below its freezing point. Then the heat deficit which must be made up to restore the temperature to its freezing point gives a measure of the ice formed over open water. A small section in "BEECH" is responsible for finding the melting of ice from below, or the formation below, and subroutine "CEDAR" calculates the melting from above. All these increases or decreases in ice volume are then put into subroutine "PINE" which distributes them. This entire procedure is shown in FLOW CHART 2-14. The ice distribution is as follows, where:

EISN - is the ice formed over open water
EISTI - is the ice added to the existing layer
EISD - is the ice lost due to melting from below
and EISM - is the ice lost due to melting from above.

Next EISN is divided by the thickness of the existing ice (EIS) to give an increment to the ice area. Then EISTI, EISD and EISM are summed algebraically and added to the total ice thickness divided by the new areas of ice, AEIS. This may also be seen in FLOW CHART 2-14.

The formulae used to calculate EISN, EISTI, EISD and EISM are as follows:

$$EISN = - HEAT/(ELAT*DENE) \qquad 2.14(1)$$

$$EISTI = - HTL/(ELAT*DENE) \qquad 2.14(2)$$

$$EISD = - RESHT/(ELAT*DENE) \qquad 2.14(3)$$

and

$$EISM = THAW/(ELAT*DENE) \qquad 2.14(4)$$

where ELAT is the latent heat of fusion for ice (taken as 80 cal gm^{-1})

DENE is the density of sea ice (taken as 0.912 gm cm^{-3})

This particular system preserves the ice volume and, further, it allows only one ice thickness to exist at any given point. One further criterion is specified; the first time that ice is formed at a grid point it forms at no less than a standard thickness. This thickness is called CRITH and for the program is set at 4.0 cm. Thus, no ice can exist with a thickness of less than this value. The methods outlined here were formulated while

CALCULATION OF THE FORMATION, GROWTH AND MELTING OF ICE

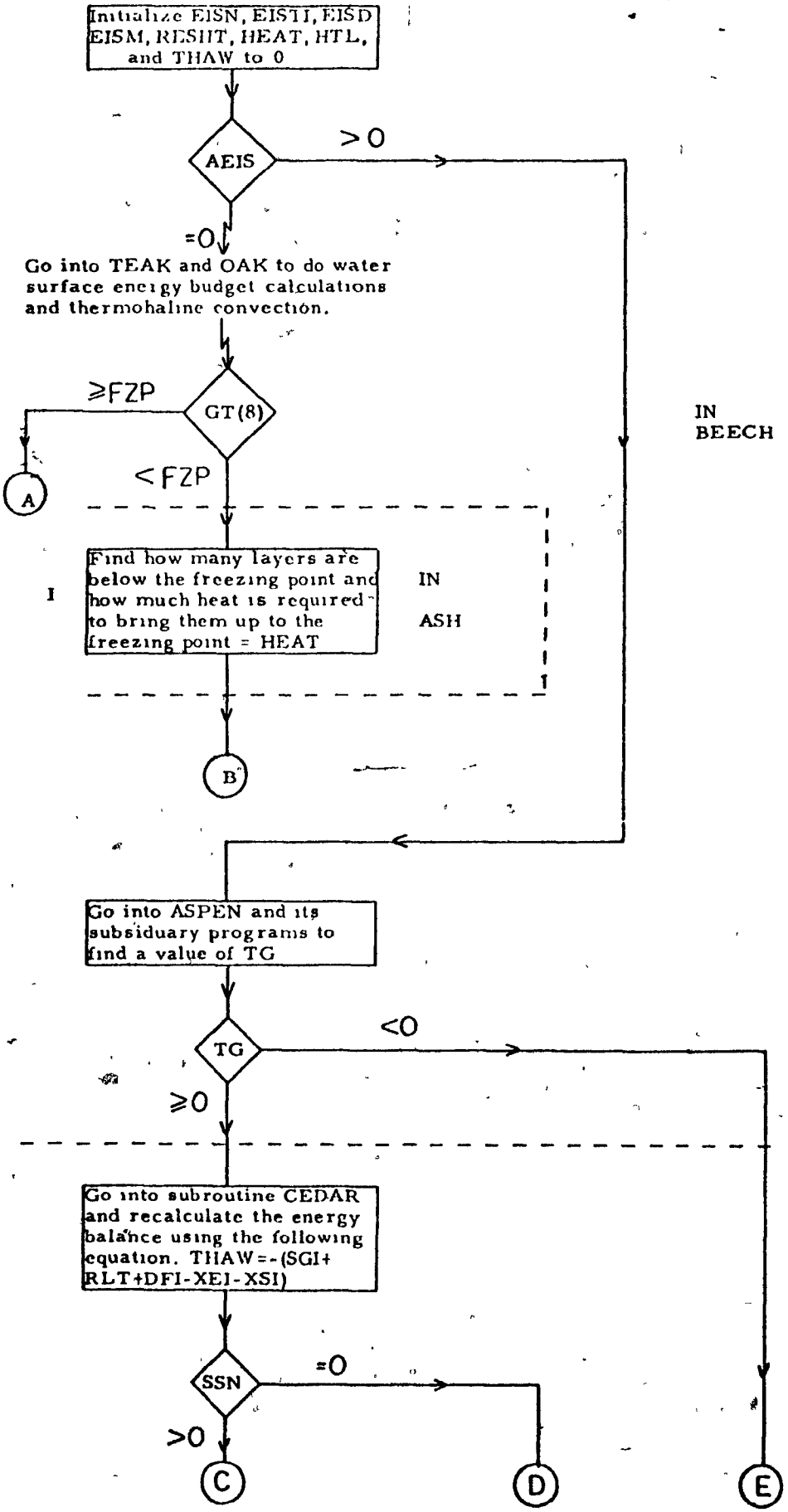

FLOW CHART 2-14

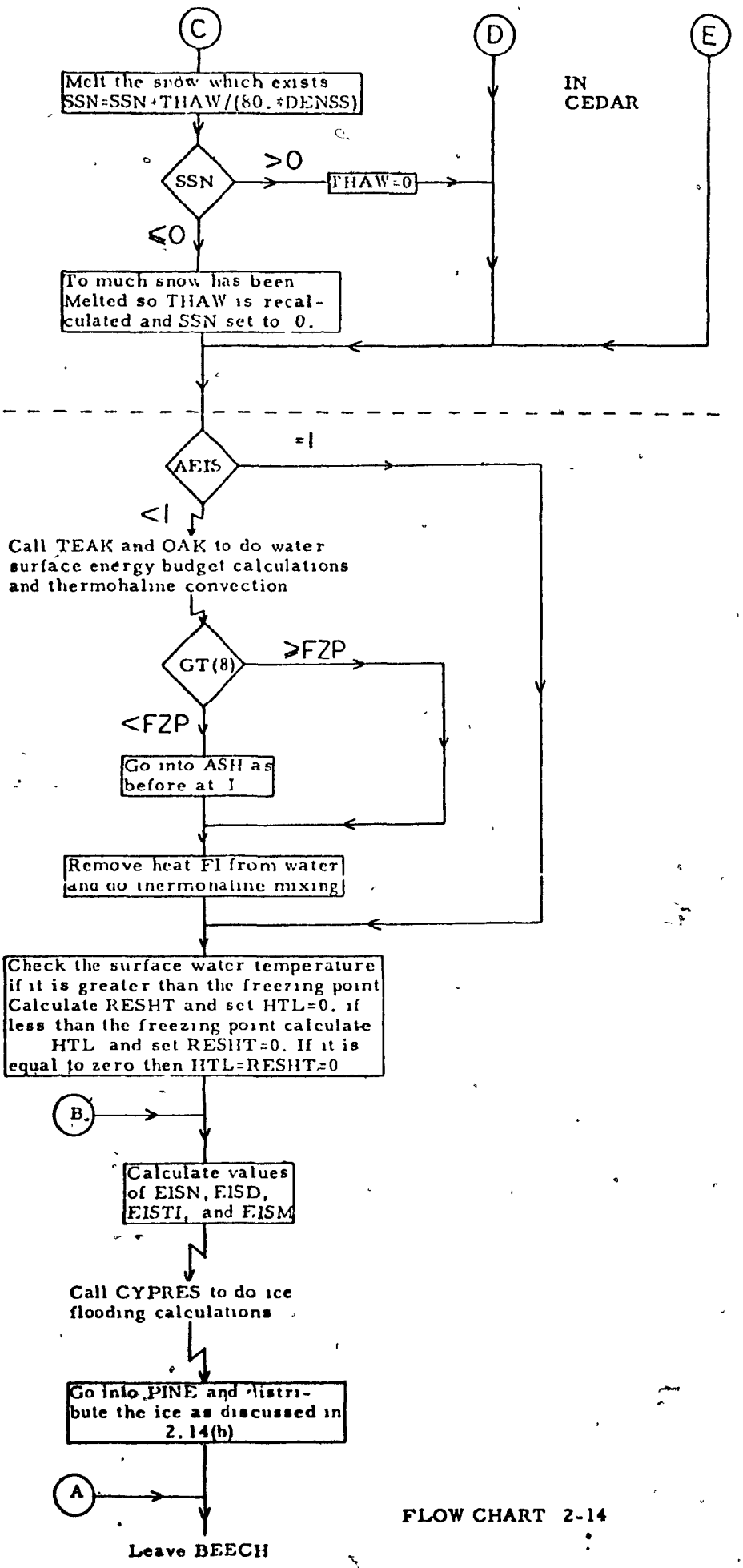

FLOW CHART 2-14

doing tests on a single grid point with no ice advection.

2.15 Ice Salinity and Brine Migration

(a) Ice forming from sea water retains only a portion of the salt contained in that water. The remaining salt is found in pockets of high salinity water, called brine cells. These migrate through the ice layer and some of them fall out at the bottom of the ice sheet. The amount of salt remaining in the ice is dependent upon the temperature at which the ice forms. Thus it can be seen that as ice will form at different temperatures it will contain different amounts of salt. The brine cells in the ice do not all drop out at the same time but do so over a period of time. The mechanics of this migration is well outlined in Pounder (Po65).

(b) As with other parameters which determine the structure of the ice, the inclusion of the salt results in many complexities. Greater than any other, from a practical point of view, is the computer space required to store the values of these many parameters. Thus brine migration and the inherent time lag have been neglected and the only consideration has been that the ice is given a salinity value. In this model all ice which is formed from sea water is given a salinity of $5^{o}/oo$. Only the average ice salinity is carried between time steps, so that ice that forms from melting snow tends to lower this salinity. Further, all the salt in the water other than this $5^{o}/oo$ is immediately dropped out into the top layer of water, where it tends to increase the salinity of the water. This then allows the water to undergo thermohaline convection while still leaving provision for an ice salinity of the correct magnitude.

2.16 Flooding of Ice and the Resultant Snow Ice

(a) When the weight of the snow cover lying on the ice becomes sufficient the ice surface becomes submerged. The resultant flooding causes the snow and sea water to mix and form a layer of snow ice above the existing ice layer.

(b) The simulation of this process is carried out in subroutine "CYPRES". To test for flooding, the snow is converted to ice of the same density as

that which exists, then the mass of this total layer which remains above water is calculated, (SRAW). The snow ice layer formed is then the difference between the thickness of snow in equivalent ice density (SSE), less SRAW.

$$\text{Thus, STIE} = \text{SSE} - \text{SRAW} \qquad 2.16(1)$$

Then SRAW is converted back into snow of the appropriate density.

2.17 The Horizontal Processes

(a) Possibly the most important horizontal process in an area such as the Gulf of St. Lawrence is the water movement due to the currents. These currents transport heat and salt and ice when it is present. There are several publications which deal with currents in the Gulf. They include a short discussion of the summer surface current pattern, as shown in Trites (Tr70). The winter geostrophic currents for portions of the Gulf has been calcualted by El Sabh and Johannessen (EJ71). Also, Forrester (Fo67) has done work on the currents of the St. Lawrence River estuary. The summer surface current pattern from Trites agrees fairly well with El Sabh's calculations in the River and estuary regions, as well as through the Gaspé passage. Also, the counterclockwise circulation near the western end of the Jacques Cartier passage appears in both current maps. However agreement is not good between them in the eastern portions of the Gulf, north of the Laurentian Channel, where the currents may be completely opposite in direction. The north portion of Cabot Strait also shows the two current patterns with completely opposite direction. Trite's summer current pattern cannot be compared to the winter geostrophic currents over the Magdelan Shallows or Northern shore of the Gulf, as the latter have not been calculated there. Variability of current speeds, where they correspond in direction, is not too large but on the order of 25%. The other areas are not really comparable. The currents shown by Trites have two advantages over those of El Sabh. First, they are formed using observations and, secondly, they represent a consistent current pattern over the entire Gulf area.

Subsurface current data are much more limited and are usually confined

to such areas as the Cabot Strait, Belle Isle Strait and the estuary. To the author's knowledge no detailed picture of the subsurface current pattern of the Gulf area exists. Further, there is no detailed knowledge of the depth to which the surface currents extend.

Thus, though a pattern of surface currents exists any use of these currents is constrained by the lack of information on their vertical profiles.

(b) The result of the above mentioned constraint is that the surface currents may be used insofar as no knowledge of their vertical nature is required. This then does not allow the transport of heat and salt by the currents as mass conservation is not readily achievable under the constraint.

One essential process which can be included is ice advection, as this requires only knowledge of the surface current pattern. Thus, ice advection has been included in the model. The current pattern used for this purpose is based on Trite's summer current pattern which is assumed constant over the entire year. This assumption is probably erroneous, but is the best available.

The effects of both wind and currents on the drift of ice are used to advect that ice in subroutine "WILLOW". The wind is used to drift the ice at 2% of the wind speed and in the direction of the isobars, after Zubov (Zu43). The ice also drifts with the current at its own speed. No provision is made for the deflection of the ice from geographical barriers due to the deflection of the wind. A further constraint is that the ice is not allowed to move more than 37 km in one day, though it may move less. This is a computational criterion as the grid length is 37 km.

In a grid square model of this type a distinct ice edge may not be represented as such. If an ice edge moves into an area to cover five tenths of the area, then the entire area is considered to have five tenths ice coverage for each unit area, no matter where it is located. This means that ice from grid square may advect into the next one, in the program, which would not happen in reality unless conditions specifically allowed it. This is to say that the program may suffer from spurious ice advection. To overcome this a criterion is introduced which does not allow ice to advect from a given grid square until that grid square contains at least two tenths

of ice area. One further comment is due; though the ice is allowed to pile up on windward shores, all ice has an average thickness over the entire square as does the snow cover over the ice.

2.18 Summary

The processes considered have now been outlined and discussed. The entire picture of how these fit into the model as a whole is to be seen in the FLOW CHART 2-18 which sketches out the order of the operations. The subroutines of Morin (Mo73) are placed at the head of this flow chart to derive all the meteorological parameters used in the subroutines shown in FLOW CHART 2-18. An appendix (A) has been included which contains a portion of Morin's work. For more detail and the appropriate subroutines, the reader is referred to Morin's work (Mo73). An appendix (B) has also been included, containing all the present author's subroutines for the calculation of the surface energy budget and the water processes that respond to it.

A SKETCH OF THE MODEL AS A WHOLE

FLOW CHART 2-18

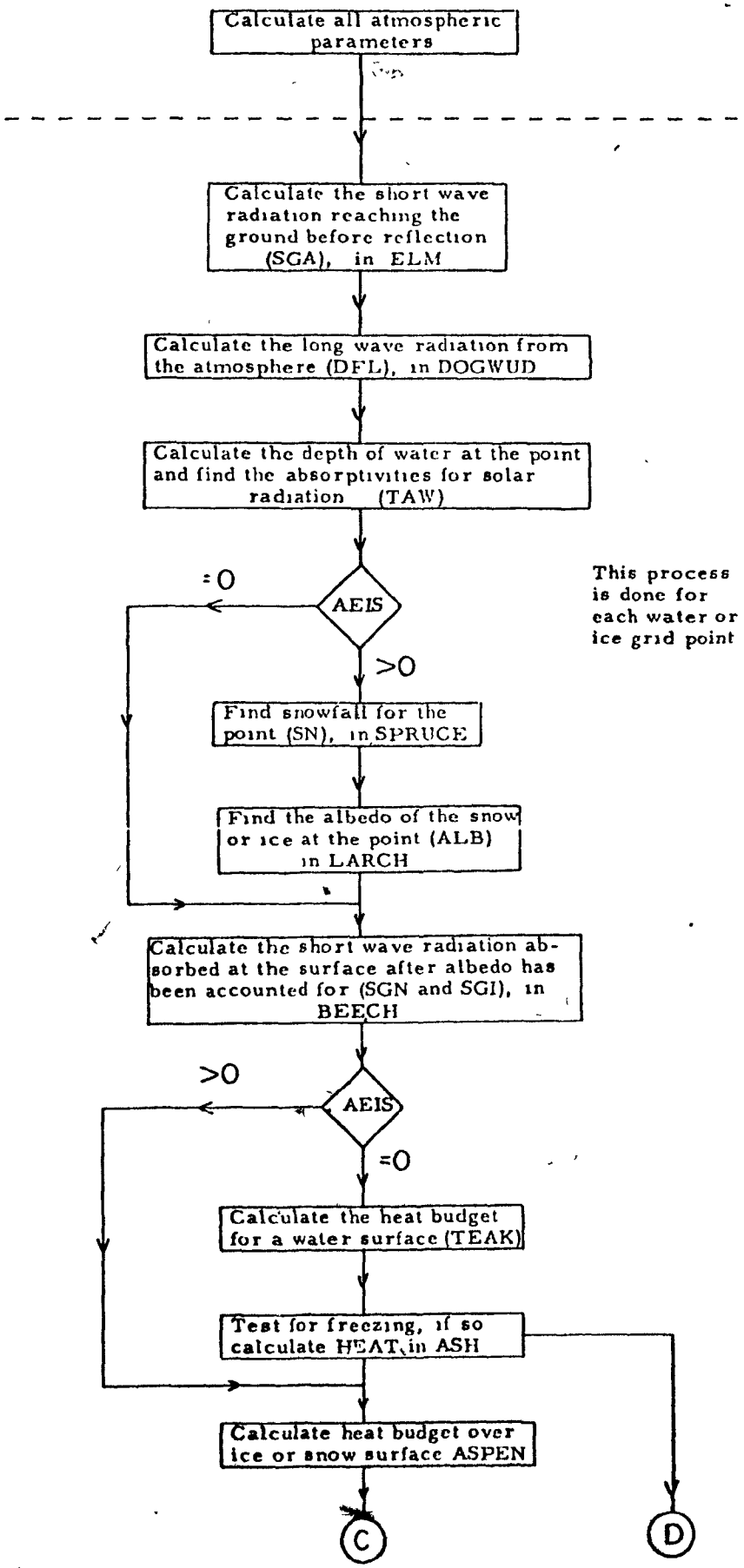

FLOW CHART 2-18 (cont.)

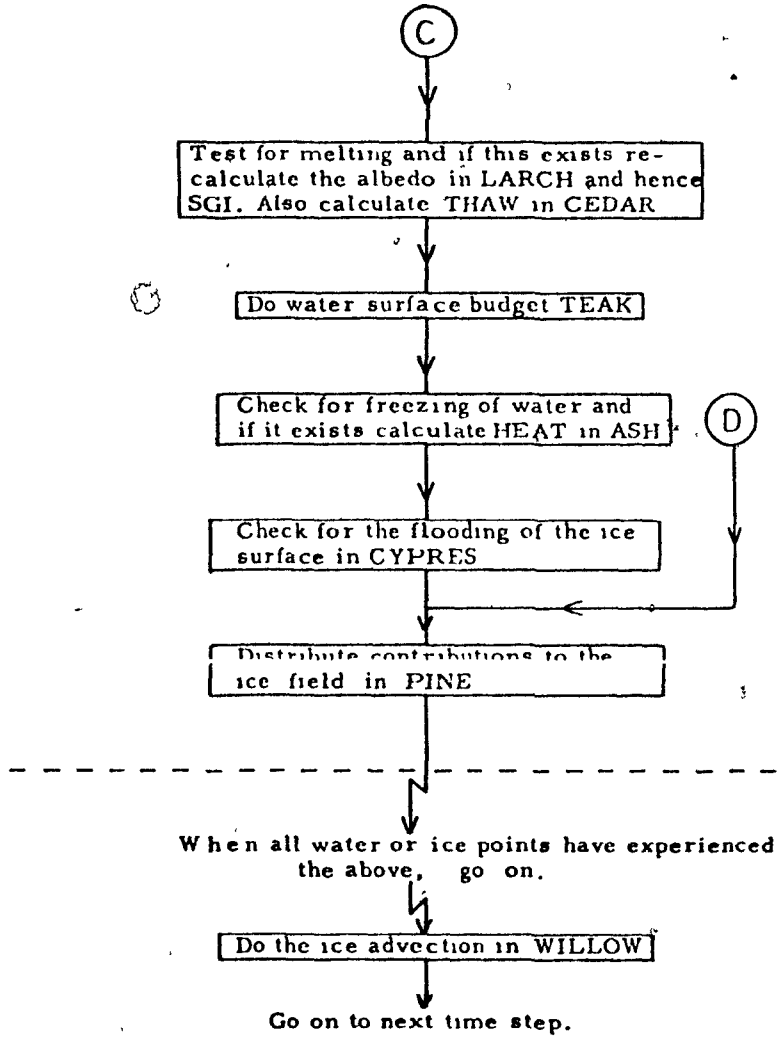

FLOW CHART 2-18 (cont.)

CHAPTER 3

THE INITIALIZATION AND RUNNING OF THE MODEL

3.1 Initialization of the Grid

The grid chosen consists of 550 points with dimensions 22(E-W) by 25(N-S), the orientation is as seen in Figure 3.1-1. It is overlaid on the Gulf of St. Lawrence area to include the maximum water area and tries to allow for the geographical location of the narrow straits and passages in the region. The grid points are identified by a matrix ITDM, shown in Figure 3.1-2, where the numbers on the grid represent

0 land points
1 water points with no ice
2 water points with ice
5 boundary points around the water
and 6 island points.

The dimension of each grid square is 37 km by 37 km for a total area of 17347 square kilometers. The values of all necessary meteorological parameters which come from Morin's model exist for 17 levels in the vertical for each of the 550 points.

3.2 Initialization of the Water Body

The water points are represented on a second grid which consists of 167 points. This has been done to save space in the computer and is simply a method of storing the data. There are eight possible water layers at each of these 167 points. The thickness of each of these layers is shown in table 3.2.1, where the maximum possible depth that a point may reach is 120 meters. This figure was chosen as the lowest level of seasonal change, based on Coombs (Co62) estimate of 100 m and Lauzier's (La57) estimate of 120-145 m. Not all points have depths as great as 120 m and therefore a matrix is specified to indicate the real number of layers a point requires to represent it's depth. Also, the real depth of all points is required for the short wave absorptivity criteria mentioned in section 2.11. These

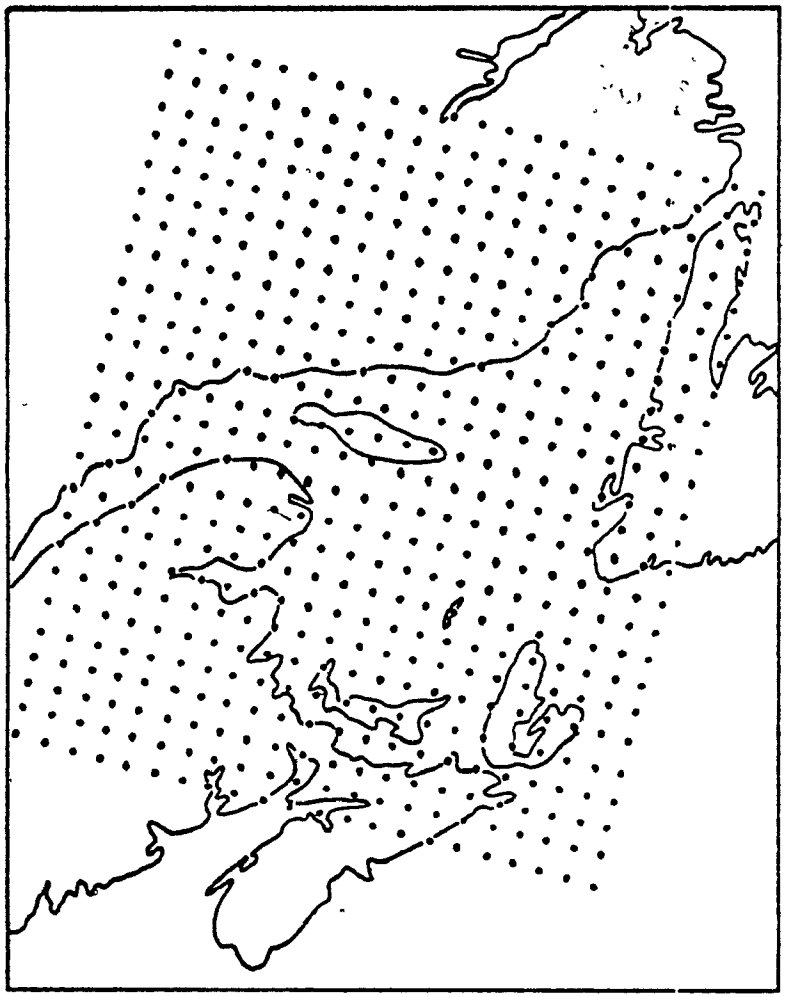

THE 550 POINT GRID AS IT IS FITTED OVER THE GULF OF ST. LAWRENCE

FIGURE 3·1-1

```
0 0 0 0 0 0 0 0 0 0 0 0 0 0 0 0 0 0 5 5 5 0   1
0 0 0 0 0 0 0 0 0 0 0 0 0 0 0 0 0 0 5 5 1 5 0   2
0 0 0 0 0 0 0 0 0 0 0 0 0 0 0 0 0 5 5 1 5 5 0   3
0 0 0 0 0 0 0 0 0 0 0 0 0 0 0 0 5 5 1 1 5 0 0   4
0 0 0 0 0 0 0 0 0 0 0 0 0 0 0 0 5 1 1 1 5 0 0   5
0 0 0 0 0 0 0 0 0 0 0 0 0 0 0 0 5 5 1 1 1 5 0 0 6
0 0 0 0 0 0 0 0 0 0 0 0 0 0 0 0 5 1 1 1 1 5 0 0 7
0 0 0 0 0 0 0 0 0 0 0 0 0 0 5 5 5 1 1 1 1 5 0 0 8
0 0 0 0 0 0 0 0 0 0 5 5 5 5 1 1 1 1 1 1 1 5 0 0 9
0 0 0 0 0 0 5 5 5 5 5 1 1 1 1 1 1 1 1 1 1 5 0 0 10
0 0 0 5 5 5 1 1 1 1 1 1 1 1 1 1 1 1 1 1 1 5 0 0 11
0 0 5 5 1 1 1 1 6 6 6 6 6 1 1 1 1 1 1 1 1 5 5 0 12
0 0 5 1 1 1 1 1 1 1 1 6 6 6 1 1 1 1 1 1 1 1 5 0 13
0 5 5 1 1 1 1 1 1 1 1 1 1 1 1 1 1 1 1 1 1 5 5 0 14
5 5 1 1 1 5 5 5 5 1 1 1 1 1 1 1 1 1 1 1 1 5 5 0 15
5 1 1 1 5 5 0 5 5 1 1 1 1 1 1 1 1 1 1 1 1 1 5 0 16
5 1 5 5 5 5 5 5 1 1 1 1 1 1 1 1 1 1 1 1 1 1 5 0 17
5 5 5 0 5 1 5 1 5 1 1 1 1 1 1 6 1 1 1 1 1 1 5 0 18
0 0 0 0 5 5 1 5 5 1 1 1 1 1 1 1 1 6 1 1 1 5 0 19
0 0 0 0 0 5 5 5 5 1 6 1 1 1 1 1 1 6 5 5 5 0 20
0 0 0 0 0 0 0 0 5 1 6 6 6 6 6 1 1 5 5 0 0 0 0 21
0 0 0 0 0 0 0 0 5 1 1 1 1 1 1 1 5 5 0 0 0 0 0 22
0 0 0 0 0 0 0 0 5 5 5 5 5 5 5 5 5 0 0 0 0 0 0 23
0 0 0 0 0 0 0 0 0 0 0 0 0 0 0 0 0 0 0 0 0 0 0 24
0 0 0 0 0 0 0 0 0 0 0 0 0 0 0 0 0 0 0 0 0 0 0 25

1 2 3 4 5 6 7 8 9 10  12  14  16  18  20  22

X-DIRECTION

Y - DIRECTION
```

THE IDENTIFICATION MATRIX "ITDM"

FIGURE 3·1-2

Layer Number	Depth of the top surface of the layer in cm	Depth of the bottom surface of the layer in cm	Thickness of the layer in cm
8	0 (surface)	250	250
7	250	500	250
6	500	1000	500
5	1000	2000	1000
4	2000	3000	1000
3	3000	5000	2000
2	5000	8000	3000
1	8000	12000	4000

Layer Numbers, Depths and Thicknesses

TABLE 3.2.1

two requirements are combined in the matrix LDMX with dimensions 22 by 25. In this matrix a zero represents a non-water point while a four figure group, when it exists is interpreted as layer number and depth. The figures chosen as real depths of the grid point are areal averages and thus may not represent either the shallow or deep portion of any given grid point near the shore. The values of LDMX are shown in Figure 3.2-1. The second step in initializing the water body is the specification of the values of temperature and salinity for each level at each point on the grid. This was accomplished using the data from the cruise of CNAV "Sackville" where measurements were taken throughout the Gulf area from November to 18th to 28th of 1971. The positions at which measurements were taken are shown in the map of Figure 3.2-2. The values of temperature and salinity for the mid-points of each layer were extracted from the salinity-temperature-depth profiles (STD's) and plotted on maps of the Gulf area. Isolines of temperature and salinity were drawn and grid point values extracted by overlaying a grid.

Finally, the currents used in ice advection were resolved and assigned as components of velocity at each grid point. The currents of Trites (Tr70) were used, augmented by the values of current speed used by the Ice Forecasting Central in those cases when the former were deficient. The resultant x and y components (ICDX and ICSY) are shown in Figures 3.2-3 and 3.2-4. The components are for the grid and do correspond to the north-south geographical directions. These currents were held constant for the duration of the experiment.

3.3 Initialization for the Atmospheric Model

Morin's (Mo73) subroutines use synoptic surface and radiosonde data for 0000Z and 1200Z. The data used were from the stations listed in Table 3.3.1. All these stations need not report for Morin's programs to function. The map of Figure 3.3-1 shows the distribution of these stations around the Gulf of St. Lawrence. For further information on the initialization of Morin's atmospheric model, his paper should be consulted.

3.4 Running of the Model

The complete model proved to be extremely large in terms of computer

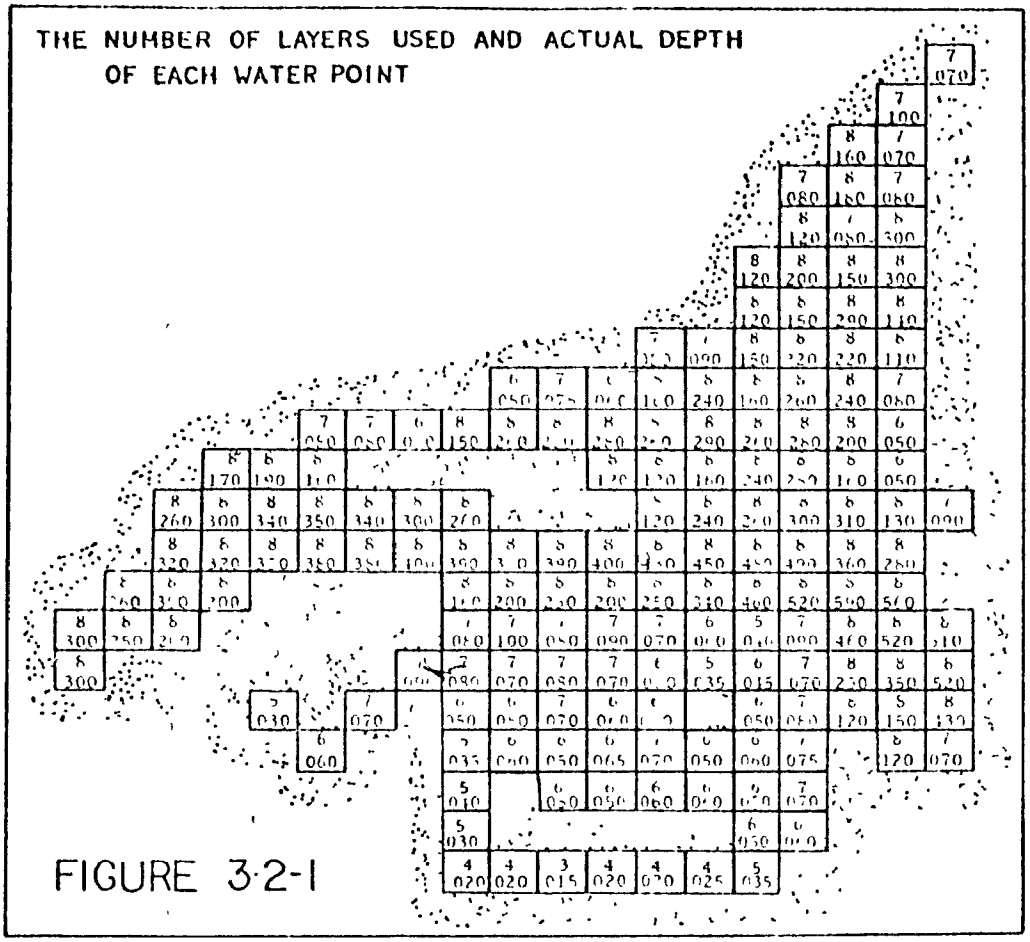

FIGURE 3·2-1

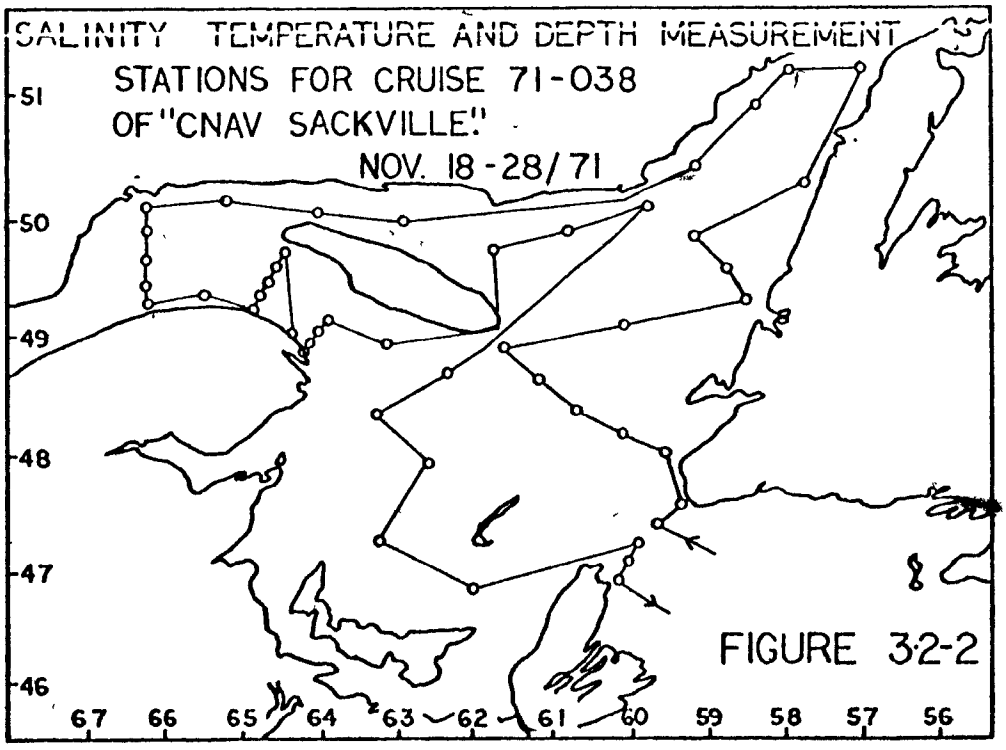

FIGURE 3·2-2

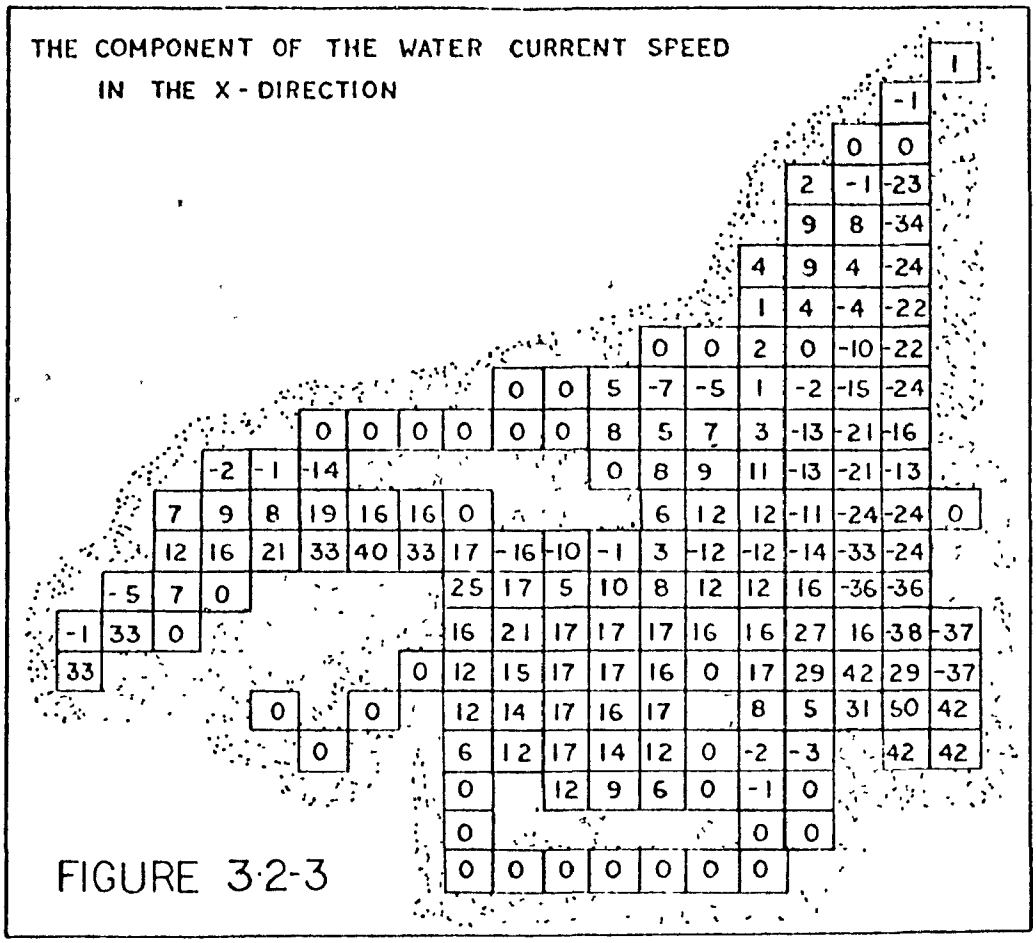

FIGURE 3·2-3

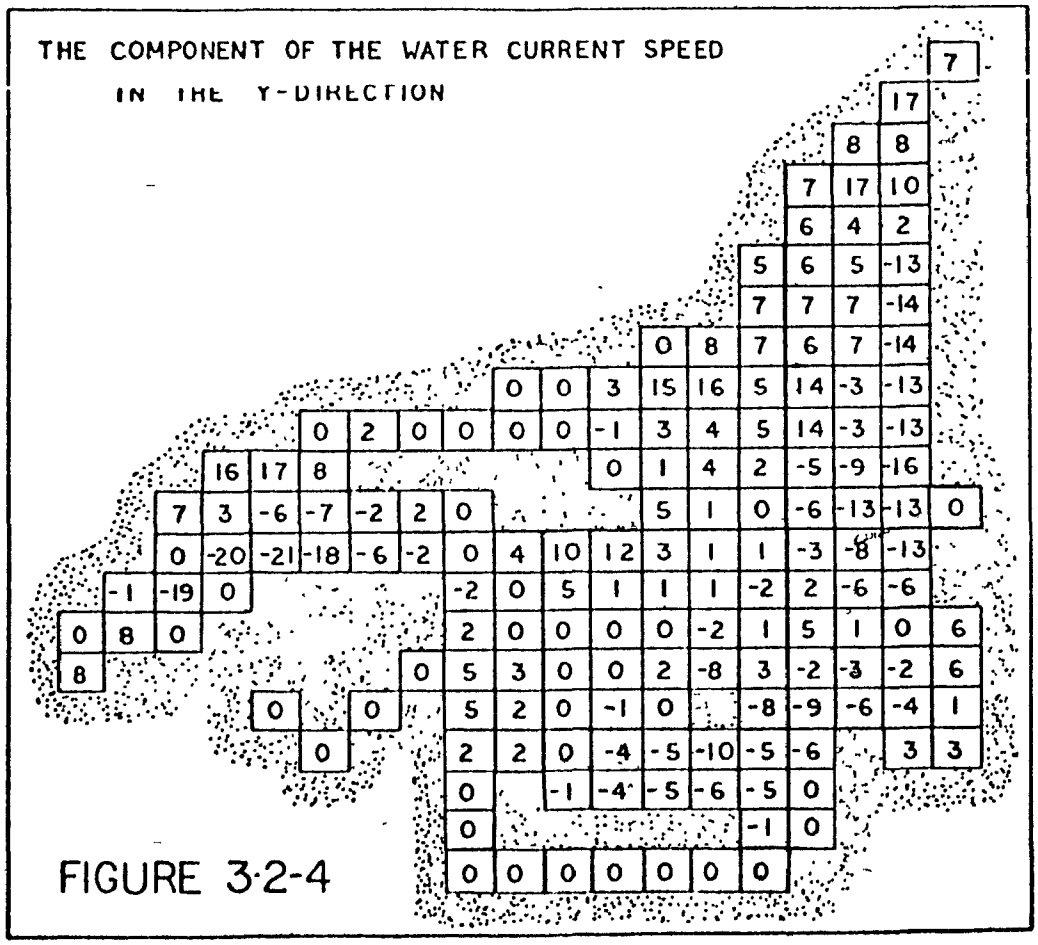

FIGURE 3·2-4

NAME OF STATION	LETTER IDENTIFIER	STATION TYPE
Churchill Falls, Labrador	UM	Surface Synoptic
Goose Bay, Labrador	YR	Radiosonde
Blanc Sablon, Québec	BX	Surface Synoptic
St. Anthony, Newfoundland	AY	Surface Synoptic
Wabush Lake, Labrador	WK	Surface Synoptic
Lake Eon, Québec	EO	Surface Synoptic
Harrington Harbour, Québec	HR	Surface Synoptic
Daniel's Harbour, Newfoundland	DH	Surface Synoptic
Deer Lake, Newfoundland	DF	Surface Synoptic
Natashquan, Québec	NA	Surface Synoptic
Sept Isles, Québec	ZV	Radiosonde
Port Menier, Québec	PN	Surface Synoptic
Stephenville, Newfoundland	JT	Radiosonde
Burgeo, Newfoundland	BD	Surface Synoptic
Port aux Basques, Newfoundland	ZB	Surface Synoptic
Fox River, Québec	FQ	Surface Synoptic
Baie Comeau, Québec	BC	Surface Synoptic
Mont Joli, Québec	YY	Surface Synoptic
Charlo, New Brunswick	CL	Surface Synoptic
Miscoe Island, New Brunswick	MC	Surface Synoptic
Grindstone, Magdelan Islands	GR	Surface Synoptic
Sydney, Nova Scotia	QY	Surface Synoptic
Charlottetown, Prince Edward Is.	YG	Surface Synoptic
Summerside, Prince Edward Is.	SU	Surface Synoptic
Chatham, New Brunswick	CH	Surface Synoptic
Caribou, Maine, U.S. of A.	CAR	Radiosonde
Fredricton, New Brunswick	FC	Surface Synoptic
Moncton, New Brunswick	QM	Surface Synoptic
Truro, Nova Scotia	TQ	Surface Synoptic
Copper Lake, Nova Scotia	VW	Surface Synoptic
Canso, Nova Scotia	OQ	Surface Synoptic
Sable Island	SA	Radiosonde

Meteorological Observing Stations used in Morin's Air Mass Transformation Model

TABLE 3.3.1

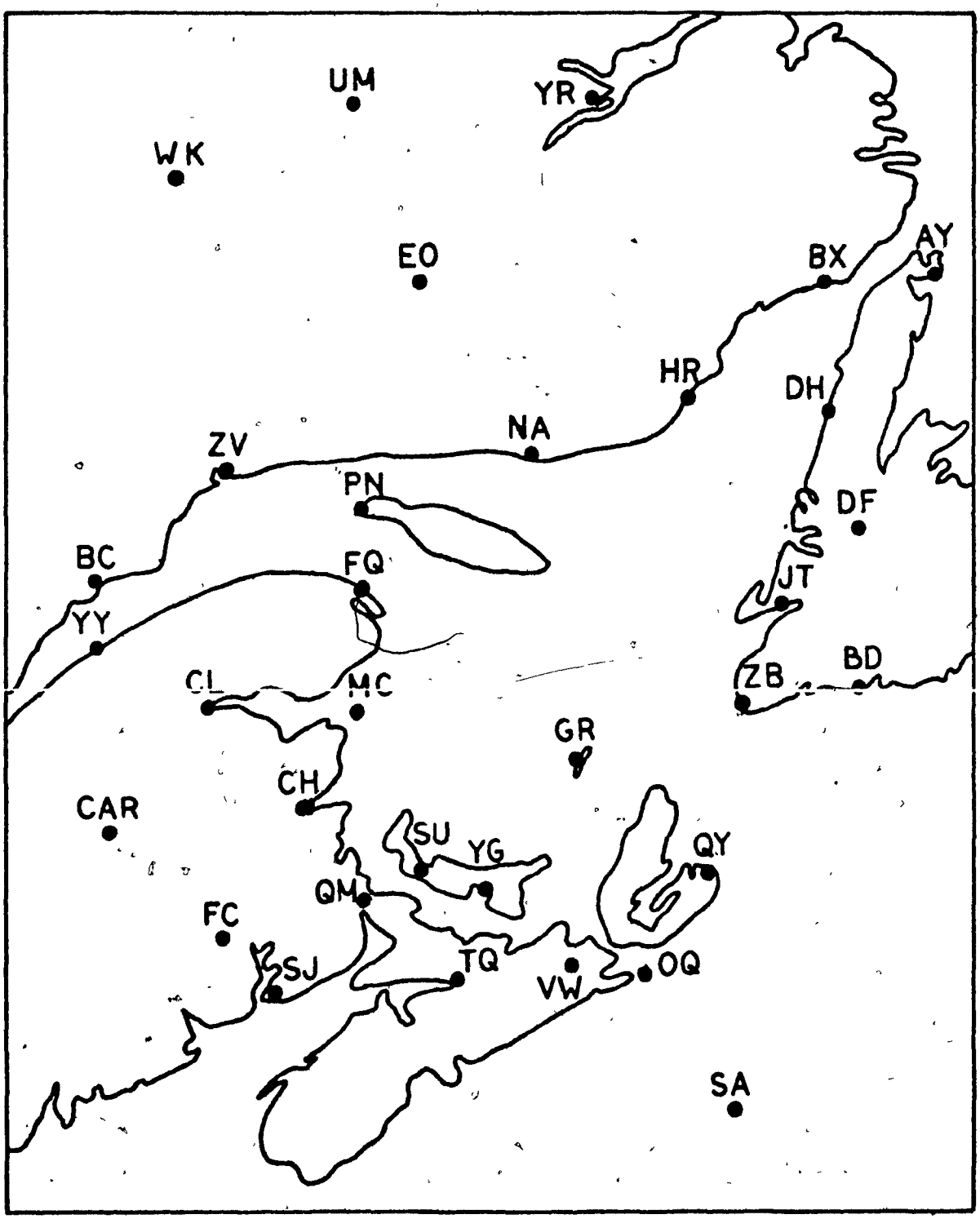

SOME OF THE METEOROLOGICAL OBSERVING STATIONS USED FOR ATMOSPHERIC DATA

FIGURE 3·3-1

core space required, namely 400K bytes. The running times also proved to be quite long, namely on the order of 30 minutes for each week of data processed. This precluded any long-period run of this model. Thus it was only possible to do calculations for the period November 18, 1971 to February 02, 1972. It is unfortunate that the spring period of melting ice could not be observed. The brief running period did, however, show some very interesting results.

3.5 Constant Values Used for the Water and Ice

Constants used in the model may be found in Table 3.5.1 along with their values.

One further point must be made about the design of the model. There are no external sources of ice, though a sink of ice was allowed by permitting ice export through Cabot Strait. The lack of ice sources will probably cause difficulties in the St. Lawrence River and esturary where it is well known that ice drifts down the river to cover large areas of the region below a Baie Comeau -Mont Joli line.

SYMBOL	DESCRIPTION	VALUE	UNITS
TIMUTS	Time units of one time step	42, 300	Seconds
TIMFAC	For Conversion from integer	1.	Pure Number
CISF	Ratio of ice drift speed to the current speed	1.	Pure Number
WISF	Ratio of ice drift speed to the wind speed	.02	Pure Number
CONE	Thermal conductivity of ice	19.8	Cal $cm^{-1}K^{-1}hr^{-1}$
CONS	Thermal conductivity of snow	1.8	Cal $cm^{-1}K^{-1}hr^{-1}$
DENSS	Density of all snow made by the model	.2	Gm cm^{-3}
DENE	Density of all ice result-from sea water	.918	Gm cm^{-3}
SLAT	Latent Heat for melting snow	80	Cal gm^{-1}
ELAT	Latent Heat for melting ice	80	Cal gm^{-1}
CRITH	Critical thickness for all ice formed by freezing over open water	4	Cm
EISSAL	Salinity of all ice made from sea water	5	$^{o}/_{oo}$
TOPL	Thickness of the top layer of water	250	Cm
WATALB	The albedo for the water	.095	Pure Number
SUE	Time Step for all budget Calculations	12	Hours

Constants used in the model

TABLE 3.5.1

CHAPTER 4

ANALYSIS AND RESULTS

4.1 The present chapter contains the results of the one computer run which was made using the water body model described in Chapter 2. The water body was forced by the surface energy budget which in turn used Morin's atmospheric model for many of it's calculations. At all points throughout this discussion attempts will be made to explain any discrepencies which occur when computer fields are compared to real fields. The real fields in this chapter consist of the ice maps as analyzed by the Ice Forecasting Central in Ottawa. These real fields, as shown with geographical names in Figure 4.1-1 , are compared to fields produced by the computer. To ensure no subjective input into the results of the model, no attempt has been made to interpret the computer results in terms of real geography. To alleviate confusion, a map showing how the geographical features of the Gulf of St. Lawrence appear on a computer produced map, are shown in Figure 4.1-2. Where some points are referenced by number the reader should refer to Figure 4.1-3 for their respective locations.

4.2 The Areal Extent of the Ice Cover

In this section the ice maps of the model are compared to the real charts considering only the occurance or non-occurance of ice at given grid points. The actual area of ice at any single grid point will be considered in section 4.3.

The first ice map showing real ice coverage is for December 23, 1971. This map shows ice in the western tip of the Bay of Chaleur and in the Northumberland Strait, as well as patches of new ice along the Northern Shore of the Gulf. Also, there is ice covering most of the St. Lawrence river above the Baie Comeau - Mont Joli line, which is just off the model's grid area. The model produces ice for the first time in the Northumberland Strait and western tip of the Bay of Chaleur, agreeing completely with the actual map of this date. The model does not, however, show any ice being formed along the Northern shore of the Gulf. The next day for which a real

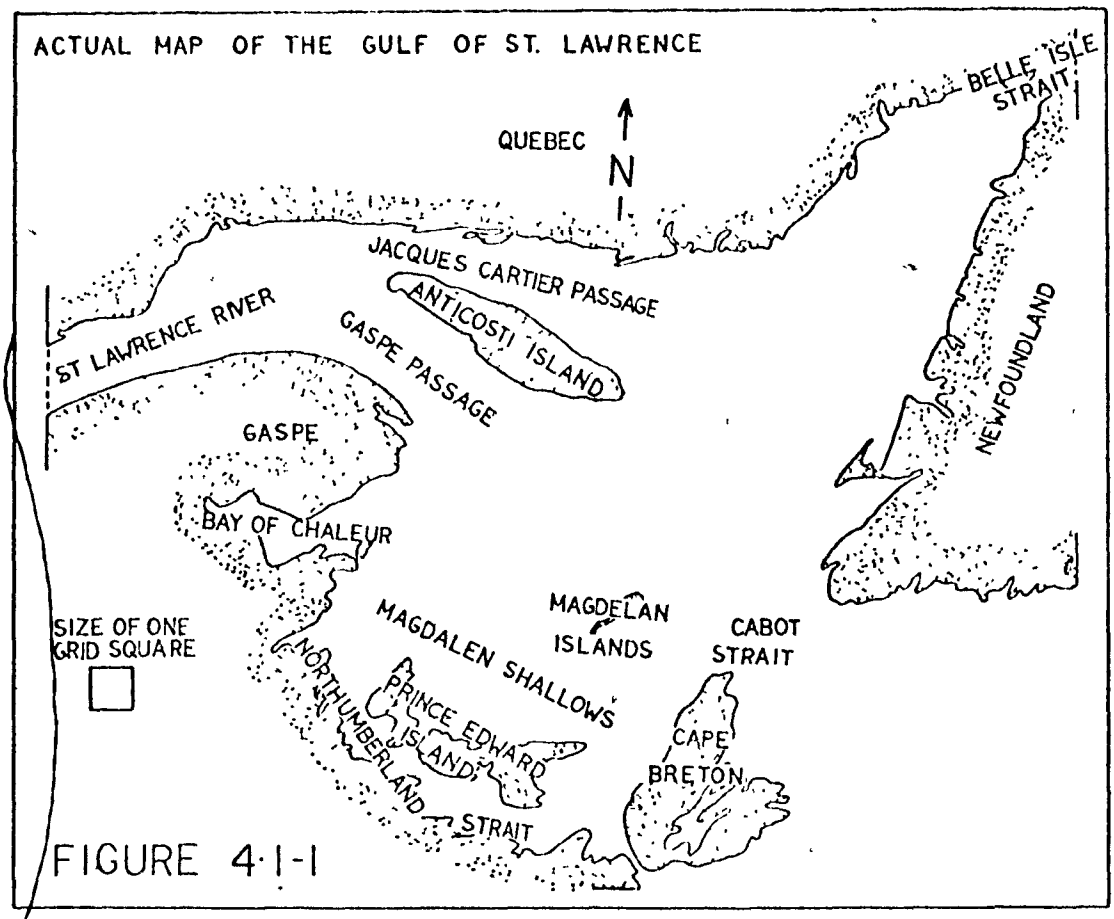

FIGURE 4·1-1

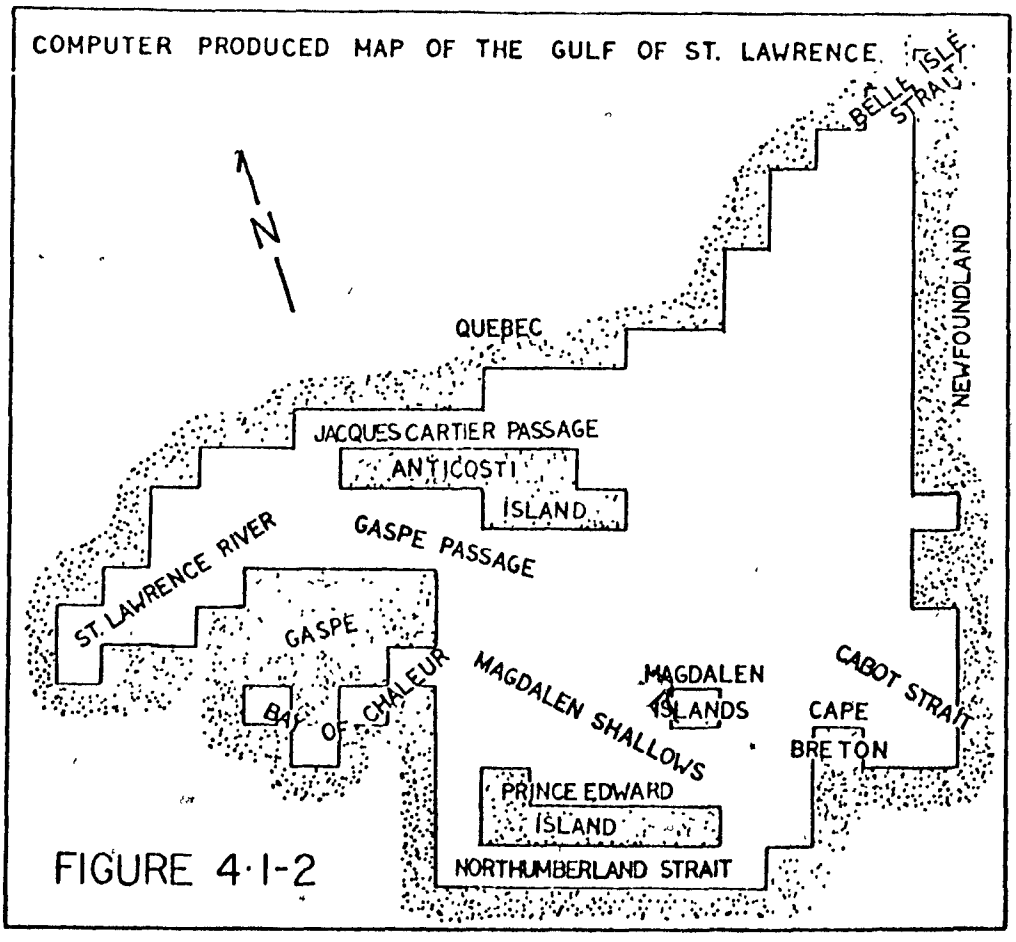

FIGURE 4·1-2

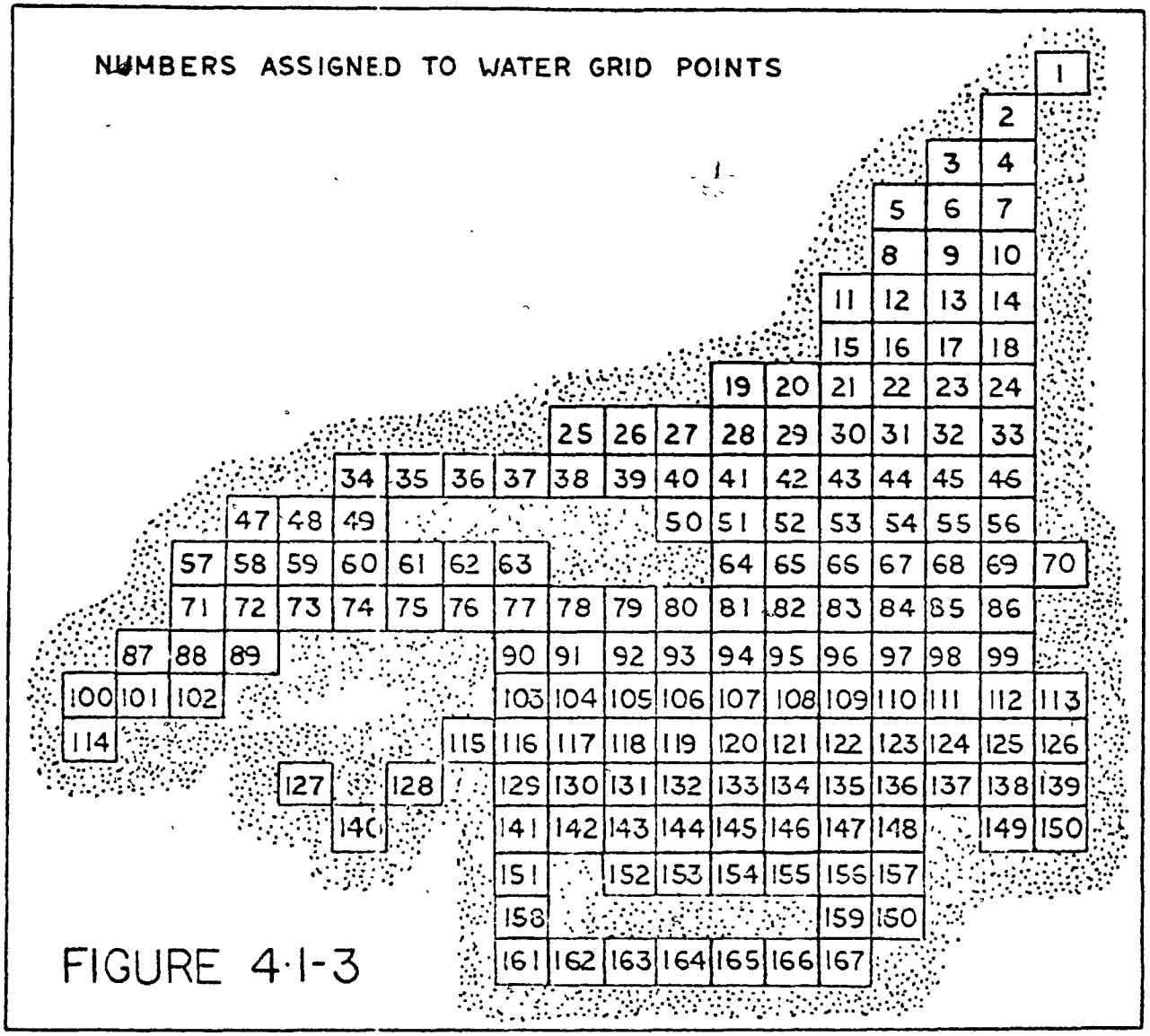
NUMBERS ASSIGNED TO WATER GRID POINTS
1
2
3 4
5 6 7
8 9 10
11 12 13 14
15 16 17 18
19 20 21 22 23 24
25 26 27 28 29 30 31 32 33
34 35 36 37 38 39 40 41 42 43 44 45 46
47 48 49 50 51 52 53 54 55 56
57 58 59 60 61 62 63 64 65 66 67 68 69 70
71 72 73 74 75 76 77 78 79 80 81 82 83 84 85 86
87 88 89 90 91 92 93 94 95 96 97 98 99
100 101 102 103 104 105 106 107 108 109 110 111 112 113
114 115 116 117 118 119 120 121 122 123 124 125 126
127 128 129 130 131 132 133 134 135 136 137 138 139
140 141 142 143 144 145 146 147 148 149 150
151 152 153 154 155 156 157
158 159 160
161 162 163 164 165 166 167

FIGURE 4·1-3

ice map exists in December 31, 1971, as shown in Figure 4.2-1(a), which is compared to the ice produced by the model as shown by Figure 4.2-1(b). In these two maps the ice area seems to be faithfully represented by the model at the western end of the Bay of Chaleur, the Northumberland Strait and over most of the Magdelan Shallows. There is some discrepancy in the Magdelan Shallows area, which is attributable to the size of the grid squares used in the model, making the open area northwest of Prince Edward Island impossible to resolve. More major discrepancies exist elsewhere, however.

One of the most obvious discrepencies is in the area of the St. Lawrence River and its esturary. The condition imposed upon the model (Chapter 3), that no external source of ice should exist, is the probable cause of this problem. The fact is that ice existed up river from Baie Comeau prior to the 23rd of December, and it seems probable that some of this ice would drift downriver with the water currents. To ascertain if this reasoning is plausible, calculations may be made on the winds and currents during the period Dec. 23 to 31, 1971. This was done, assuming that the currents used in the model itself were representative of the real currents in the area. The result was that the ice would drift a total of 240 kilometers during this 8 day period. If this had been done in the model, the ice cover produced by it would have agreed very well with the real ice cover. This would seem to indicate that the St. Lawrence River itself is a fairly large source of ice during the early weeks of the ice season.

The second most obvious area of discrepancy is along the Northern Shore of the Gulf. As shown in the real ice map this ice appears to form in a very narrow band quite close to the shore and then broaden out as some of it drifts southward. In actual fact the ice here probably forms in shallow water. This shallow water ice formation does occur in the model to a certain extent. In Figure 4.1-3 it may be noted that points 25 and 27 (60 meters) do produce ice at the appropriate time, but other points to the east do not as their depths are too great. The reason their depths are exaggerated is that the grid point area must represent a topographical region which is both very shallow and very deep due to the steepness of the bottom in this location

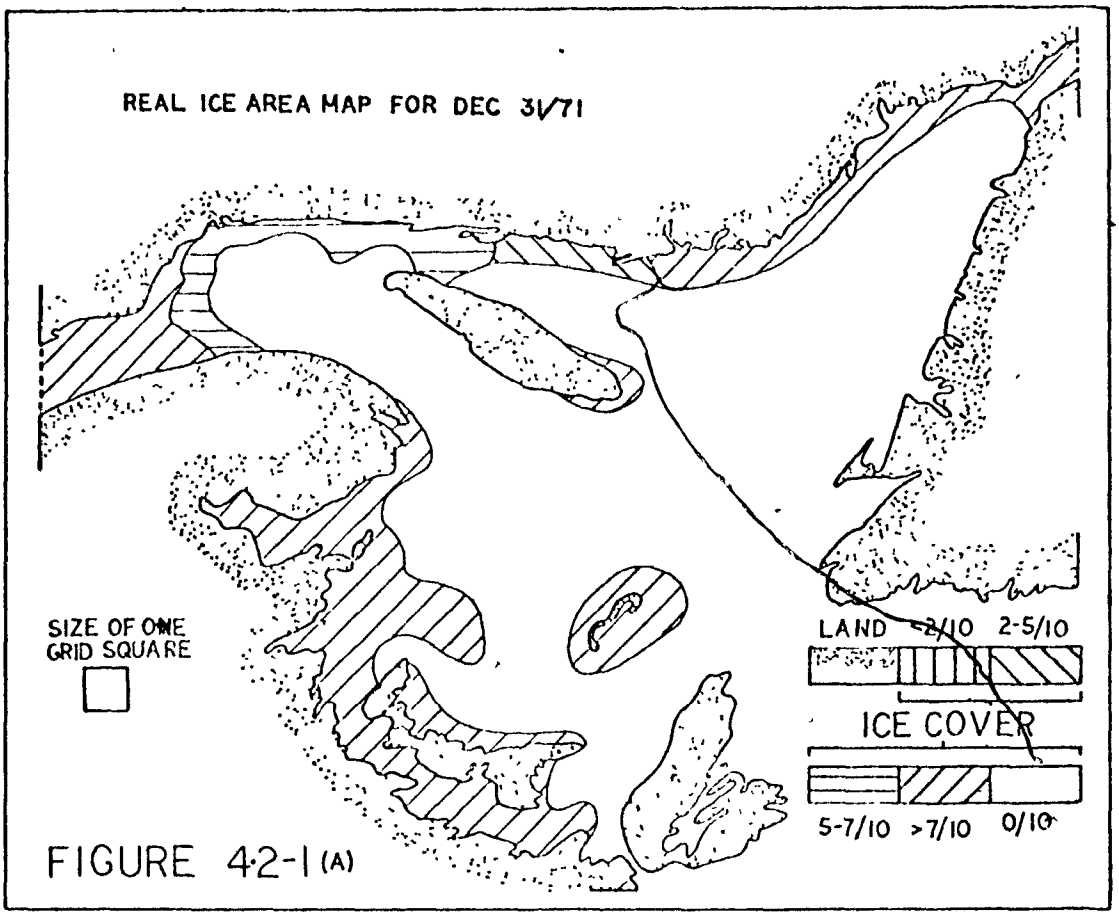

FIGURE 4·2-1 (A)

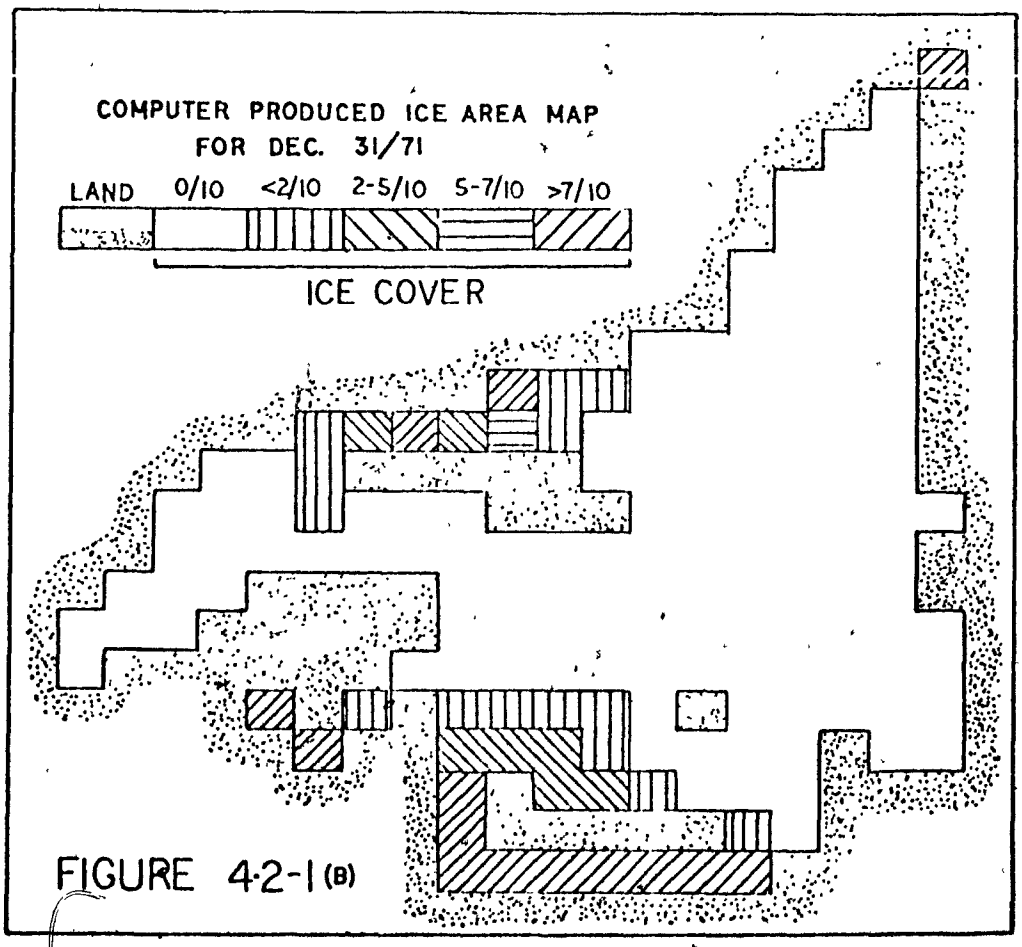

FIGURE 4·2-1 (B)

The compromise of an average depth therefore creates the discrepency. There are two alternative solutions to this problem. The first is to use a finer grid, which could cause computer memory storage problems. The second is subjectively to make the depth of the point shallow to allow the ice edge to assume its correct position. This second alternative could have unforeseen consequences, though one definite consequence is an overestimate of the ice volume produced at that point.

This same depth problem occurs in other areas as well. It occurs on the eastern tip of Anticosti and to a certain extent at the eastern tip of The Gaspé peninsula to the north of the mouth of the Bay of Chaleur. This latter area probably suffers from other problems as well, especially right in the mouth of the Bay of Chaleur. The depth of the water at the grid point in the mouth of the Bay of Chaleur is quite representative of the real depth in this area. Another reason must therefore be sought for the discrepency in this area.

Examining the grid system in the area of the Bay of Chaleur it may be noted that the slight "V" shape which actually exists here is overemphasized on the grid. In reality any westerly flow which does not have too large a northerly component will push ice eastward out of the Bay. This is not the case in the model, where any northerly component whatsoever will stop any ice advection to the east. The winds at Miscoe Island for this period show a strong westerly component, but significantly a small, northerly component as well. Thus the model does not move ice eastward where in reality it should. This then leaves an ice free area in the model where none really exists.

Finally, the last area of discrepency for the period Dec 23 to Dec 31st is seen over the Magdelan Islands where there is a large area covered by ice in reality but not in the model. The simple reason for this is that the grid near the Magdelan Islands was made a non-water point. If it had been made a water point, it would have proved to be much more shallow than the points around it which could easily have caused it to freeze on time.

The next pair of ice maps are for January 6, 1972, (Figures 4.2-2(a), (b)). This pair of maps shows similar discrepencies to the maps of Dec 31, 1971, except now ice is beginning to form near the Baie Comeau - Mont Joli

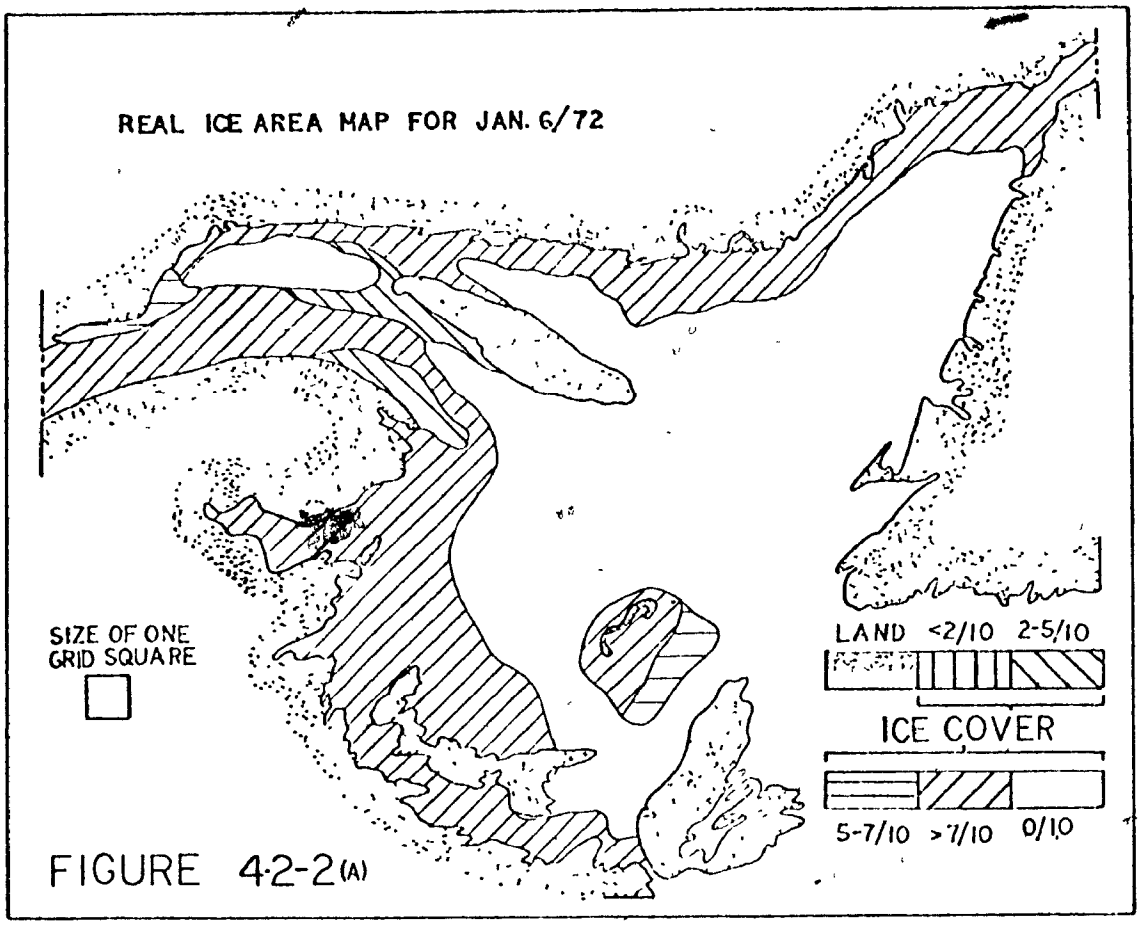

FIGURE 4·2-2(A)

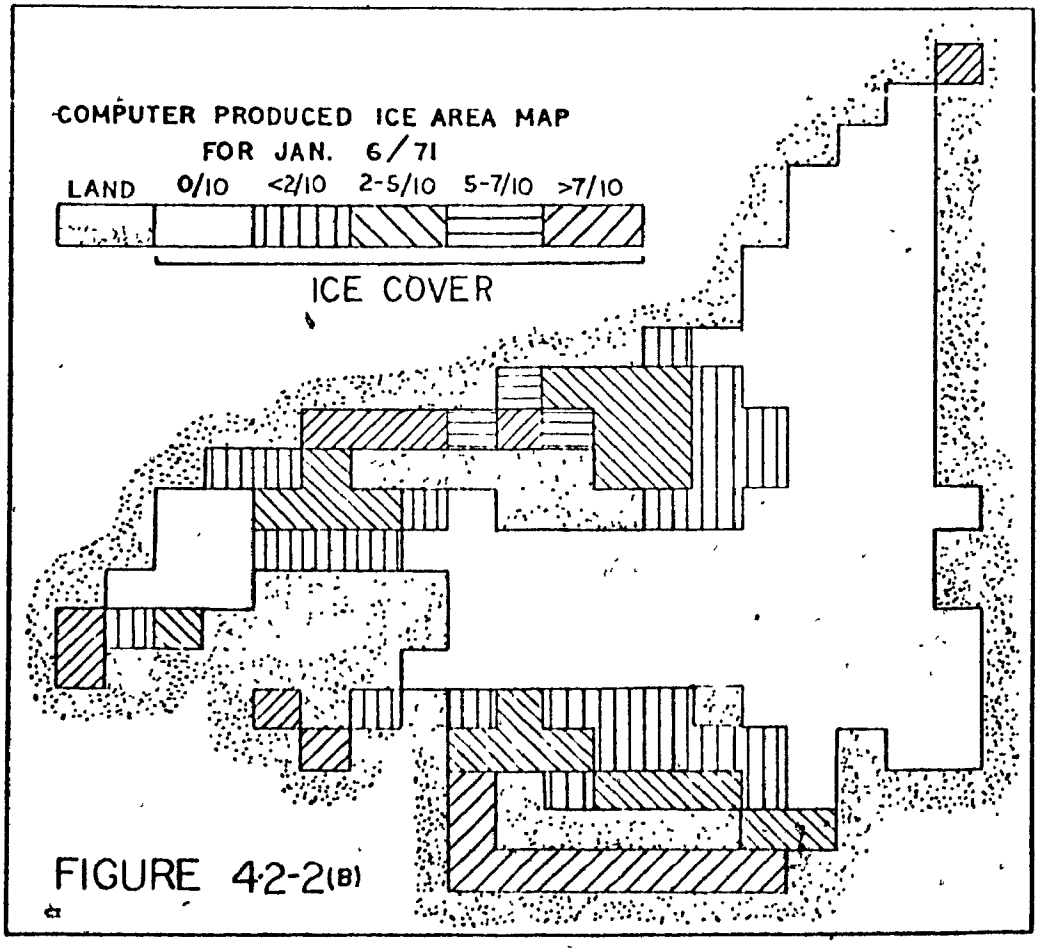

FIGURE 4·2-2(B)

region of the river. This would seem to indicate that even if ice did not advect down the river, this area would become ice covered by forming its own ice. Thus lack of downriver advection simply delays the time of ice coverage. Note also the over extensive ice coverage in the Magdelan Shallows. Much of this ice covers less than two tenths of the grid square area, thus is most probably just an extension of the ice cover nearby. As mentioned in section 2.17, these ice edge extensions are not easily shown with the grid resolution shown here.

Just as before the Gaspé - Bay of Chaleur area is void of ice on the computed map, but now a new reason comes in to play. Ice which has already been advected downriver by Dec 31, 1971 on the actual maps would be carried still further eastward, filling the Gaspé passage. In the model this ice never existed and thus there is not enough ice in the Gaspé Passage to overcome the "two-tenths criterion" and advect southward into this area, as it should do. This fact illustrates the cascade effect of errors in the earlier fields interfering with correct results in later fields.

The maps for January 10, 1972 appear in Figures 4.2-3(a), (b) and are to be used in conjunction with those of January 14, 1972, Figures 4.2-4 (a), (b). These two charts illustrate the inherent weakness of the simple "two-tenths" criterion. Prior to January 10 there is a predominantly northerly flow of air which causes the ice which exists along the Northern Shore of the Gulf to drift southward. This is quite adequately shown by the map for the 10th, made by the computer program. During the period Jan 10 to Jan 14 however this air flow changes to become predominantly southerly. In the real map for Jan 14 the ice edge is seen to retreat northward quite a substantial distance. This is not the case in the ice field made by the model. Much of the most southerly ice in this area is less than two tenths in grid square area and so, of course, cannot move. This same phenomenon may occur at the southern ice edge of the Magdelan Shallows, where a southerly wind extends the ice field northward, but a return to northerly flow does not reduce the areal extent. In the case of the ice on the north shore, an examination of the individual grid square areas does show northward ice advection. Points 40, 41 and 43 show decreases in area while 19, 20, 22,

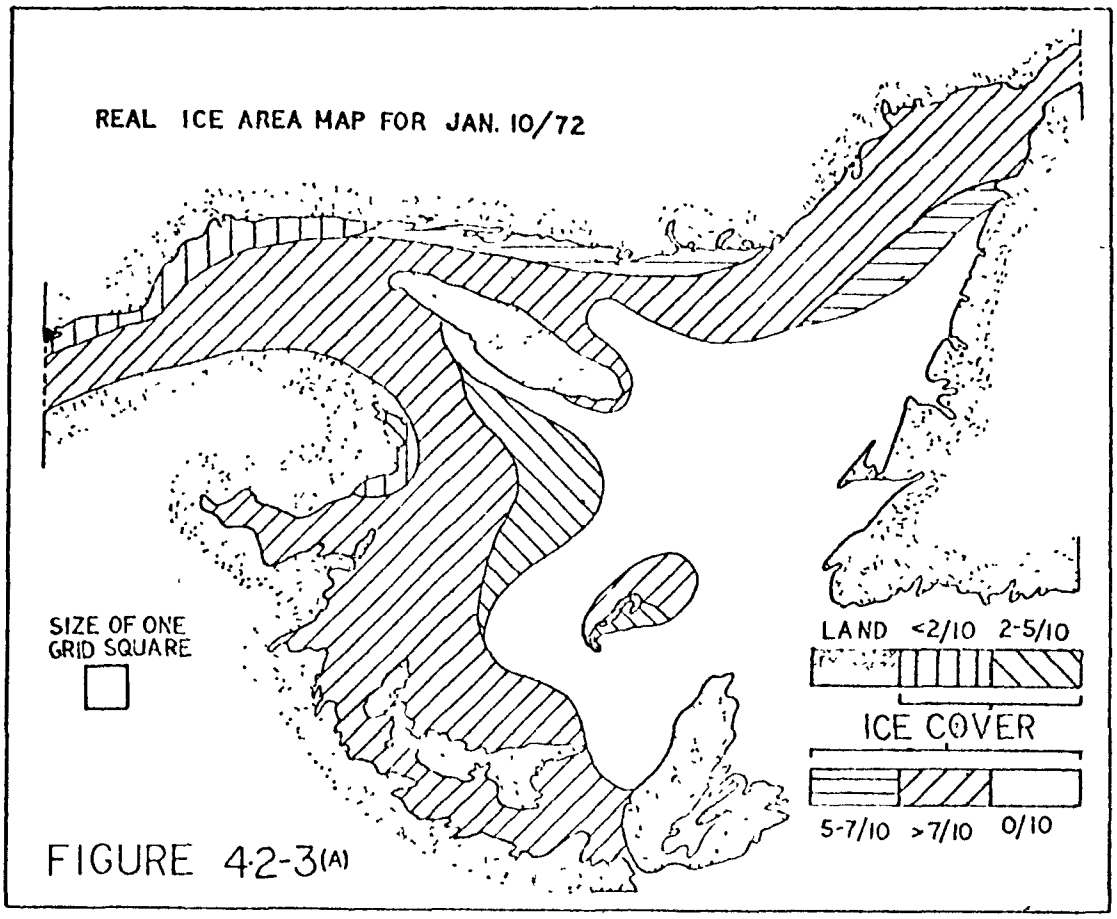

FIGURE 4-2-3(A)

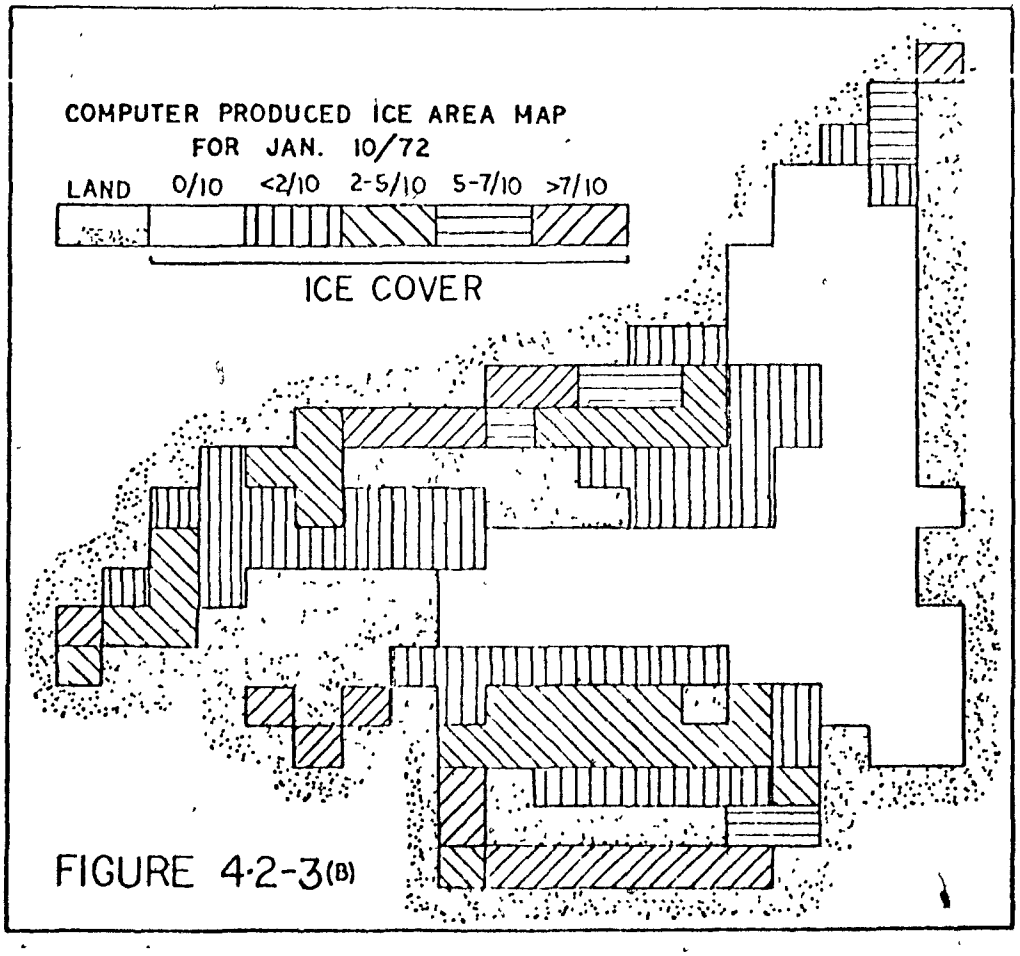

FIGURE 4-2-3(B)

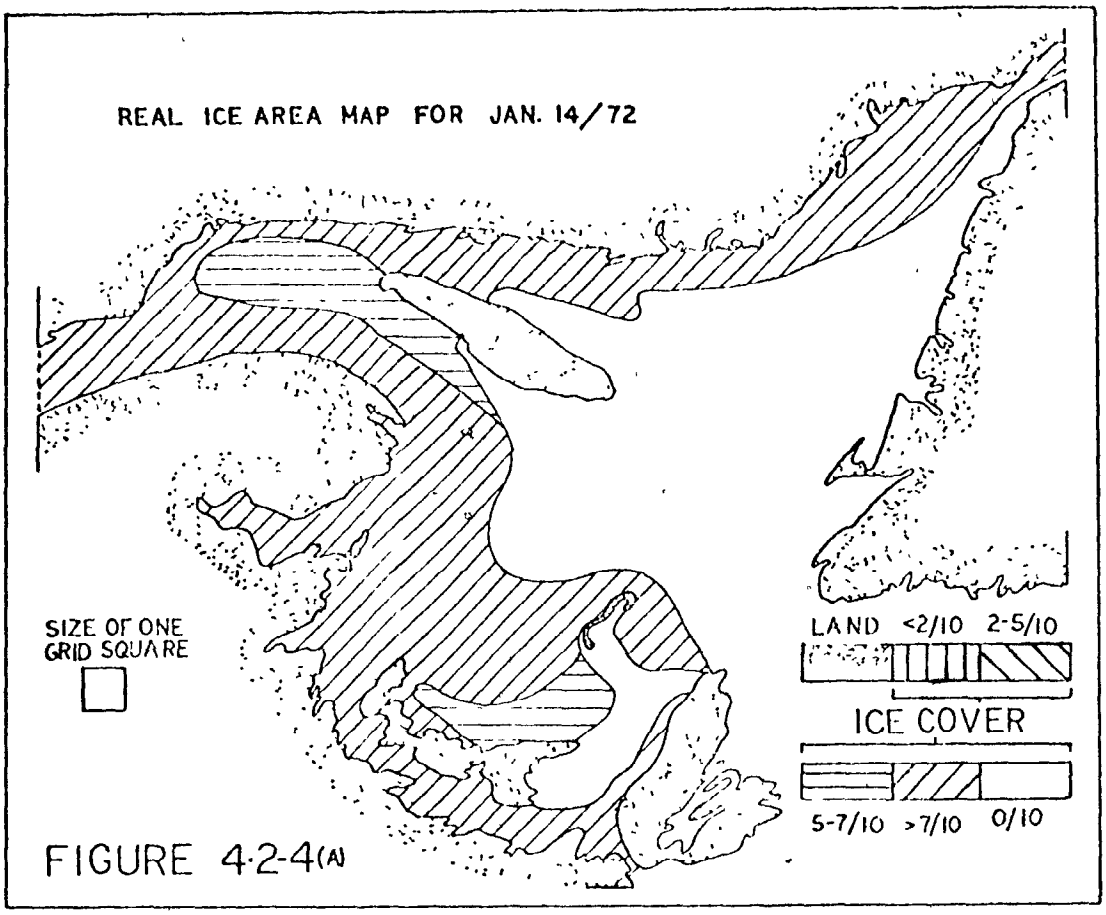

FIGURE 4·2-4(A)

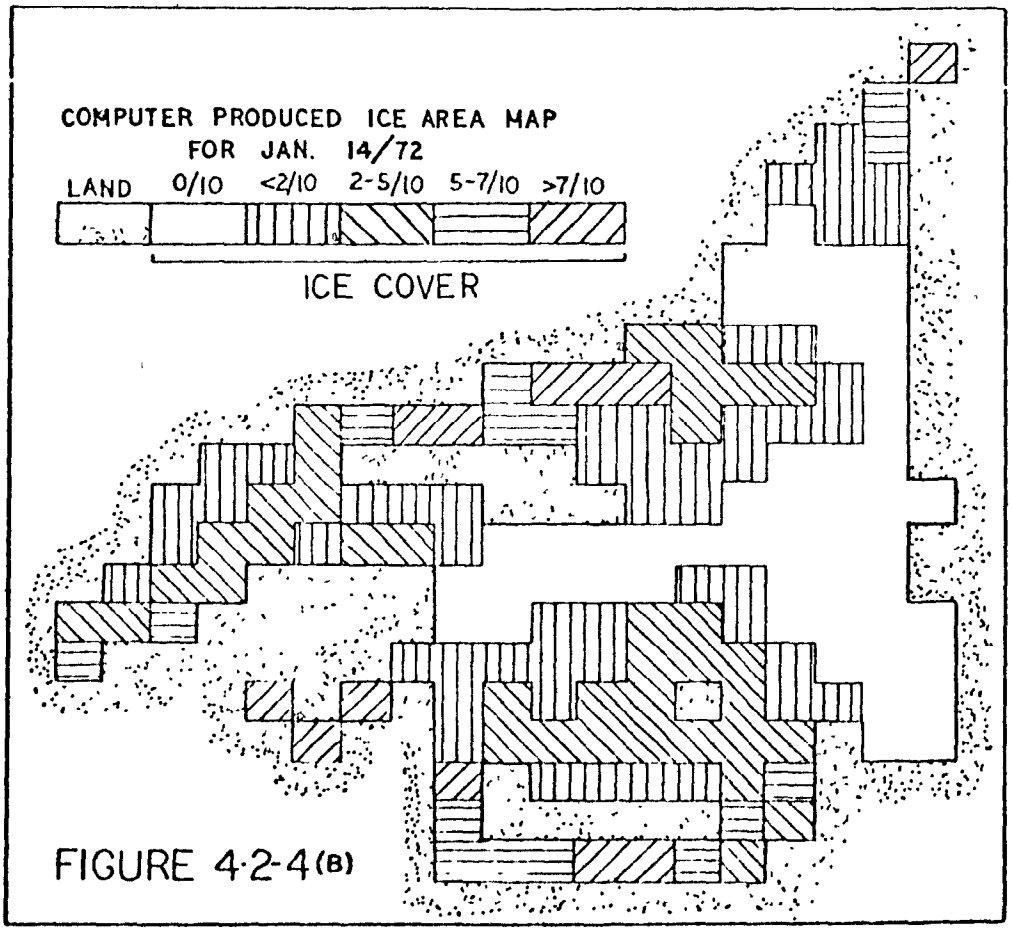

FIGURE 4·2-4(B)

27 and 28 show increases, primarily due to advection.

Thus the "two-tenths criterion" does not adversely affect the areal picture if wind reversals either do not exist or are of short duration, but any long term reversal makes this criterion untenable.

To sum up this section, the model as it exists gives quite a reasonable approximation of the ice cover's areal extent considering the limitations imposed on that model at the time of initialization.

4.3 Ice Area at Individual Grid Squares

The maps of February 2, 1972, Figures 4.3-1(a), (b), illustrate one point which is present in all the other maps but best shown at this date. The ice areas at individual grid points in the computer produced maps are extremely discontinuous. The real maps show little if any discontinuity between adjoining areas. The discontinuous nature of the computer produced field must surely lie in the method of ice increment distribution. That is the problem must be in subroutine "PINE" and in particular is probably the manner in which the ice formed over open water is incorporated into the field as described in section 2.14. The method in effect adds any new ice formed to the existing ice, preserving the existing ice thickness. Thus for similar atmospheric and open water conditions, the thicker the ice the less the areal increment. This particular method was devised by testing on a single grid point where there was seldom if ever any open water in existence after the first day of ice formation. This method of testing at a point did not, therefore, allow for the dispersive nature of ice advection which gives the field in this case a great deal of open water.

An additional effect of so much open water is probably an overestimate of the total ice volume in the Gulf of St. Lawrence. This will be investigated in section 4.5.

4.4 The Formation, Import and Export of Ice from Grid Points

An analysis is done in this section to determine the formation, import and export qualities of the grid points. It is this type of analysis which can only be made on a high resolution model with specific grid areas. The

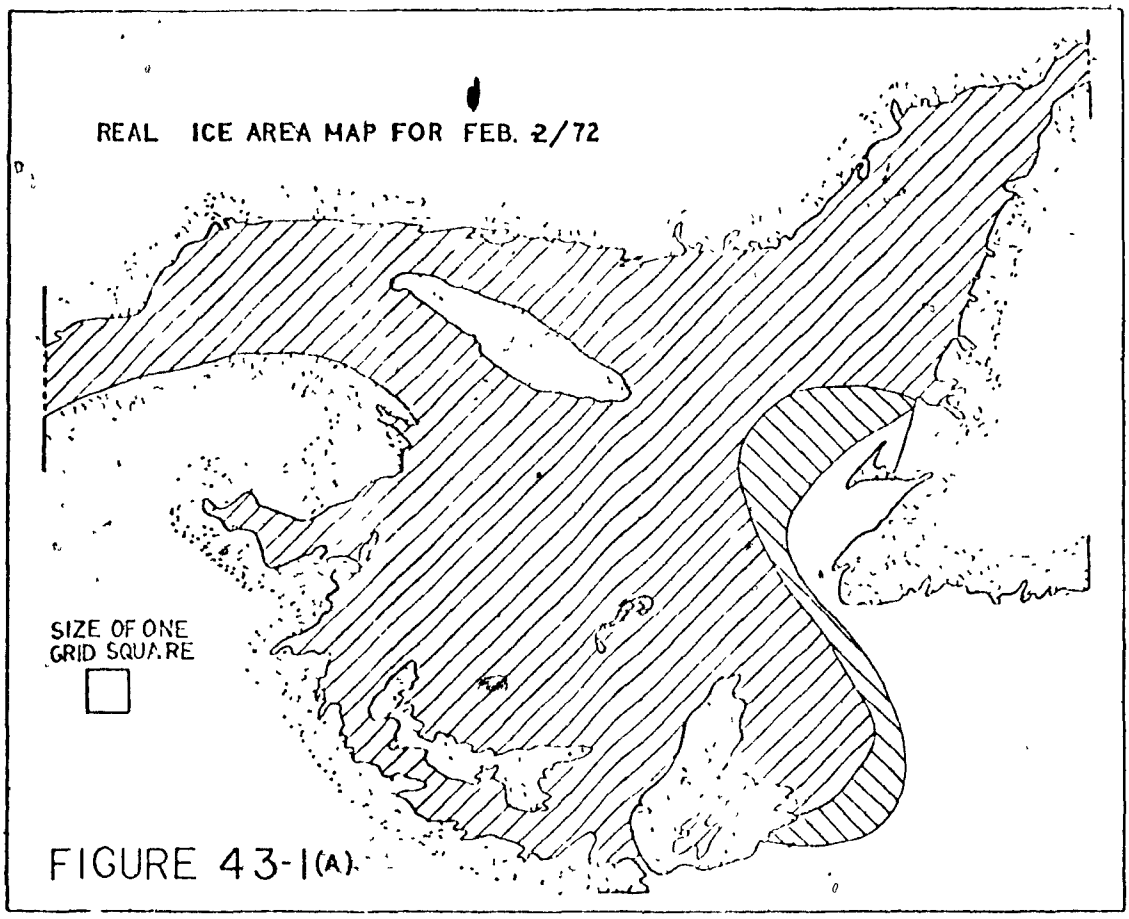

FIGURE 43-1(A)

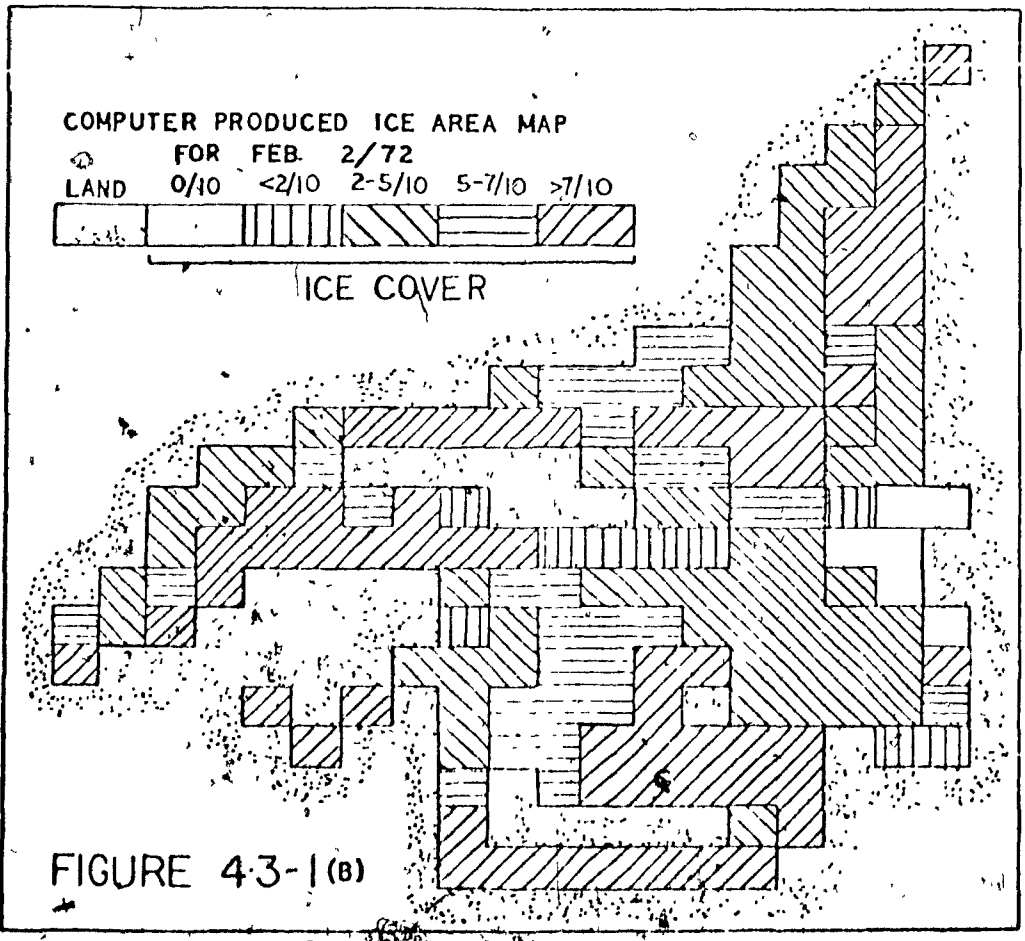

FIGURE 4·3-1(B)

analysis was carried out for the period Dec 23, 1971 to January 18, 1972 which has been broken into several smaller periods. Each period has three maps, where map (a) contains the ice formed at each grid point, map (b) the volume existing at each point at the end of the period and map (c) the ice imported (+) or exported (−) by each point.

The first of these periods is from Dec 23,to Dec 31 of 1971, Figures 4.4-1(a), (b), (c). At the end of this period there are 34 points at which ice exists. Of these 34 points there are 12 which melt the ice located over them. These melting points reduce the total ice volume formed by 3.2%. More important than the melting points is the fact that 5 of the 34 points produce 60% of all the ice which exists. Thus many other points which have ice receive it by advection from the 5 major ice forming points. Also worthy of note is the fact that the seven points in the Northumberland Strait (points 161-167) form 34% of all ice, but at the end of the period these same points account for 44% of the total ice volume. Thus, even though this area is a large ice producer it is a relative ice sink by virtue of its net import. Now, if only points external to the Northumberland Strait are considered then the five points (25, 36, 127, 141 and 151) out of a total of 27 points produce 90% of the ice which exists. These points show quite clearly on the ice import-export map as the chief exporters of ice.

The next map series is from Dec 31, 1971 to January 6, 1972; Figures 4.4-2(a), (b), (c). On these maps the same five points now produce only 33% of all the ice in the Gulf, while the Northumberland Strait points have dropped to 16%. The Northumberland Strait does, however, contain 32% of all ice existing on January 6 and thus its import increases though its production goes down.

If to the five above mentioned points are added five more points, (100, 34, 35, 27 and 158) then out of a total of 67 points where ice exists on Jan 6th these 10 points are responsible for 70% of all ice production. Further, if the Northumberland Strait is again neglected, these points represent 83% of all Gulf Ice production. Again looking at the import-export charts these 10 points prove to be the major ice exporters in the Gulf.

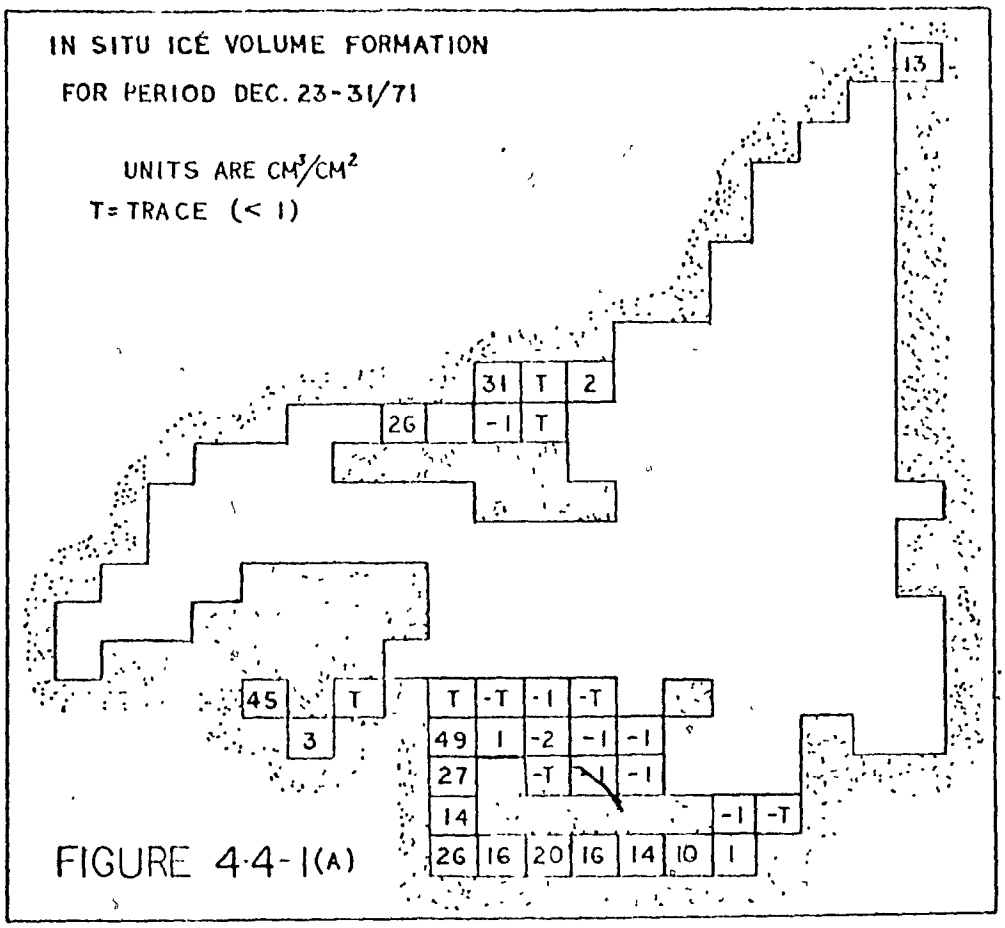

FIGURE 4·4-1(A)

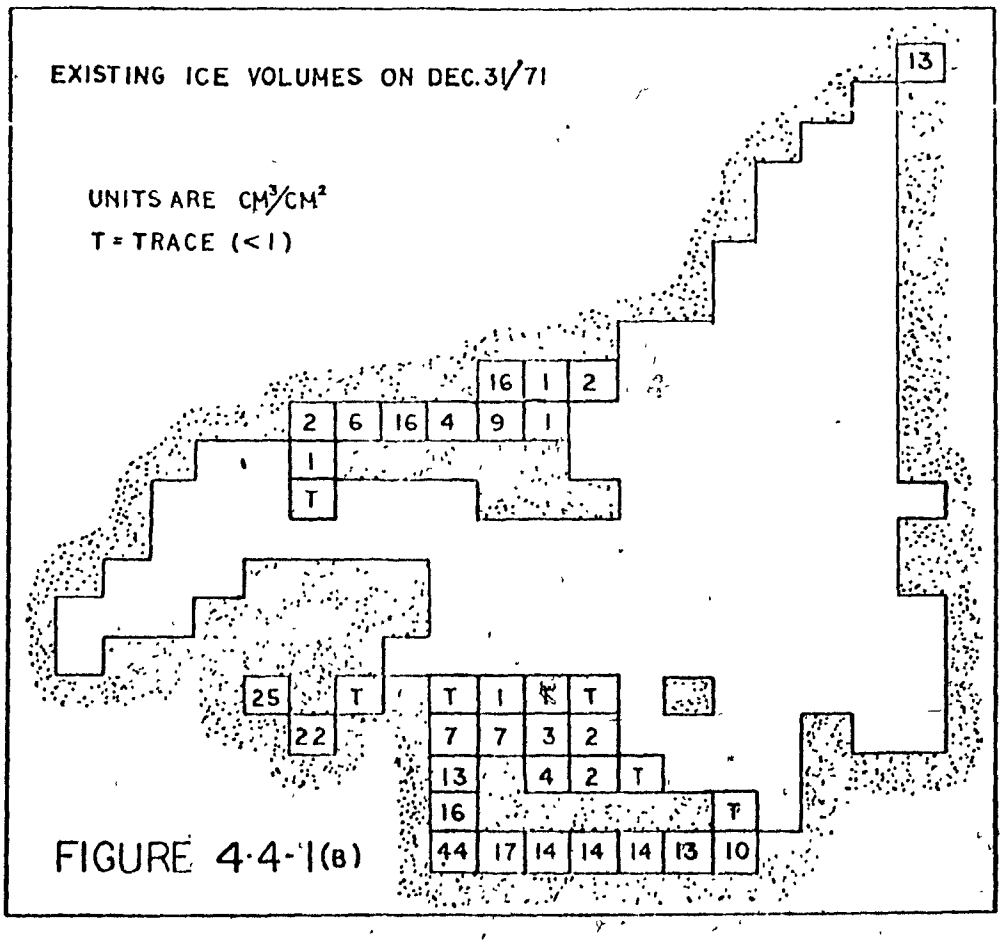

FIGURE 4·4-1(B)

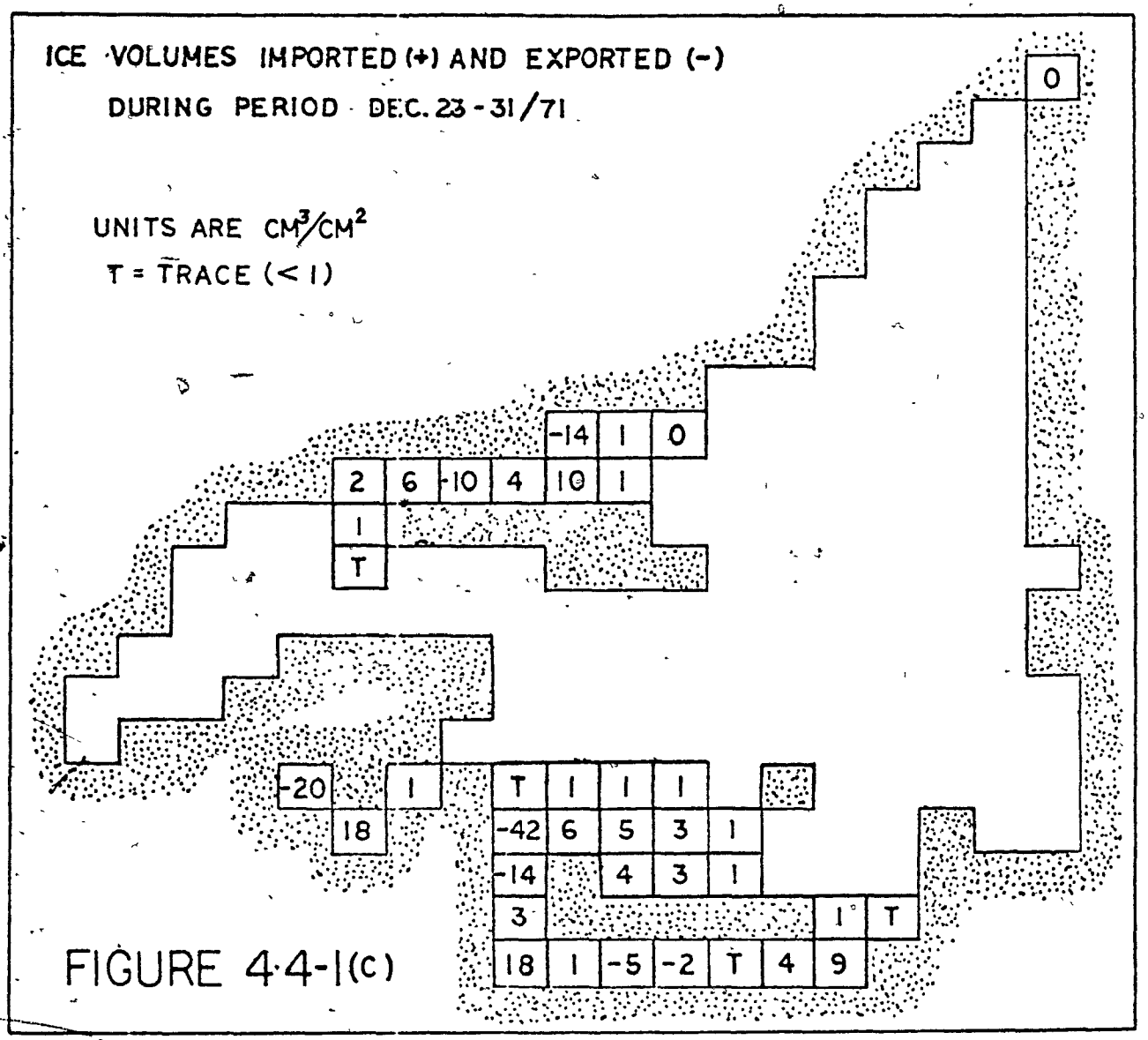
ICE VOLUMES IMPORTED (+) AND EXPORTED (-)
DURING PERIOD DEC. 23 - 31/71
UNITS ARE CM³/CM²
T = TRACE (< 1)
0
-14 1 0
2 6 -10 4 10 1
1
T
-20 1
18
T 1 1 1
-42 6 5 3 1
-14 4 3 1
3 1 T
18 1 -5 -2 T 4 9

FIGURE 4.4-1(c)

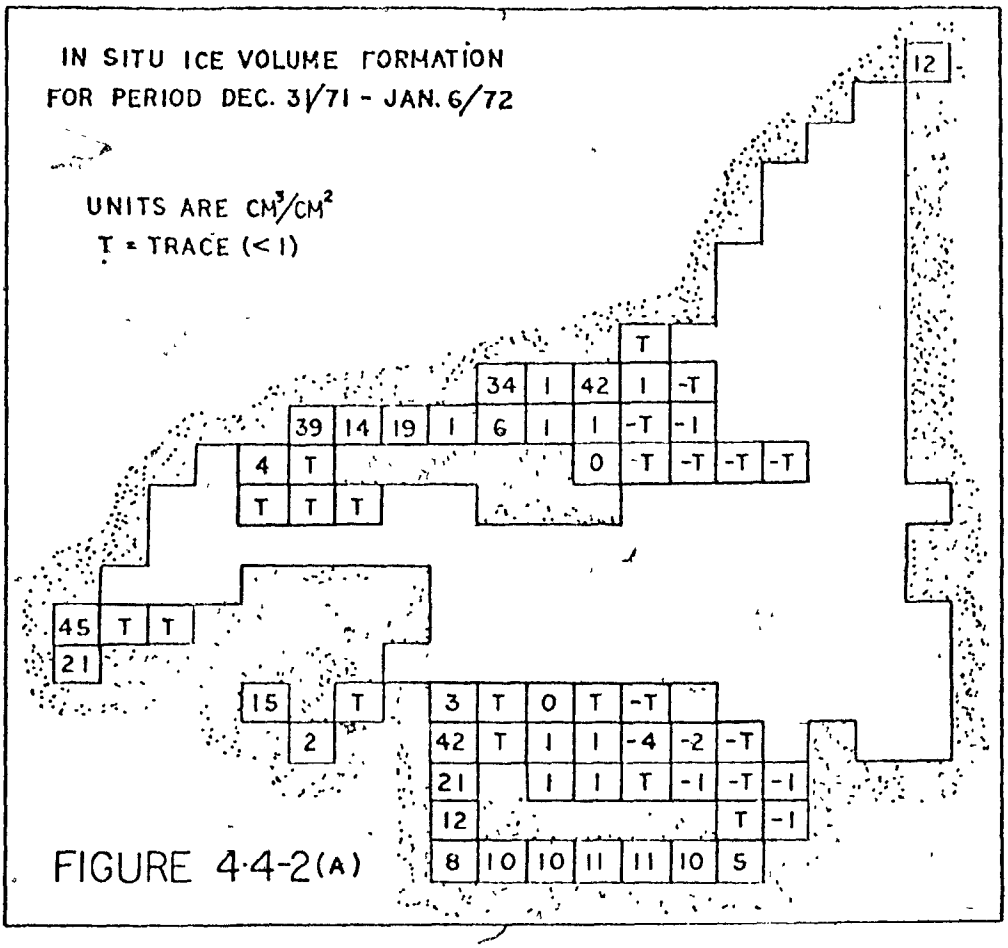

FIGURE 4·4-2(A)

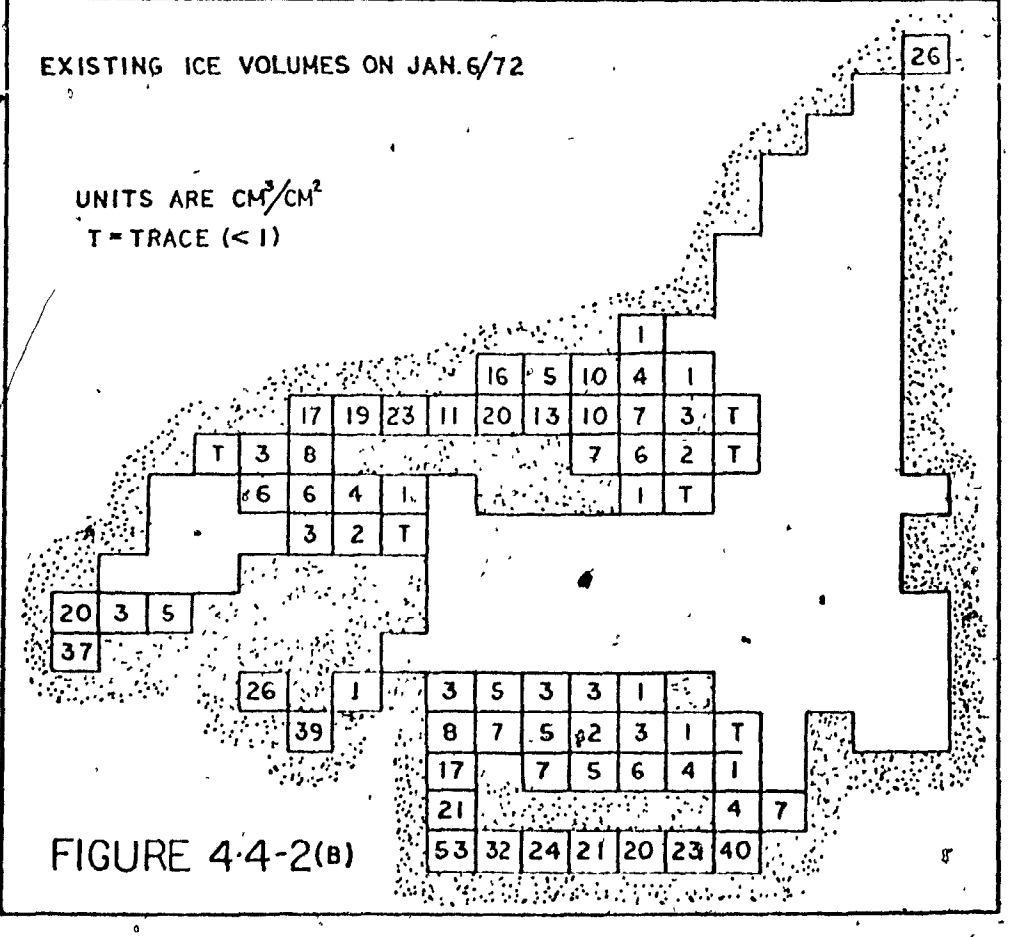

FIGURE 4·4-2(B)

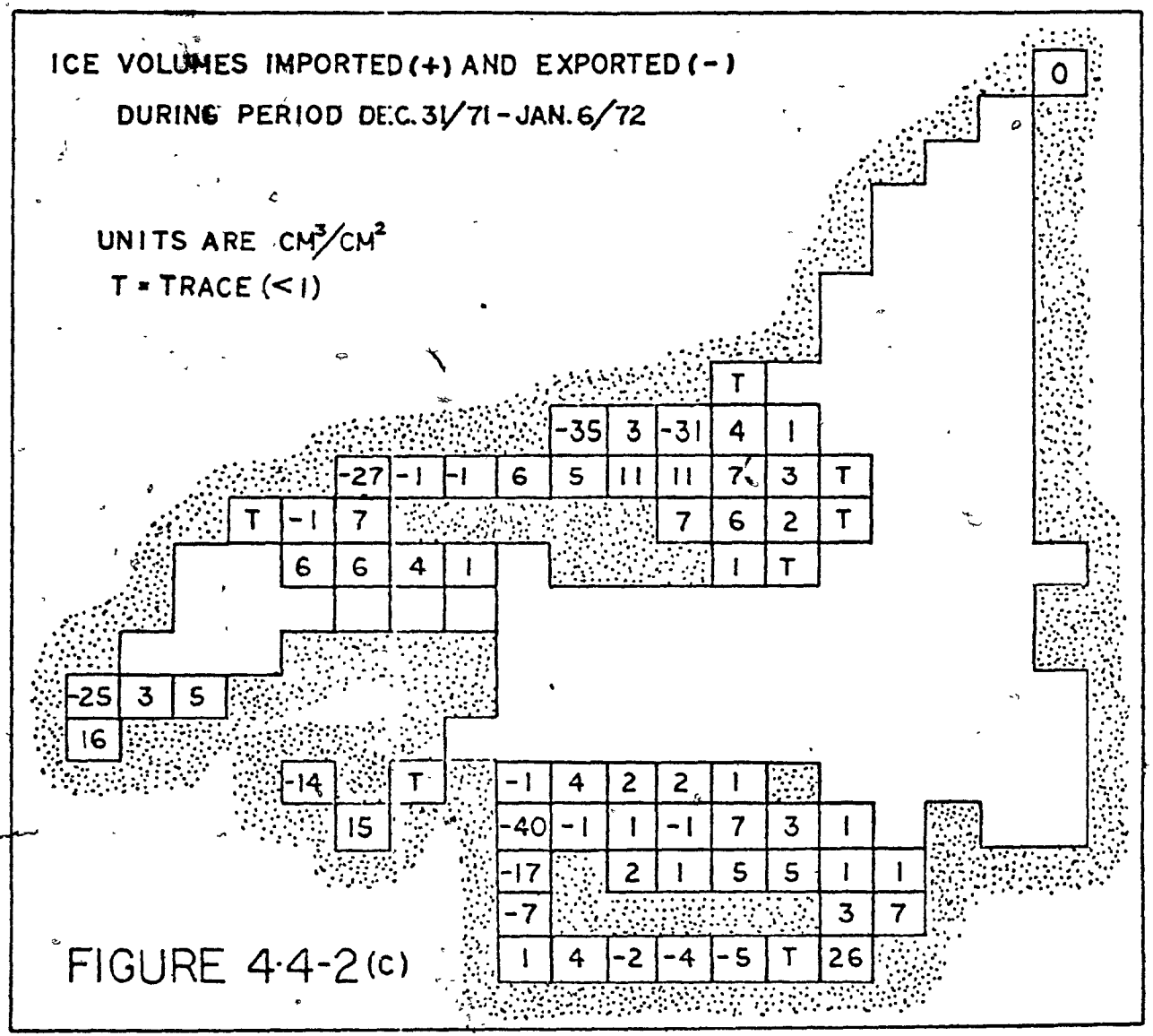
ICE VOLUMES IMPORTED (+) AND EXPORTED (-)
DURING PERIOD DEC. 31/71 - JAN. 6/72
UNITS ARE CM³/CM²
T = TRACE (<1)
0
T
-35 3 -31 4 1
-27 -1 -1 6 5 11 11 7 3 T
T -1 7 7 6 2 T
6 6 4 1 1 T
-25 3 5
16
-14 T
15
-1 4 2 2 1
-40 -1 1 -1 7 3 1
-17 2 1 5 5 1 1
-7 3 7
1 4 -2 -4 -5 T 26

FIGURE 4·4-2(c)

Finally, the whole period is considered in the maps of Figures 4.4-3 (a), (b), (c), for Dec 23, 1971 to Jan 18, 1972. In Table 4.4.1 are the results for 16 major points in the Gulf out of the 126 at which ice exists. These points produce 66% of all the existing ice in the Gulf. The total amount of ice exported by all exporting points is 50% of all the ice existing in the Gulf. Of this export 94% comes from these 16 points. Thus, less than 20% of the Gulf area produces 66% of all existing ice and 50% of all existing ice coverage is by virtue of the export from these points.

There are certain general characteristics which these 16 points share. They are nearly always shallow points. They are nearly always found on the lee shores and are considered shore points. This means that they form ice earliest and export it rapidly with the favourable off shore winds. These results are not new, but the relative magnitudes of ice produced must certainly be of importance and interest.

Bearing in mind the errors discussed in the previous sections, the quantative values from this model are probably not totally correct, but qualitatively speaking the results should be valid. These points should exist in reality and their relative effects should be reasonable. The percentages would be lower if the advection from the St. Lawrence river were accounted for, but this does not negate the effects at the 16 points but only emphasizes the additional importance of the St. Lawrence input.

These results suggest possibilities for simpler models which could be run for only shore points and include advection. This would allow works such as Coombs (Co62) to be of additional value. Such a model would be good for calculations of the early present of ice. Further tests run with the high resolution model described in this text could help to evaluate the real importance of these ice producing shore points.

4.5 The Volume of Ice in the Gulf of St. Lawrence

The area of the Gulf of St. Lawrence is not truly represented on the grid point map due to the highly irregular shape of the geographical region. Thus, rather than compare the actual volumes of ice an average thickness is used. The average thickness calculation is done in the following manner.

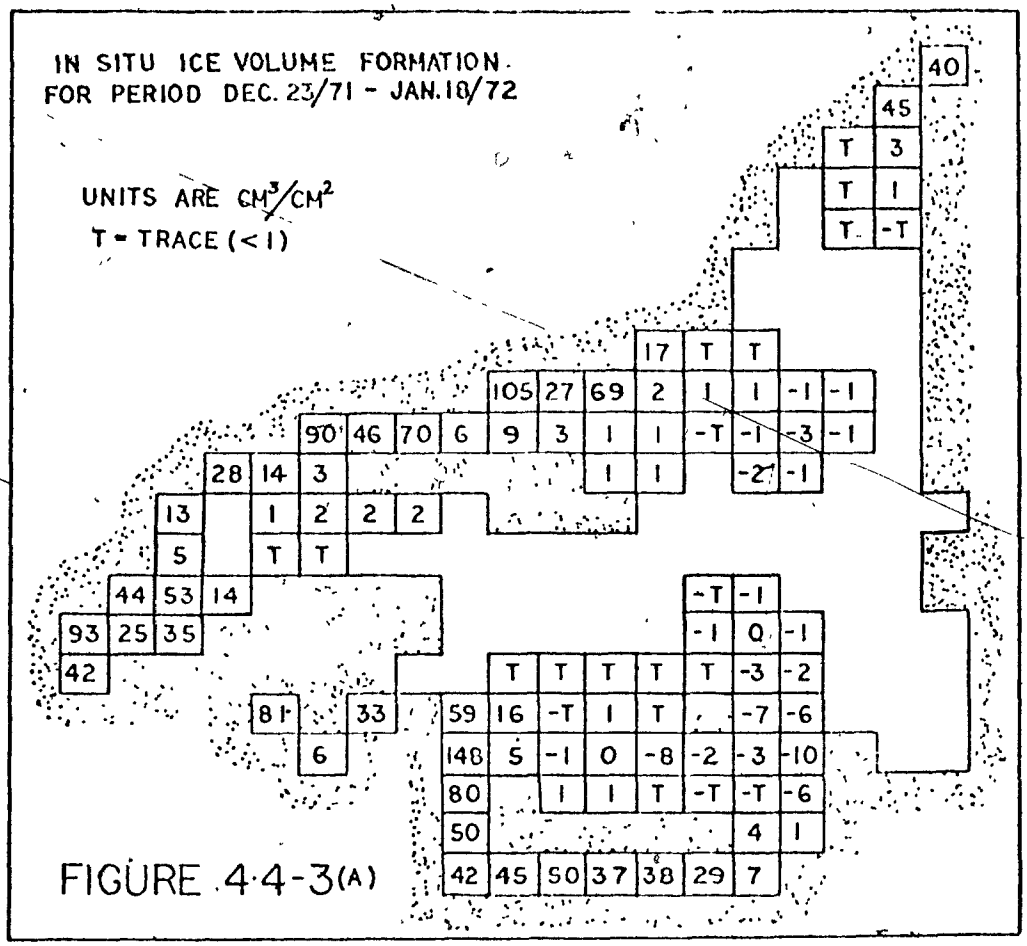

FIGURE 4-4-3(A)

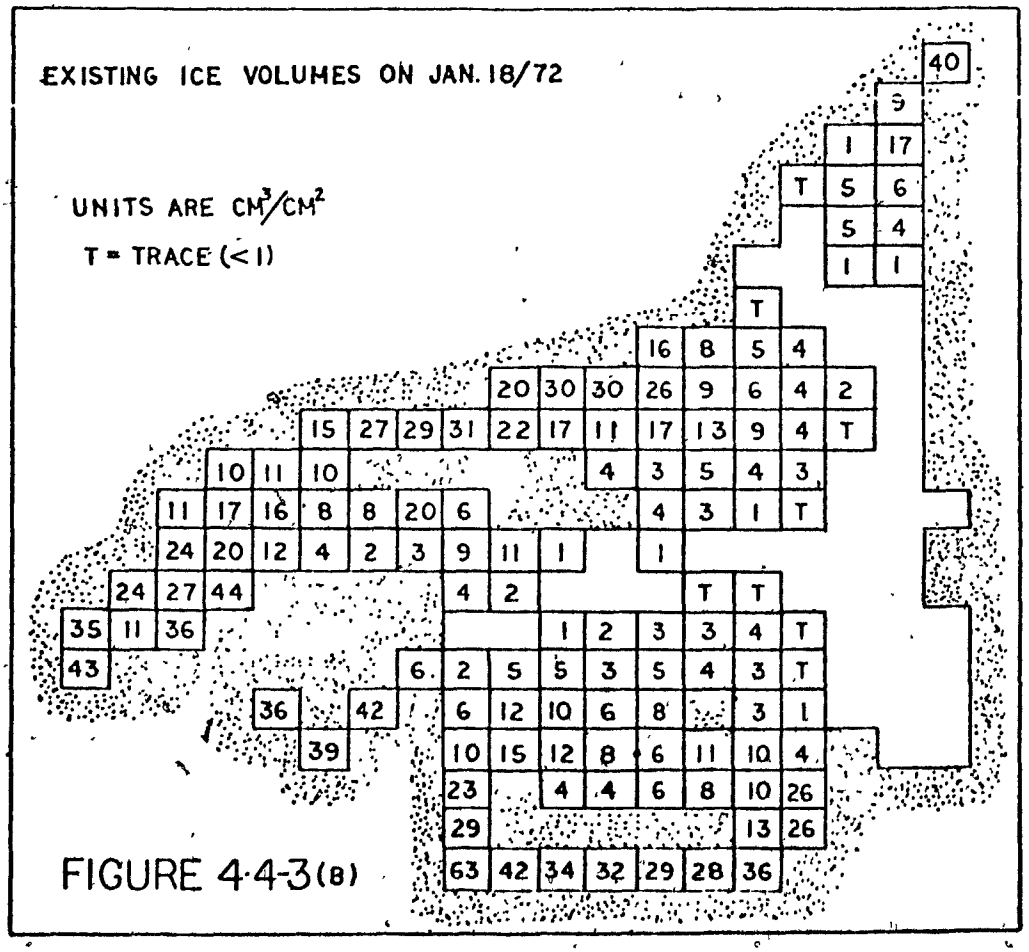

FIGURE 4-4-3(B)

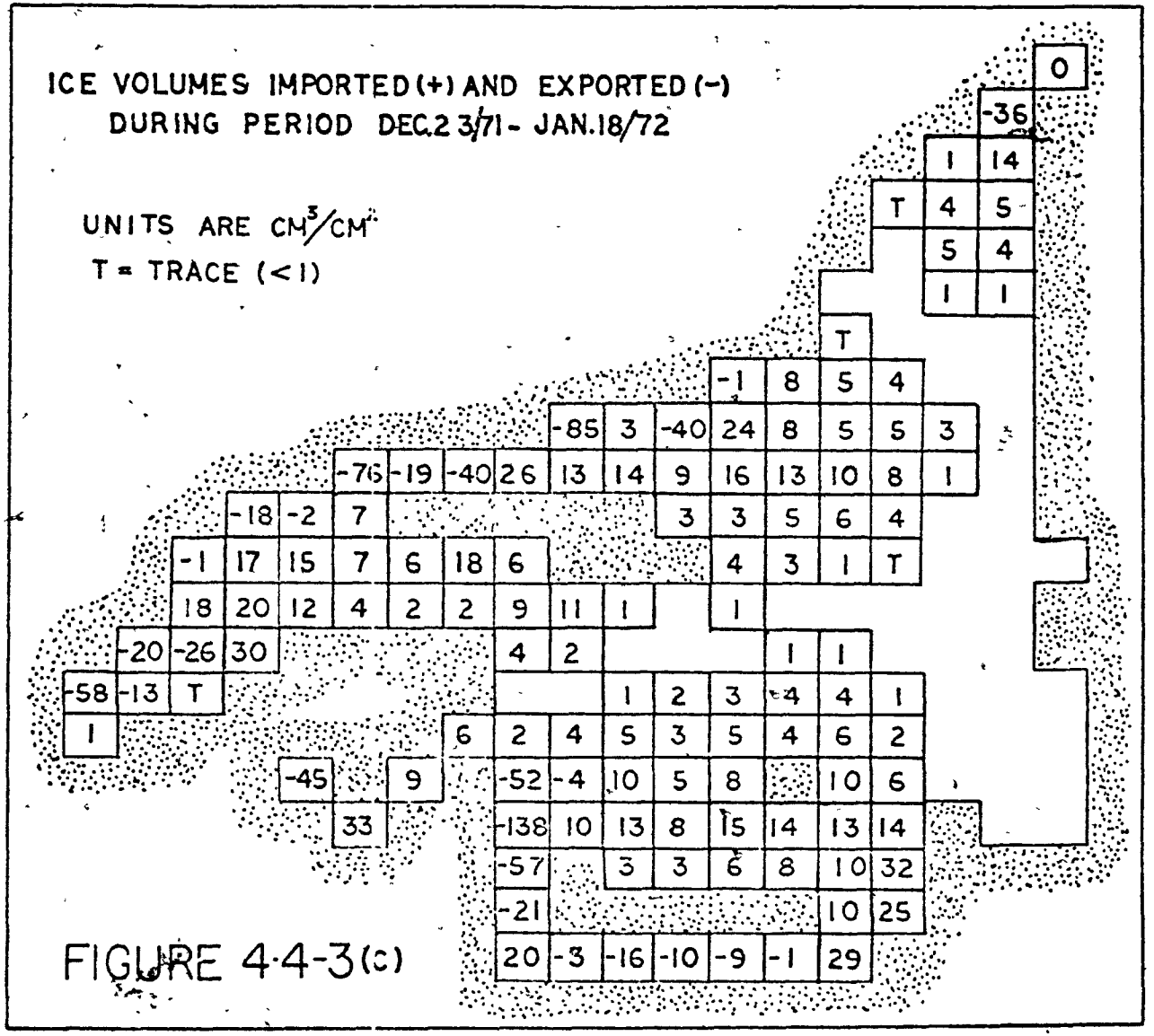
ICE VOLUMES IMPORTED (+) AND EXPORTED (-)
DURING PERIOD DEC. 23/71 - JAN. 18/72
UNITS ARE CM³/CM²
T = TRACE (<1)
0
-36
1 14
T 4 5
5 4
1 1
T
-1 8 5 4
-85 3 -40 24 8 5 5 3
-76 -19 -40 26 13 14 9 16 13 10 8 1
-18 -2 7 3 3 5 6 4
-1 17 15 7 6 18 6 4 3 1 T
18 20 12 4 2 2 9 11 1 1
-20 -26 30 4 2 1 1
-58 -13 T 1 2 3 4 4 1
1 6 2 4 5 3 5 4 6 2
-45 9 -52 -4 10 5 8 10 6
33 -138 10 13 8 15 14 13 14
-57 3 3 6 8 10 32
-21 10 25
20 -3 -16 -10 -9 -1 29

FIGURE 4-4-3(c)

Point No.	Percent of in situ ice formation in the gulf	Percent of in situ ice formed at point which is exported	Percent of total ice export from all exporting points
2	2.7	80	4.5
25	6.4	81	10.8
27	4.2	57	4.9
34	5.5	84	9.5
35	2.8	41	2.3
36	4.2	58	5.1
47	1.7	65	2.3
87	2.6	46	2.5
88	3.2	49	3.3
100	5.6	62	7.3
101	1.5	55	1.8
127	4.9	56	5.7
129	3.6	89	6.6
141	8.9	93	17.4
151	4.9	71	7.2
158	3.0	42	2.6

Break down of the contributions to ice production and export of the more important grid points

TABLE 4.4.1

The actual ice volume is calculated for the real ice field and that of the model which is th[illegible] divided by the area over which some ice exists. This area must not be confused with the actual ice area but rather it is a summation of grid areas where any amount of ice exists. This then will serve to normalize the thickness values and make them comparable. It is also most useful to pick a day when the ice edge pattern of both the real and modelled ice fields are similar. Such a day is February 2, 1972, as seen in Figures 4.3-1(a), (b).

Before going on to the results of the calculation it is worthy of note that the volume of the real ice field as shown in the ice charts cannot be calculated exactly. Some interpretation of ice thickness must be carried out and only the maximum and minumum ice volume are readily calculated. From Figure 4.5-1(a) it may be seen that each ice area has a four figure group attached to it. These numbers represent certain ice types with certain thickness ranges associated with them. For any four digit group, say "ABCD" the interpretative data is shown in Table 4.5.1. If any type of ice is not present a slash is put in its place.

As seen in Table 4.5.1 for ice type "A" there exists a wide range of thickness values. The author assumed that type "A" thick ice would probably not exist except in areas where ice piles up along shorelines. The resolution of the model does not allow for such cases of pile-up and they are not shown on ice maps produced by Ice Central. Therefore this type of ice was neglected.

The average thickness of ice for the model is quite easily calculated from the computer output, while the real ice map required many area calculations. The results of the calculations for the real ice field are shown in Table 4.5.2 which also shows the thickness used to represent the different ice types. The value of average thickness found in the model ice field was 34.3 centimeters. From the results shown in Table 4.5.2 it is quite obvious that this fits quite well into the range of possible values. It is somewhat larger than the average value of 29.2 cm for the real field. In the case of the real field, not all the ice which exists came from the same grid area as in the model as the St. Lawrence River supplies some ice

ICE TYPE	DESCRIPTION		THICKNESS RANGE
A	First Year	Thick	> 120 cm
		Medium	70 - 120 cm
		Thin	30 - 70 cm
B	Grey - White		15 - 30 cm
C	Grey		10 - 15 cm
D	Nilas or new ice		5 - 10 cm

Interpretative Tables for Department of Environment Ice Charts

TABLE 4.5.1

Thicknesses used for the calculation				Average Thickness
A	B	C	D	
120	30	15	10	44.58 (max.)
30	15	10	5	15.88 (min.)
70	22.5	12.5	7.5	29.21 (avge)

Thickness used for each type of ice and the average thickness derived therefrom for the Feb. 2, 1972 ice field.

TABLE 4.5.2

in the early stages, as has been shown above. This would have a tendency to lower the maximum and minimum limits if this ice were removed from consideration. No really definite statement can be made on the numbers calculated, though one may generalize and say that the model tends to form ice close to the upper possible limit. In this case it may form more ice than is really produced.

More conclusive results on the details of these ice volume calculations must await a better method of estimating real ice volumes and the design of a model with more of the refinements mentioned previously.

CHAPTER 5

CONCLUSIONS

The model as presented in this thesis has proved to be capable of yielding reasonable resultant ice fields, considering the initial constraints placed upon it. It has good areal resolution and can easily be run to produce diagnostic fields, though the computer expenses incurred do put limitations on its use.

The general pattern of ice and non-ice areas were quite good and improved with time as the Gulf area became more ice-bound. The initial condition which did not allow the advection of ice down the St. Lawrence River created an erroneous non-ice field in this area. It did, however, serve to show that this advection is an important process in making up the Gulf's ice field. It further showed that even if this advection could be stopped the area would simply become ice bound at a later date due to insitu ice formation. Non-presence of ice along the northern shore of the Gulf of St. Lawrence resulted from the water-depth initialization in this area being to deep. The field in this area was hence incorrect. The problem itself is inherent in the resolution of the model. The fact that such a problem exists is indicative of the importance of shallow water along this shore.

The inability of a grid point model to define the ice edge for areas smaller than one grid length is another inherent problem of this type of model. The author attempted to resolve this difficulty with the "two tenths criterion". In an area such as the Gulf of St. Lawrence which has, in general a northwesterly air flow such a criterion is not too deficient. It does, however, cause problems when opposing air flows existing for time periods of over three or four days. In areas of varying flow patterns a simple criterion such as this would have to be replaced by a more sophisticated one.

The real power of a grid point, short time step model such as this one is in the fact that the detailed formation and movement of ice may be

traced. The model showed up areas where large ice formation and export could exist. These points are in general of shallow depth (30-60 meters), and are found on lee shores where the air flow is usually northwesterly. As previously mentioned correcting the deficiencies in the model may change the magnitudes calculated, but the presence of such points should remain.

The average ice thickness calculated from the model falls easily within the maximum and minimum limits of average thickness calculated for the observed ice field. These limits are too wide to allow much more to be said, then that the model gives a value greater than the average value calculated from the real field.

BIBLIOGRAPHY

(Anon68), ----, 1968: "Ocean Thermal Forecasting in the Northeast Atlantic", Section 2. Meteorology and Oceanographic Div., Hydrographic Dept., Ministry of Defence, London, pp. 21.

(Bu64), Budyko, M.I., 1964: "Guide to the Atlas of the Heat Balance of the Earth". Translated by the Office of Climatology, U.S. Dept. of Commerce, WB/T-106.

(Co62), Coombs, J.A., 1962: "A Preliminary Investigation of the Heat Budget in the Gulf of St. Lawrence", (Unpubl. Man.). Bedford Institute of Oceanography, Report B.I.O. 62-1, Dartmouth, Nova Scotia, pp. 50.

(De61), Defant, A., 1961: "Physical Oceanography", Volume I. The MacMillan Co., New York, pp. 88-109.

(DY65), Dingle, A.N. and C. Young, 1965: "Computer Applications in the Atmospheric Sciences". Dept. of Meteorology and Oceanography, Univ. of Michigan, pp. 36-54.

(EJ71), El Sabh, M.I., and O.M. Johannessen, 1971: Winter Geostrophic Circulation in the Gulf of St. Lawrence, Marine Sciences Report number 18. McGill Univ., Montreal, pp. 19.

(Fo67), Forrester, W.D., 1967: "Currents and Geostrophic Currents in the St. Lawrence Estuary", (Unpubl. Man.). Bedford Institute of Oceanography Report B.I.O. 67-5, Dartmouth, Nova Scotia, pp. 171.

(Ga72), Gagnon, R.J., 1972: "Influence of the Surface Energy Budget on Crop Yield", (Unpubl. M.Sc. Thesis), McGill University, Montreal, P.Q., pp. 175.

(La60), Laevasta, T., 1960: "Factors Affecting the Temperature of the Surface Layer of the Sea". Commentationes Physico-Mathematicae XXVI, Societ as Scientianum Fennica, pp. 136.

(La68), Langleben, M.P., 1968: "Albedo Measurements of an Arctic Ice Cover from High Towers". Journal of Glaciology, 7, pp. 289-298.

(La57), Lauzier, L., and W.B. Bailey, 1957: "Features of the deeper Waters of the Gulf of St. Lawrence". Bull. Fish. Res. Bd. Canada, No. 111, pp. 213-250.

(Ma67), Matheson, K.M., 1967: "The Meteorological Effect on Ice in the Gulf of St. Lawrence". Publ. in Meteorology No. 89, McGill University, Montreal, pp. 110.

(Mo73), Morin, P.L.J., 1973: "Air Mass Modification over the Gulf of St. Lawrence". (Unpubl McGill M.Sc. Thesis), McGill University, Montreal.

(MU69), Maykut, G.A., and N. Untersteiner, 1969: "Numerical Prediction of the Thermodynamic Response of Arctic Sea Ice to Environmental Changes". The Rand Corporation Memorandum RM-6093-PR, pp. 171.

(Po65), Pounder, E.R., 1965: "The Physics of Ice". Pergamon Press, pp. 143.

(Ro65), Roll, H.U., 1965: "Physics of the Marine Atmosphere", Int'l Geophysics Series, Volume 7. Academic Press, pp. 247-253.

(Sc62), Schwerdtfeger, P., 1962: "Energy Exchange through an Annual Ice Cover". (Unpubl. Ph.D. Thesis), McGill University, Montreal, pp. 144.

(Se65), Sellers, W.D., 1965: "Physical Climatology, University of Chicago Press, pp. 275.

(Tr70), Trites, R.W., 1970: "The Gulf of St. Lawrence as a Physical System". Second Gulf of St. Lawrence Workshop held at Bedford Institute of Oceanography, Dartmouth, N.S., pp. 32-64.

(VO72), Vowinckel, E., and S. Orvig, 1972: "EBBA. An Energy Budget Programme". Publication in Meteorology, No. 105, McGill University, Montreal, pp. 47.

(Zi72), Zillman, J.W., 1972: "A Study of Some Aspects of the Radiation and Heat Budgets of the Southern Hemisphere Oceans". Met. Study no. 26, Bureau of Meteorology, Dept. of the Interior A.G.P.S., Canberra, Australia.

(Zu43), Zubov, N.N., 1943: "Arctic Ice" (Izdatel'stvo Glavsemorputi), Moscow. Translated for AFCRC by U.S. Naval Oceanographic Office and American Meteorological Society).

Appendix A

Air Mass Transformation Description from Morin (Mo73)

3.5 Air Mass Transformation-Model

For the calculation of freeze-up and ice formation over a given area, a detailed knowledge of the energy budget terms is required. Considering foregoing processes, it is doubtful whether simple interpolation programs as discussed so far would result in sufficiently accurate meteorological fields.

Burke (1945) devised methods of predicting the final surface air temperature by using the following parameters: initial air temperature and humidity, sea surface temperature, lapse rate, and distance travelled over water. As a second approximation for required data fields, an air mass transformation program "AIRMTR" was devised by the present author. The underlying principal is an extension of the "Burke" technique applied over a large area.

3.5.1 Advection of Air Parcels

The model used by the author is an extension of one developed by Vowinckel (personnal communication). This model calculates intermediate temperature, cloud, and humidity profiles along a streamline - all the while taking into account the varying sea surface temperature, winds, and sea level pressure. This redefined field is then assumed to be in steady state for the next 12 hours during which energy budget computations are executed.

To effect the transformation of certain meteorological parameters in the lower levels, all boundary and ice or water grid points of Figure 2 (see Figures 3.1-1 and 3.1-2 main tent) have been specially identified. Next, all points along the Gulf shore are examined to determine if the advection of their profile by the geostrophic wind (veered 8°) is towards land or ice/water surfaces. Profiles overlying regions with offshore

winds will then be advected by the subroutine TRAJEC. This subroutine calculates displacement from one grid line between two grid points to another grid line between two different grid points. The maximum allowable displacement in 1.44 * DX where DX is the grid spacing. From one grid line to another, flux exchanges at the interface are calculated and redistributed in the vertical, and the modified protion of the profile is recorded at two nearby points. Following this, the entire profile is advected. The grid spacing was chosen as 37 km so as to include significant bays and straits.

3.5.2 Sensible Heat Distribution

Each advected profile has its meteorological parameter changes executed in the subroutine "TEPHI" which simulates the temperature and humidity soundings on a tephigram.

The sensible heat exchange for ice and water surfaces is calculated in the subroutine "HEMLOK" and the subroutine "SCFLEX" appropriately weights the flux contribution from ice and water surfaces. "HENLOK" is an extension of the subroutine "VERA" (Vowinckel and Orvig, 1972). Following this, the subroutine "EATDST" distributes the sensible heat into the sounding. The level of modification is limited by the maximum lapse rate allowable, and by the magnitude of the sensible heat exchange. Each time the lapse rate is exceeded, another layer is included in the modification process. Examination of several profiles traversing the Gulf and passing over Stephenville showed a lapse rate usually near the midway of the moist and dry adiabat.

In situations of cooling by an underlying surface, the depth of cooling is greatly dependent on the stability of the profile and wind shear. Sellers (1965) summarizes various studies on stability. In general, strong stability is usually characterized by a Richardson number of .25, and -.7 for the unstable situation. The subroutine "RICRON" determined if an advected profile woudl develop a low level surface inversion or a cooled layer with a dry adiabatic lapse rate. For a Richardson number greater than -.2, a surface inversion not exceeding 1 layer (about 25 mbs) was allowed to occur, otherwise cooling was extended to include the two bottom

layers (about 50 mbs). Linearly interpolated low level winds, the temperature profile, and the height field were involved in the calculation of the Richardson number. The model was designed to simulate changes in the lower atmosphere which are predominantly effected by underlying surface features and which in turn, almost wholly affect the energy budget of the underlying surface. Therefore, changes occuring in the higher levels due to warm or cold air advection and large scale vertual motion will not be possible. To include such processes would require advection of an atmosphere divided into several layers, with each layer consisting of a similar grid point array and each layer moving independantly of the others with exchanges of moisture and heat occuring between grid points of each layer.

3.5.3 Latent Heat Distribution

With respect to moisture, the latent heat is equally added to all modified layers by the subroutine "HUMAST". Following this, the vertical moisture profile is analysed in the cloud formation program called "CLOUD". Each layer is checked to see if the relative humidity exceeds 70%, after which cloud formation is allowed to proceed if the interpolated cloud field indicates that cloud does exist for that particular layrr at that grid point. Once overcast conditions are achieved, the maximum relative humidity allowed is 85%. Ninomaya (1964) shows that clouds with a water content of .43 g kg^{-1} had a relative humidity exceeding 85%. Since the Gulf area is not marked by extensive modification as is the air over the Japan Sea, the author chose an upper limit of 85%. After overcast conditions are attained, and after the relative humidity reaches 85%, the excess moisture is transported to the next upper level where it is used to increase cloud/or humidity. The clouds are assumed to have a liquid water content of .2 g kg^{-1} (Squires, 1958; Warner, 1955) and the highest mean value obtainable is .3 g kg^{-1} under states of very strong convective activity.

3.5.4 Islands

Islands such as Anticosti and Prince Edward act as sinks for sensible and latent heat acquired by air masses having passed over ice/water surfaces. These two islands as well as the Magdelan Shallows and the northern portion

of Cape Breton Island were treated as solid ice surfaces having a defined temperature - the temperature being that of the nearest reporting station as no ground temperatures are available. During the winter season, the recorded air temperature will generally approximate the surface temperature. For regions lying on the windward shores, the temperature will be largely modified and not representative.

3.5.5 Interface Temperature

One parameter essential in calculating the flux exchange at the interface is the ice/water surface temperature. As previously stated, air parcels are advected from one grid line to another. In the case where the initial and final grid points are water, the water temperature for the first half of the step displacement is the linearly interpolated temperature of the 2 grid points bounding the grid line. Similarly, the temperature of the last half of the displacement is the linearly interpolated temperature of the 2 last grid points involved. In the case of all ice cover, ice temperatures are substituted. For a mixture of ice and water surfaces, the flux contributions from ice and water are calculated and then weighed according to the areal extent of ice or water. The temperatures in these situations are areally weighed.

3.6 Water Body Model

In periods prior to ice formation over the Gulf, the high flux exchange rates associated with cold arctic outbursts will gradually reduce the finite heat supply of the Gulf. This resulting heat loss, reflected by a drop in the surface water temperature, is a principal factor in determining the flux exchange rate. An accurate extimate of the flux exchange demands a reasonable estimate of the air-sea temperature difference. Preceding sections dealt with the unrepresentativeness of certain meteorological fields in the lower atmospheric levels as generated by simple interpolation techniques applied to meteorological data. In this section a method is described, which regenerates the parameters essential in evaluating the latent and sensible heat flux exchanges between the atmosphere and the underlying water body. Used in conjunction with a water body model

(see appendix) developed by Lally (1973), and initialized at a date for which there exist scattered vertical soundings of temperature and salinity for the Gulf, surface water temperature distributions are obtained from time step to time step through energy budget considerations and iterative energy balance schemes incorporating modified and unmodified atmospheric and water parameters.

Chapter IV section 1.1 examines the limitations of the air model by examining an actual sounding advected over the Gulf with a sounding recorded twelve hours later, and section 4.1.2 discusses the results of applying the advection scheme over the entire Gulf region whose ice/water temperatures are regulated by a water body model.

Appendix B

Program & Subroutines

```
C THIS IS THE MAIN WHICH IS USED WHEN WORKING WITH THE INTERPOLATED
C  DATA SETS WHICH HAVE BEEN STORED ON TAPE
C
      INTEGER*2 ICLDHT(22,25),ICDX(22,25),ICSY(22,25),PROTMX(22,25)
      INTEGER*2 ITDM(22,25),NZLVL(6),LDMX(22,25),MTH(550),MTXFLX(170)
      DIMENSION TN(22,25,17),SHH(22,25,17)
      DIMENSION DPSHH(22,25,17),DPTN(22,25,17),CC(22,25,17)
      DIMENSION TW(22,25),TGS(22,25),TGI(22,25),TG(22,25),FSAV(22,25)
      DIMENSION SAIC(22,25),TUFI(22,25)
      DIMENSION X(22,25),SS(22,25),PR(22,25)
      DIMENSION EIS(22,25),AEIS(22,25),SSN(22,25),SX(22,25),SY(22,25)
      DIMENSION PN(22,25),TX(22,25)
      DIMENSION  GT(167,8),SAL(167,8)
      DIMENSION GTIO(8),SALIO(8),EISEXP(6),UF(17)
      DIMENSION ETA(5),RO(8),SL(8),GF(8),TWL(8),TAH(8),TAW(8),DF(17)
      DIMENSION ABSORP(8,3),C(17),SHN(17),P(17),T(17),SA(17),CHH(17)
      DIMENSION ALBEDO(22,25),Z(22,25,6),DPCC(22,25,8)
      DIMENSION EVD(22,25),SVD(22,25),AED(22,25)
      DIMENSION TEMALB(22,25),STWT(22,25)
      DIMENSION SRLU(22,25),SFG(22,25),SQE(22,25),SQS(22,25)
      DIMENSION SSGT(22,25),SDFT(22,25),HCWR(22,25)
C
      DATA ROT,CLWC,CRI/.288,.2,.65/
      DATA TIMFAC,CASF,TIMUTS/1.,1.,42300./
      DATA NL,NLX,NLT,TOPL/17,16,8,250./
      DATA CONE,CONS,DENSS,DENE,SPH/19.8,1.8,.2,.918,.5/
      DATA SLAT,ELAT,CRITH,EISSAL,DIA/2*80.,4.,.005,99./
      DATA ISZ,JSZ/22,25/
      DATA ORAD,AG,RA,TSUN,EXC/1.495E08,102.,695560.,5890.,.0167/
      DATA OZ,COL,DUST,DUA,DUB,V/.0124,.23986,0.,0.,.5,.05/
      DATA FLO,BR,TI,SR,LU/0.,48.,363.,11.,1/
      DATA ALB/.7/
      DATA LZELM/272/
      DATA EISEXP/6*0./
      DATA NZLVL/17,11,6,4,2,1/
      DATA TWL/4000.,3000.,2000.,1000.,1000.,500.,250.,250./
      DATA ETA/.5,.75,.9,.95,1./
      DATA P  /150.,300.,400.,500.,600.,700.,730.,760.,790.,820.,850.,
     1      875.,900.,925.,950.,975.,1000./
      DATA ABSORP/0.,0.,0.,.001,.006,.032,.065,.896,0.,0.,0.,0.,.001,
     1.012,.053,.934,0.,0.,0.,0.,0.,.009,.040,.951/
C
      SUE = 12.
      NCOUNT=0
      NTPERD = 0
      DX=.37E+07
      WISF=.02*.7
C
C SUBROUTINE START READS IN CERTAIN MATRICES OF CONSTANTS WHICH HELP
C CONTROL THE PROGRAM (LDMX,PROTMX,MTXFLX,ICDX AND ICSY)
C
      CALL START (PROTMX,MTXFLX,LDMX,ICDX,ICSY)
C
C SUBROUTINE RDWMDT READS IN INITIAL WATER BODY MODEL DATA
C
      CALL RDWMDT (GT,SAL,TGI,TGS,FSAV,EIS,SSN,AEIS,SAIC,ALBEDO,ITDM,TG)
C
      CONR = CONE/CONS
 1010 DAY=1.
 1015 CONTINUE
      LYE_M=LZELM + SUE*15. - 3.
C
C THIS READS IN THE PREVIOUSLY INTERPOLOLATED INITIAL ATMOSPHERIC FIELDS
C FROM TAPE
      READ(8,END=1008) IT,IDTG,NRAD,NSYN,TN,SHH,CC,SX,SY,PN,PR,Z,ICLDHT
C
      II = IT .
```

```
C
C SUBROUTINE AIRMTR IS RESPONSIBLE FOR TRANSFORMING THE AIR MASS.
C
      CALL AIRMTR(ITDM,SX,SY,Z,PN,SHH,TN,TW,TG,AEIS,P,DPTN,DPSHH,CC,X,
     1ROT,ICLDHT,DPCC,DX,TOE,TOS)
C
C
C CALCULATE THE SUNS DECLINATION ANGLE WITH HELENA
C
 1040 CALL HELENA(TI,FUT,SIS,ORAD,AG,RA,TSUN,EXC)
C
      BEISA=0.
      BEISV=0.
C
C BEGIN LOOP WHICH CALCULATES POINT BY POINT THE SURFACE ENERGY BUDGET FOR
C WATER AND ICE POINTS.
      DO 1050 J=1,JSZ
      DO 1051 I=1,ISZ
      IF(LDMX(I,J).EQ.0) GO TO 1089
      P(NL)=PN(I,J)
      PS=P(NL)
      DP=(PS-850.)/6.
      DO 1055 K=1,5
 1055 P(17-K)=PS-DP*K
      DO 1058 N=1,16
      C(N)=CC(I,J,N)*.1
      SHN(N)=SHH(I,J,N)
      T(N)=TN(I,J,N)
      CHH(N)=(P(N+1)-P(N))*C(N)*10.
 1058 CONTINUE
      T(17)=TN(I,J,17)
      SHN(17)=SHH(I,J,17)
      C(NL) = 0.
      CHH(NL) = 0.
      TDZ = DEW(SHN(NL),PS)
      SAA=0.
      S300=0.
      SN=0.
C
C CALCULATE SHORT WAVE RADIATION REACHING THE GROUND FOR THE POINT.
C
      CALL ELM(NLX,NL,P,SHN,FUT,SIS,SAA,CHH,SGA,S300,BR,OZ,DUST,DUA,V,
     1          DUB,SUE,LZELM,LYELM)
C
C CALCULATE LONG WAVE RADIATION FROM THE ATMOSPHERE TO THE GROUND.
C
      CALL DOGWUD(T,P,SHN,C,UF,DF,NLX,NL,LU,COL)
C
      TZ = T(NL)
      DFL = DF(NL)
      F = SQRT(SX(I,J)**2 + SY(I,J)**2) * .01 * .7
      PCPN = PR(I,J)
      BPCPN=BPCPN+ PCPN
      FWS = FSAV(I,J)
      FWSSAV = FWS
      KTS = (J-1)*22 + I
      MP = MTH(KTS)
      DO 1060 M = 1,NLT
      GTIO(M) = GT(MP,M)
      SALIO(M) = SAL(MP,M)
 1060 CONTINUE
      ALBIJ=ALBEDO(I,J)
      SSNIO = SSN(I,J)
      TGIO = TG(I,J)
      TGSIO = TGS(I,J)
      SAICIO = SAIC(I,J)
      TGIIO = TGI(I,J)
      IF(EIS(I,J).GE.249.) EIS(I,J) = 249.
      EISIO = EIS(I,J)
      AEISIO = AEIS(I,J)
C
C CALCULATE DEPTH OF POINT AND NUMBER OF LAYERS AT THE POINT.
C
      NLW = LDMX(I,J)/1000
      DEPTH = LDMX(I,J) - (NLW * 1000)
```

```
      LX = NLT + 1
      DO 1065 JX= 1,NLW
      TAH(LX-JX)= TWL(LX-JX)
 1065 CONTINUE
C SET UP SOLAR RADIATION ABSORPTIVITIES (TAW).
      LJ = 1
      IF(DEPTH.LE.200.) LJ = 2
      IF(DEPTH.LE.100.) LJ = 3
      DO 1070 N = 1,NLT
      TAW(N) = ABSORP(N,LJ)
 1070 CONTINUE
      IF(AEISIO.LE.0.) GO TO 1075
C
C DETERMINE SNOWFALL FOR THE POINT IF THERE IS ANY.
      CALL SPRUCE(PCPN,TZ,DENSS,DENE,TGIIO,TGSIO,TGIO,SAICIO,EISIO,
     1            SSNIO,SN)
C
C DETERMINE ALBEDO (ALB) FOR THE POINT.
      CALL LARCH(TZ,TGIO,EISIO,SSNIO,ETA,PCPN,SN,ALB,F,ALBIJ)
C
 1075 CONTINUE
C
C DO ALL SURFACE ENERGY BUDGET AND ICE FORMATION, GROWTH AND MELT CALCULATIONS
C IN BEECH
C
      CALL BEECH(TZ,TDZ,PS,NL,SGA,DFL,SUE,ALB,DENSS,DENE,CONE,ETA,
     1           CONS,CONR,SPH,ELAT,CRITH,TOPL,DAY,EISSAL,DIA,F,FWS,
     2           SLAT,SSNIO,SN,TAW,GF,TGIO,TGIIO,TGSIO,SAICIO,GTIO,
     3           SALIO,TAH,NLW,NLT,AEISIO,EISIO,SGW,SGI,RLW,RLI,FW,
     4           FI,XEW,XEI,XSW,XSI,DFW,DFI,HEAT,THAW,RESHT,HTL,
     5           TVEIS,TNVEIS,VNEIS,ALBIJ,STIE)
C
      TUFI(I,J)=TUFI(I,J)+ UF(I)*12.
      SRLU(I,J) = RLI+RLW
      SFG(I,J) = FI+FW
      SQE(I,J) = XEI+XEW
      SQS(I,J) = XSI+XSW
      SSGT(I,J) = SGI+SGW
      SDFT(I,J) = DFI+DFW
      DO 1080 N = 1,NLT
      GT(MP,N) = GTIO(N)
      SAL(MP,N) = SALIO(N)
 1080 CONTINUE
      BEISV=BEISV+ (EISIO*AEISIO)
      BEISA=BEISA+ AEISIO
      ALBEDO(I,J)=ALB
      TW(I,J) = GTIO(NLT)
      AEIS(I,J) = AEISIO
      EIS(I,J) = EISIO
      TG(I,J) = TGIO
      TGS(I,J) = TGSIO
      SAIC(I,J) = SAICIO
      TGI(I,J) = TGIIO
      SSN(I,J) = SSNIO
      FSAV(I,J) = FWS
      ITDM(I,J)=2
      IF(AEIS(I,J).LE.0.) ITDM(I,J) = 1
      IF(PROFMX(I,J).NE.-1) GO TO 1051
      HCONWA = 0.
      DO 1082 KX = 1,NLW
      KXX = NLT +1 - KX
      HCONWA = (GTIO(KXX) - (-2)) * TAH(KXX) * 1. /
     1                 SVDL(SALIO(KXX),GTIO(KXX),0.) + HCONWA
1082  CONTINUE
C
C GIVES A DETAILED WRITE OUT OF ALL PARAMETERS FOR A FEW SELECTED POINTS
C
      CALL WRTEI(KIND,IT,IDTG,I,J,ITDM(I,J),TZ,TDZ,PS,PR(I,J),ALB,S300,
     1      SAA,SGA,DFL,ICLDHT(I,J),TGI(I,J),TGS(I,J),SAIC(I,J),SSN(I,J),
     2      STIE,HCONWA,EIS(I,J),AEIS(I,J),SHN,SALIO,C,ICDX(I,J),
     3      ICSY(I,J),LDMX(I,J),MP,NLW,DEPTH,FWS,SN,SGI,SGW,RLI,RLW,
     4      DFI,DFW,XEI,XEW,XSI,XSW,FI,FW,HEAT,HTL,RESHT,THAW,TNEIS,
     5      VNEIS,LZELM,LYELM)
```

```
 1089 CONTINUE
      TUF1(I,J)=0.
      SRLU(I,J) = 0.
      SFG(I,J) = 0.
      SQE(I,J) = 0.
      SQS(I,J) = 0.
      SSGT(I,J) = 0.
      SDFT(I,J) = 0.
 1051 CONTINUE
 1050 CONTINUE
C
C END THE POINT BY POINT LOOP.
C
      IF(BEISA.LE.0.) GO TO 2009
C
C WRITES OUT THE ICE AREA-ICETHICKNESS-ICE VOLUME AND ICE VOLUME INCREMENT
C          FOR EACH GRID POINT FOR THE IN SITU FORMATION STAGE
C
      CALL WRTE12(SSGT,SDFT,AEIS,EIS,X,TX,167,0,IDTG)
C
C SETUP ITDM FOR IMPORT EXPORT CALCULATIONS
      DO 2000 J = 15,20
      ITDM(21,J) = 1
2000  CONTINUE
C
C DO ICE ADVECTION
C
      CALL WILLOW(ICDX,ICSY,ITDM,SX,SY,DX,TIMUTS,EVD,SVD,AED,TIMFAC,
     1            CISF,WISF,AEIS,EIS,SSN,ISZ,JSZ,ALBEDO,TEMALB,STWT,
     2            01,02,03)
C
      BEISEX=0.
      DO 2001 J = 15,20
      ITDM(21,J) = 5
      EISEXP(J-14) = EISEXP(J-14) + AEIS(21,J)*EIS(21,J)
      BEISEX=BEISEX + EISEXP(J-14)
      AEIS(21,J) = 0.
      EIS(21,J) = 0.
2001  CONTINUE
      BEVAW=0.
      BEAAW=0.
      DO 2005 I=1,22
      DO 2005 J=1,25
      IF(ITDM(I,J).NE.2)   GO TO 2005
      BEVAW=BEVAW + (EIS(I,J)*AEIS(I,J))
      BEAAW=BEAAW + AEIS(I,J)
 2005 CONTINUE
C
C WRITES OUT THE ICE AREA-ICE THICKNESS-ICE VOLUME AND ICE VOLUME INCREMENT
C             AFTER ADVECTION HAS TAKEN PLACE
C
      CALL WRTE12(SSGT,SDFT,AEIS,EIS,X,TX,167,1,IDTG)
C
2009  CONTINUE
      LZELM = LYELM + 3
      IF((360.-LZELM).LT.(SUE*15.-3.)) LZELM = LZELM-360.
2010  CONTINUE
C
C WRITES OUT THE FIELDS OF SGA,RLU,DFL,QE,QS,FG,UFL FOR THE TIME PERIOD
C
      CALL WRTE13(SFG,SSGT,SRLU,SDFT,SQS,SQE,TUF1,IDTG,TX,X,167)
C
      IF(DAY.EQ.0.)   GO TO 2028
      DAY=0.
      GO TO 1015
2028  CONTINUE
C
C CALCULATES AND WRITES OUT THE HEAT CONTENT FOR EACH GRID POINT WATER COLUMN
C
      CALL WRTE14(SSGT,X,GT,SAL,TAH,IDTG)
C
      NCOUNT = NCOUNT + 1
      IF(NCOUNT.GE.7) GO TO 2030
      GO TO 1010
```

```
2030  CONTINUE
      NCOUNT = 0
C
C PUNCHES ALL END OF WEEK DATA ON CARDS FOR THE RE-INITIALIZATION OF THE MODEL
C
      CALL WRTE15(GT,SAL,TGI,TGS,FSAV,EIS,AEIS,SAIC,SSN,ALBEDO,ITDM)
C
C
      GO TO 1010
1008  CONTINUE
      NTPERD = NTPERD + 1
C
C *0*0*0*0*0*0*0*0*0*0*0*0*0*0* TAPE READ PARAMETER *0*0*0*0*0*0*0*0*0*0*0*0*0*0*0
C
      IF(NTPERD.LT.3) GO TO 1010
C
C *0*0*0*0*0*0*0*0*0*0*0*0*0*0* TAPE READ PARAMETER *0*0*0*0*0*0*0*0*0*0*0*0*0*0*0
C
   13 STOP
      END



      SUBROUTINE ASH (GT,TAH,SAL,NLW,NLT,HEAT)
C
C CALCULATES THE AMOUNT OF ICE FORMED OVER OPEN WATER BY CALCULATING THE HEAT
C  REQUIRED TO RAISE THE WATER TEMPERATURE BACK UP TO THE FREEZING TEMPERATURE
C
      DIMENSION GT(NLT),SAL(NLT),TAH(NLT)
      L = NLT + 1
      DO 10  N = 1,NLW
      DENL = 1./SVOL(SAL(L-N),GT(L-N),0.)
      FZP = FP(SAL(L-N))
      IF(GT(L-N).LT.FZP) GO TO 12
      GO TO 18
  12  DIF = GT(L-N) - FZP
      GT(L-N) = FZP
  10  HEAT = HEAT + (DIF*TAH(L-N)*DENL*0.96)
  18  CONTINUE
      RETURN
      END



      SUBROUTINE ASPEN(TZ,TDZ,PS,F,XX,SUE,AEIS,EIS,SSN,TGI,TGS,
     1                 CONE,CONS,CONR,NLT,DENE,XEI,XSI,FI,RLI,SGI,DFI,
     2                 TG,TGW)
C
C CALCULATES THE SURFACE ENERGY BUDGET FOR SNOW AND ICE SURFACES
C
C  *-*-*-*-*-*-*-*-*-*-*-*-*-*-*-*-*-*-*-*-*-*-*-*-*-*-*-*-*-*-*-*-*-*-*-*-*-*
C
C SETS UP THE BALANCE LOOP PARAMETERS USED IN THE ITERATIVE SCHEME IN "YEW"
      XRX = 0.
      XN = 1.
      ZZ = 0.
      J = 0
      IJ = 0
C  *-*-*-*-*-*-*-*-*-*-*-*-*-*-*-*-*-*-*-*-*-*-*-*-*-*-*-*-*-*-*-*-*-*-*-*-*-*
      U = 1.
  10  IF(SSN.LE.0.) GO TO 20
C
C CALCULATES GROUND FLUX WHEN BOTH ICE AND SNOW EXIST
C
      CONST = (SSN/EIS) * CONR
      TGI = (TGS + (CONST*TGW)) / (CONST + 1.)
      FI =-(TGS - TGI) * (CONS/SSN) * SUE * AEIS * 1.3
      TG = TGS
      GO TO 30
C
C CALCULATES GROUND FLUX WHEN ONLY AN ICE SURFACE EXISTS
C
```

```
   20  FI =-(TGI - TGW) * (CONE/EIS) * SUE * AEIS * 1.3
       TG = TGI
   30  RLI =(-(1.1707 E -7 *(TG  + 273.16) **4) / 24.) * SUE * AEIS
       CALL HEMLOK(TG,TZ,TDZ,F,XE,XS,U,PS,XX,SUE)
       XEI = XE * AEIS
       XSI = XS * AEIS
C
C BALANCE LOOP WHICH DERIVES A NEW SURFACE TEMPERATURE (TG)
C
       CALL YEW(SGI,RLI,DFI,FI,XEI,XSI,XRX,XN,ZZ,J,IJ,RB,TG)
       IF(ABS(RB).LT.10.) GO TO 50
       IF(ABS(XN).LE..001) GO TO 50
       IF(J.GT.20) GO TO 40
       IF(SSN.LE.0.) TGI = TG
       TGS = TG
       IF(TG.GE.0.) RETURN
       GO TO 10
   40  WRITE(6,400) J,XRX,RB,RLI,XEI,XSI,SGI,DFI,XN,TGI
  400  FORMAT(1H0,'NO BALANCE J=',I3,8F8.0,F8.3)
C
C REDISTRIBUTE ANY HEAT LEFT AFTER THE BALANCE IS ATTAINED OR 20 ITERATIONS
C
   50  RFI = SGI+RLI+DFI+FI-XEI-XSI
       XA = ABS(XEI) + ABS(XSI) + ABS(FI) + ABS(RLI)
       XEI = XEI + ABS(XEI)/XA * RFI
       XSI = XSI + ABS(XSI)/XA * RFI
       RLI = RLI - ABS(RLI)/XA * RFI
       FI = FI - ABS(FI)/XA * RFI
       IF(SSN.LE.0.) TGI = TG
       TGS = TG
       RETURN
       END
```

```
       SUBROUTINE BEECH(TZ,TDZ,PS,NL,SGA,DFL,SUE,ALB,DENSS,DENE,CONE,
      1        ETA,CONS,CONR,SPH,ELAT,CRITH,TOPL,DAY,EISSAL,DIA,F,FWS,
      2       SLAT,SSN,SN,/TAW/,GF,TG,TGI,TGS,SAIC,GT,SAL, TAH ,NLW,NLT,
      3            AEIS,EIS,SGW,SGI,RLW,RLI,FW,FI,XEW,XEI,XSW,XSI,DFW,
      4            DFI,HEAT,THAW,RESHT,HTI,TVEIS,TNVEIS,VNEIS,
      5            ALBEDO,STIE)
C
C CALCULATES THE SURFACE ENERGY BUDGET OVER ANY TYPE OF SURFACE . CALLS FOR ICE
C  DISTRIBUTION AND DOES ICE SALINITY CHANGES
C
       DIMENSION TAW(NLT),TAH(NLT),GF(NLT),GT(NLT),SAL(NLT),ETA(5)
C
C  -------------------------INITIALIZE VALUES ------------------------
C
       TAH(NLT) = TAH(NLT) - (AEIS * EIS)
       WATALB=.095
       TNVEIS = 0.
       TVEIS = 0.
       VNEIS = 0.
       SALEX = 0.
       SALAD = 0.
       RLI = 0.
       RLW = 0.
       FI = 0.
       FW = 0.
       XEI = 0.
       XSI = 0.
       XEW = 0.
       XSW = 0.
       EISN = 0.
       EISD = 0.
       EISM = 0.
       EISTI = 0.
       STIE = 0.
       RESHT = 0.
       NALB = 1
       M = NLT + 1
```

```
      HTL = 0.
      THAW = 0.
      HEAT = 0.0
      SGW = SGA*(1. - AEIS)*(1. - WATALB)
      SGI = SGA*AEIS*(1. - ALB)
      DFI =  DFL  *SUE*AEIS
      DFW =  DFL * SUE*(1. - AEIS)
      TGW =  GT(NLT)
C
C  ---------------------- VALUES INITIALIZED -------------------------
C     CONSIDERS WHETHER THERE IS AN ICE SURFACE OR NOT. IF THERE IS ICE
C
  20  IF(AEIS.GT.0.) GO TO 30
C
C CALCULATES THE BUDGET OVER A WATER SURFACE
C
      XX = 1.
C
      CALL TEAK(GT,XEW,XSW,FW,SGW,RLW,DFW,TZ,TDZ,PS,XX,AEIS,NLW,NLT,TAH,
     1          TAW,SUE,GF,SAL,FWS,TOPL,F)
C
C   THERMOHALINE CONVECTION
C
      CALL OAK(GT,SAL,TAH,NLW,NLT)
C
      IF(GT(NLT).GE.FP(SAL(NLT))) GO TO 24
C
C FORMATION OF ICE OVER OPEN WATER
C
      CALL ASH (GT,TAH,SAL,NLW,NLT,HEAT)
      IF(HEAT.NE.0.) GO TO 45
  24  TGW = GT(NLT)
      GO TO 400
  30  CONTINUE
C
C CALCULATES THE SURFACE ENERGY BUDGET WHEN SNOW AND ICE EXIST AT A GRID POINT.
C  IF THE AREA IS TOTALLY ICE COVERED IT WILL BYPASS THE WATER BUDGET
C
      XX = 2.
      CALL ASPEN(TZ,TDZ,PS,F,AA,SUE,AEIS,EIS,SSN,TGI,TGS,
     1                   CONE,CONS,CONR,NLT,DENE,XEI,XSI,FI,RLI,SGI,DFI,
     2                   TG,TGW)
      IF(TG .LT.0.) GO TO 40
C
C IF MELTING IS FOUND TO OCCUR, THE SURFACE ALBEDO IS RECALCULATED
C
      IF(NALB.GT.1) GO TO 35
      CALL LARCH(TZ,TG,EIS,SSN,ETA,PR,SN,ALB,F,ALBEDO,I,J)
      NALB = NALB + 1
      SGI = SGA * AEIS * (1. - ALB)
      GO TO 30
  35  CONTINUE
C
C CALCULATES THE MELTING FROM ABOVE
C
      XX = 2.
      CALL CEDAR(TG,SGI,RLI,DFI,XEI,XSI,FI,THAW,DENSS,SLAT,SUE,
     1                   AEIS,TZ,TDZ,XX,F,PS,SSN)
      IF(THAW.LT.0.) GO TO 36
      GO TO 40
  36  IF(SSN.LE.0.) GO TO 40
      SSE = SSN * (DENSS/DENE)
      SAIC = (SAIC * EIS)/(SSE + EIS)
      EIS = EIS + SSE
      SSN = 0.
      TGI = TG
  40  IF(AEIS.EQ.1.) GO TO 42
      XX = 1.
      CALL TEAK(GT,XEW,XSW,FW,SGW,RLW,DFW,TZ,TDZ,PS,XX,AEIS,NLW,NLT,TAH,
     1          TAW,SUE,GF,SAL,FWS,TOPL,F)
      CALL OAK(GT,SAL,TAH,NLW,NLT)
      IF(GT(NLT).GE.FP(SAL(NLT))) GO TO 42
      CALL ASH (GT,TAH,SAL,NLW,NLT,HEAT)
```

```
   42  CONTINUE
       ROSW = (1./SVOL(SAL(NLT),GT(NLT),0.))
       GT(NLT) = GT(NLT) - FI/(TAH(NLT)*ROSW)
       CALL DAK(GT,SAL,TAH,NLW,NLT)
       FZP = FP(SAL(NLT))
       IF(GT(NLT).EQ.FZP) GO TO 72
       IF(GT(NLT).LT.FZP) GO TO 74
       HTL = 0.
       IF(GT(NLT).GT.0.) GO TO 78
       GO TO 80
   72  HTL = 0.
       GO TO 80
   74  M = NLT + 1
C
C CALCULATES THE ICE LAYER INCREMENT ADDED TO AN EXISTING LYER
C
       HTL = 0.
       DO 75 K=1,NLW
       FZPT = FP(SAL(M-K))
       ROW = 1./SVOL(SAL(M-K),GT(M-K),0.)
       IF(GT(M-K).GE.FZPT) GO TO 80
       RHT = (GT(M-K)-FZPT) * TAH(M-K) * ROW
       HTL = HTL + RHT
       GT(M-K) = FZPT
   75  CONTINUE
       GO TO 80
C
C CALCULATES MELTING FROM BELOW
C
   78  RESHT = (GT(NLT) - 0.) * TAH(NLT) * ROSW
       GT(NLT) = 0.
   80  CONTINUE
       ELDE = ELAT * DENE
       EISN = - HEAT / ELDE
       EISD = - RESHT / ELDE
       EISTI = - HTL / ELDE
       EISM = THAW / ELDE
  300  TGW = GT(NLT)
C
C CHECKS FOR ICE FLOODING AND MAKES SNOW ICE IF NECESSARY
C
       CALL CYPRES(DENSS,DENE,SSN,EIS,GT,SAL,NLT,TAH,STIE,SAIC)
       TVEIS = AEIS * EIS
C
C ICE SALINITY CALCULATIONS
C
       SALEX = (TOPL - TVEIS) * (1./(SVOL(SAL(NLT),GT(NLT),0.)))*SAL(NLT)
       SALAD = (SAL(NLT) - EISSAL)*DENE*(EISTI+EISN) - (SAIC*DENE*EISM) -
      1        (SAIC*DENE*EISD)
       SAIC = (SAIC*EIS + (EISTI+EISN)*EISSAL +(EISM+EISD)*SAIC) /
      1        (EIS + EISTI + EISN + EISM + EISD)
C
C DISTRIBUTES ICE AREA AND THICKNESS INCREMENTS
C
       CALL PINE(EIS,AEIS,EISN,EISTI,EISM,EISD,AIN,HEAT,FI,THAW,RESHT,
      1SSN,SN,TGI,GT,TAH,TGW,NLT,SAL,DENE,ELAT,CRITH,TZ)
       TNVEIS = AEIS * EIS
       VNEIS = TNVEIS - TVEIS
       SAL(NLT) = (SALAD + SALEX)/((TOPL-TNVEIS)*(1./(SVOL(SAL(NLT),
      1GT(NLT),0.))))
       CALL DAK(GT,SAL,TAH,NLW,NLT)
       IF(AEIS.GT.0.) GO TO 400
       EIS = 0.
       SSN = 0.
       AEIS = 0.
       TGI = -2.
  400  FG = FI + FW
       QE = XEI + XEW
       QS = XSI + XSW
       RLU = RLI + RLW
  500  CONTINUE
       TAH(NLT) = TOPL
  630  CONTINUE
       RETURN
       END
```

```
      SUBROUTINE CEDAR(TG,SGO,RLU,DFL,QE,QS,FG,THAW,DENSS,SLAT,SUE,
     1                 AEIS,TZ,TDZ,XX,F,PS,SSN)
C
C RECALCULATES THE ENERGY BUDGET TO FIND THE HEAT OF MELTING, THEN MELTS SNOW IF
C   IT EXISTS AT THE POINT.
C
      U = 1.
      TG = -.1
      RLU =(-(1.1707 E -7 *(TG  + 273.16) **4) / 24.) * SUE * AEIS
      CALL HEMLOK(TG,TZ,TDZ,F,XE,XS,U,PS,XX,SUE)
      QE = XE * AEIS
      QS = XS * AEIS
      THAW = -(SGO + RLU + DFL - QE - QS)
      FG =0.
      IF(SSN.LE.0.) GO TO 150
      SSN = SSN + THAW/(80.*DENSS)
      IF(SSN.GT.0.) GO TO 100
      THAW = -(0. - SSN) * 80. * DENSS
      SSN = 0.
      GO TO 150
  100 THAW = 0.
  150 CONTINUE
      RETURN
      END



      SUBROUTINE CYPRES(DENSS,DENE,SSN,EIS,GT,SAL,NLT,TAH,STIE,SAIC)
C
C CALCULATES THE SNOW WHICH TURNS TO ICE DUE TO THE ICE FLOODING
C
      DIMENSION GT(NLT),SAL(NLT),TAH(NLT)
      IF(SSN.LE.0.) RETURN
      SSE = SSN * DENSS/DENE
      TEEM = SSE + EIS
      SRAW = TEEM * (1. - DENE)
      IF(EIS.GT.(TEEM-SRAW))  RETURN
      STIE = SSE - SRAW
      SSN = SRAW * DENE/DENSS
      SAIC = SAIC * EIS/(EIS+STIE)
      EIS = EIS + STIE
      RETURN
      END



      SUBROUTINE FIR(F,FS,WMF,DW,ENG,GT,TAH,SAL,NLT,NLW,AEIS,TOPL)
C
C  DOES DYNAMIC CONVECTION
C
      DIMENSION GT(NLT),SAL(NLT),TAH(NLT)
C
C  F IS IN METRES PER SECOND
C  FS IS IN KNOTS
C
C  PUT F INTO KNOTS
C
      FKN = F * 2.
      FSKN = FS
      THHOLD = TAH(NLT)
C
C   FIND THE WIND MIXING FACTOR WMF
C
      IF(FKN.LE.20.) GO TO 10
      WMF1 = 60. + (14.5 * ALOG(FKN - 19.))
      GO TO 20
   10 WMF1 = (3./20.) * (FKN**2)
   20 AVF = (FKN + FSKN)/2.
```

```
      IF(AVF.LE.20.) GO TO 30
      IF(AVF.LE.30.) GO TO 40
      IF(AVF.LE.40.) GO TO 50
      WMF2 = 360. + (18. * ALOG(AVF - 39.))
      GO TO 60
   30 WMF2 = (3./20.) * (AVF**2)
      GO TO 60
   40 WMF2 = -320. + (19. * AVF)
      GO TO 60
   50 WMF2 = -80. + (11. * AVF)
   60 WMF = AMAX1(WMF1,WMF2)
C
   90 CONTINUE
C
      FS = FKN
      WMD = 0.
      ENG = 0.
      M = NLT + 1
      TAH(NLT) = TAH(NLT) * 2.
C
      DO 200 J = 1,NLW
      JKEEP = J
      TDM = GT(M-J) - GT(NLT - J)
      CALL LINDEN(DWZ,WMF,TDM)
      IF(DWZ.LE.0.) GO TO 100
      DWZ = DWZ * 100.
      DELENG = (TAH(M-J) + TAH(NLT-J))/(2. * DWZ)
      WMD = WMD + (TAH(M-J) + TAH(NLT-J))/2.
      ENG = ENG + DELENG
      IF(ENG.GE.1.) GO TO 210
  200 CONTINUE
C
      IF(JKEEP.EQ.NLW) GO TO 220
C
  210 DIFENG = ENG - 1.
      DIN =(((TAH(M-JKEEP)+TAH(NLT-JKEEP)))/2.) * (DIFENG/DELENG)
      WMD = WMD - DIN
      ENG = ENG - DIFENG
  220 CONTINUE
      DW = WMD * (1. - AEIS)
      IF(DW.LE.0) GO TO 100
C
      TAH(NLT) = THHOLD
      TAHT = 0.0
      TMA = 0.
      WTEMP = 0.0
      WSAL = 0.
      JMN = 0
      L = NLT + 1
      DO 110 N = 1,NLW
      NR = N
      DENL = 1./SVDL(SAL(L-N),GT(L-N),0.)
      TAHT = TAHT + TAH(L-N)
      TMA = TMA + TAH(L-N) * DENL
      IF(DW.LT.TAHT) GO TO 120
      WTEMP = WTEMP + (GT(L-N)*TAH(L-N)*DENL)
      WSAL = WSAL + (SAL(L-N)*TAH(L-N)*DENL)
      TMEAN = WTEMP/TMA
      SMEAN = WSAL/TMA
      JMN = JMN + 1
  110 CONTINUE
C
      GO TO 150
C
  120 IF(DW.EQ.TAHT) GO TO 150
      TAHT = TAHT - TAH(L-NR)
      TMA = TMA - (TAH(L-NR) * DENL)
      TEMHT = DW - TAHT
      WTEMP = (TMA * TMEAN) + (TEMHT*DENL*GT(L-NR))
      TMEAN = WTEMP/(TMA + TEMHT*DENL)
      WSAL = (TMA*SMEAN) + (TEMHT*DENL*SAL(L-NR))
      SMEAN = WSAL/(TMA + TEMHT * DENL)
      GT(L-NR) = (((TAH(L-NR)-TEMHT)*GT(L-NR))+(TEMHT*TMEAN))/TAH(L-NR)
```

```
      SAL(L-NR) = (((TAH(L-NR) - TEMHT)*SAL(L-NR)) + (TEMHT*SMEAN))/
     1TAH(L-NR)
C
  150 DO 160 J = 1,JMN
      SAL(L-J) = SMEAN
  160 GT(L-J) = TMEAN
  100 CONTINUE
      TAH(NLT) = THHOLD
      RETURN
      END
```

```
      SUBROUTINE LARCH(TZ,TG,EIS,SSN,ETA,PR,SN,ALB,F,ALBEDO)
C
C CALCULATES THE SURFACE ALBEDO FOR SNOW OR ICE OR BOTH
C
      DIMENSION ETA(5)
      N=3
      ALB=0.
      IF(EIS.GT.0.)   GO TO 215
      ALB=.08
       GO TO 50
  215 IF(PR.LE.0.)   GO TO 220
      IF(SN.GT.0.)   GO TO 230
      ALB=.3
       GO TO 50
  230 IF(F.GT.10.)   GO TO 240
      ALB=.9
      GO TO 50
  220 N=2
C
C CALCULATES THE LOWERING OF ALBEDO DUE NORMAL DETERIORATION
C
      ALBPD=ALBEDO*.96
  240 IF(TG.GT.0.)   GO TO 260
      IF(SN.LE.0..AND.SSN.LE.0.)   GO TO 270
      N=N-1
      DO 30 K=1,N
C
C FINDS THE INFLUENCE OF THE UNDERLYING SURFACE ON THE ALBEDO
C
      SX=SSN
      IF(K.EQ.2)   SX=2.*SN+SX
      JN=SX/2.54
      IF(JN.LE.1) JN=1
      IF(JN.GE.5) JN=5
      CX=ETA(JN)
C
C CALCULATES THE EFFECT OF THE SURFACE TEMPERATURE ON THE ALBEDO
C
      IF(TG.GE.(-10.)) GO TO 5
      IF(TG.LE.(-31.)) GO TO 6
      ALBS = .7 - (10. - ABS(TG)) * .01
      GO TO 7
    5 ALBS=0.7-(10.-ABS(TG))*.04
      GO TO 7
    6 ALBS=0.9
    7 ALB=ALBS*CX+ALB
   30 CONTINUE
      ALB=ALB/N
      IF(N.EQ.1)  ALB=AMIN1(ALB,ALBPD)
      IF(ALB.LT..3)   ALB=.3
      GO TO 50
  270 IF(TG.GE.(-10.))   GO TO 8
      IF(TG.LE.(-31.))  GO TO 9
      ALBS=.7-(10.-ABS(TG))*.01
      GO TO 10
    8 ALBS=.7-(10.-ABS(TG))*.04
      GO TO 10
    9 ALBS=.96*ALBEDO
```

```
   10 ALB=AMIN1(.85,ALBS)
      GO TO 50
  260 ALB=.3
   50 ALBEDO=ALB
      RETURN
      END



      SUBROUTINE OAK(GT,SAL,TAH,NLW,NLT)
C
C DOES THE THERNOHALINE CONVECTION
C
      DIMENSION GT(NLT),SAL(NLT),TAH(NLT),DEN(8)
C
  100 JL = 0
      M = (NLT - 1) - NLW
      MM = (NLT - 1)
C
      DO 200 J = M,MM
      LL = 0
      DEN(J) = 1./(SVOL(SAL(J),GT(J),0.))
C
      WGT = DEN(J)*GT(J)*TAH(J)
      WGS = DEN(J)*SAL(J)*TAH(J)
      TMA = TAH(J)*DEN(J)
C
      DEN(J+1) = 1./(SVOL(SAL(J+1),GT(J+1),0.))
      IF(DEN(J).GE.DEN(J+1)) GO TO 200
      LL = J
      JL = J
  110 WGT = WGT + DEN(JL+1)*GT(JL+1)*TAH(JL+1)
      WGS = WGS + DEN(JL+1)*SAL(JL+1)*TAH(JL+1)
      TMA = TMA + TAH(JL+1)*DEN(JL+1)
      GMT = WGT/TMA
      SALM = WGS/TMA
      DENM = 1./(SVOL(SALM,GMT,0.))
      JL = JL + 1
C
      IF(JL.EQ.NLT) GO TO 190
C
      DEN(JL+1) = 1./(SVOL(SAL(JL+1),GT(JL+1),0.))
C
      IF(DENM.GE.DEN(JL+1)) GO TO 190
C
      GO TO 110
C
  190 DO 150 K = LL,JL
      GT(K) = GMT
      SAL(K) = SALM
  150 CONTINUE
  200 CONTINUE
C
      IF(JL.NE.0.) GO TO 100
      RETURN
      END



      SUBROUTINE PINE(E,AE,EN,ETI,EM,ED,AIN,H,FI,TW,RHT,SSN,SN,TGI,GT,
     1TAH,TGW,NLT,SAL,DENE,ELAT,CRITH,TZ)
C
C DISTRIBUTES CONTRIBUTIONS TO THE ICE COVER
C
      DIMENSION GT(NLT),TAH(NLT),SAL(NLT)
      AED = AE
      IF(AE.EQ.0.) GO TO 200
      IF(AE.EQ.1.) GO TO 210
```

```
C
C  FINDS THE NEW ICE AREA
C
      AIN = EN/E
      ANEW = AE + AIN
      IF(ANEW.GT.1.) GO TO 220
      AE = ANEW
      GO TO 230
  220 ETI = ETI + (ANEW - 1.) * E
      AE = 1.
      GO TO 230
  210 ETI = ETI + EN
  230 ETI = ETI + ED
C
C  FINDS THE NEW ICE THICKNESS
C
      E = E + ETI + EM
      IF(E.GE.CRITH) GO TO 250
      REDD = (AE*E)/CRITH
      AE = REDD
      E = CRITH
      AEOLD = AE
      GO TO 250
  200 AE = (EN/CRITH)
      E = CRITH
      IF(AE.LE.0.) GO TO 260
      TGI = (-2. + TZ)/2.
      IF(AE.GT.1.) GO TO 240
      GO TO 250
  240 E = AE * CRITH
      AE = 1.
  250 CONTINUE
      SSNNEW = AEOLD * SSN/ AE
      SSN = SSNNEW
      GO TO 280
  260 X = 0. - AE
      GT(NLT) = GT(NLT)       + ((X * CRITH*ELAT*DENE)/(.96*TAH(NLT)))
      TGW = GT(NLT)
      E = 0.
  280 CONTINUE
      RETURN
      END
      SUBROUTINE SPRNCE(PR,TZ,DENSS,DENE,TGI,TGS,TG,SAIC,EIS,SSN,SN)
C
C CLACULATES THE SNOWFALL IF SUCH EXISTS
C
      IF(PR.LE.0.) GO TO 100
      IF(TZ.GT..001) GO TO 50
   10 SN = (PR*2.54)/DENSS
      SSN = SSN + SN
      TGS = TZ
      TG = TGS
      GO TO 100
   50 IF(PR.LT..25) GO TO 10
      SSE = SSN * DENSS/DENE
      SAIC = SAIC * EIS/(SSE + EIS +(PR/DENE))
      EIS = EIS + SSE + (PR/DENE)
      SSN = 0.
      TG = TGI
  100 CONTINUE
      RETURN
      END




      SUBROUTINE TEAK(GT,QE,QS,FG,SBO,RLU,DFL,TZ,TDZ,PS,XX,AEIS,NLW,NLT
     1                ,TAH,TAW,SUE,GF,SAL,FWS,TOPL,F)
C
C CALCULATES THE SURFACE ENERGY BUDGET OVER A WATER SURFACE
C
      DIMENSION GF(NLT),GT(NLT),SAL(NLT),TAH(NLT),TAW(NLT)
```

```
      U = 1.
C
C INCORPORATE THE SOLAR RADIATION
C
   32 IF(SGO.EQ.0.0) GO TO 2
      L = NLT + 1
      SX = 0.
      DO 1 N = 1,NLW
      SY = SGO*TAW(L-N)
      SX = SX  + SY
      GT(L - N) = GT(L - N) + SY / TAH(L - N)
    1 CONTINUE
      IF(NLW.EQ.NLT) GO TO 2
      GT(L-NLW) = GT(L-NLW) + (SGO-SX)/((TAH(L-NLW)* 1./SVOL(SAL(L-NLW),
     1            GT(L-NLW),0.)))
    2 CONTINUE
C
C CALLS FOR THE DYNAMIC CONVECTION
C
      CALL FIR3(F,FWS,WMF,DW,ENG,GT,TAH,SAL,NLT,NLW,AEIS,TOPL)
      TGW = GT(NLT)
C
C CALCULATES THE LATENT AND SENSIBLE HEAT FLUXES
C
      CALL HEMLOK(TG,TZ,TDZ,F,XE,XS,U,PS,XX,SUE)
      QE = XE * (1. - AEIS)
      QS = XS * (1. - AEIS)
      RLU =(-(1.1707E-7 *(GT(NLT) + 273.16) **4) /24.) * SUE * (1. - AEI
     1S)
C
C CALCULATES THE GROUND FLUX OVER A WATER SURFACE
C
      FG = - ( DFL + RLU - QE - QS)
C
C INCORPORATE HEAT LOSS OR GAIN INTO THE SURFACE WATER LAYER
C
      DENT = 1./SVOL(SAL(NLT),GT(NLT),0.)
      GT(NLT) = GT(NLT) - FG / (TAH(NLT) * DENT)
      RETURN
      END
```

```
      SUBROUTINE WILLOW(/ICDX/,/ICSY/,ITDM ,/SX/,/SY/,DXT,TIMUTS,EVD,SVD
     1                  ,AED, TIMFAC,CISF,WISF,AEIS,EIS,SGN,ISZ,JSZ,
     2                  ALBEDO,TEMALB,STWT,Q1,Q2,Q3)
C
C CALCULATES THE ICE ADVECTION
C
      INTEGER*2 ICDX(ISZ,JSZ),ICSY(ISZ,JSZ),ITDM(ISZ,JSZ)
      DIMENSION SX(ISZ,JSZ),SY(ISZ,JSZ),AEIS(ISZ,JSZ),EIS(ISZ,JSZ)
      DIMENSION SSN(ISZ,JSZ),EVD(ISZ,JSZ),SVD(ISZ,JSZ),AED(ISZ,JSZ)
      DIMENSION ALBEDO(ISZ,JSZ),TEMALB(ISZ,JSZ),STWT(ISZ,JSZ)
      DIMENSION IN(4),JN(4),W(4)
      DO 10 K = 1,22
      DO 10 L = 1,25
      EVD(K,L) = 0.
      SVD(K,L) = 0.
      AED(K,L) = 0.
      TEMALB(K,L) = 0.
      STWT(K,L) = 0.
   10 CONTINUE
      DO 30 J = 2,22
      DO 29 I = 2,20
      IF(ITDM(I,J).NE.2) GO TO 28
      IF(AEIS(I,J).GT..2) GO TO 11
```

```
      EVD(I,J) = EVD(I,J) + AEIS(I,J) * EIS(I,J)
      SVD(I,J) = SVD(I,J) + AEIS(I,J) * SSN(I,J)
      AED(I,J) = AED(I,J) + AEIS(I,J)
      STWT(I,J) = STWT(I,J) + 1.
      TEMALB(I,J) = TEMALB(I,J) + (1. * ALBEDO(I,J))
      GO TO 28
   11 CONTINUE
      SAVEDX = 0.
      SAVEDY = 0.
      DIFEDX = 0.
      DIFEDY = 0.
C FINDS THE COMPONENTS OF ICE DRIFT DUE TO THE WIND
      WDX = SX(I,J) * WISF
      WDY = SY(I,J) * WISF
C FINDS THE COMPONENTS OF ICE DRIFT DUE TO THE CURRENT
      CDX = ICDX(I,J) * CISF
      CDX = CDX * TIMFAC
      CDY = ICSY(I,J) * CISF
      CDY = CDY * TIMFAC
C FINDS THE NORMALIZED COMPONENTS OF ICE DRIFT FOR A TIME PERIOD OF
C     TIMUTS IN LENGTH
      EDX = (CDX+WDX) * (TIMUTS/DXT)
      EDY = (CDY + WDY) * (TIMUTS/DXT)
      ABEX = ABS(EDX)
      ABEY = ABS(EDY)
      IF(ABEX.GE.1.) GO TO 12
      IF(ABEY.GE.1.) GO TO 14
      GO TO 18
   12 SAVEDX = EDX
      SAVEDY = EDY
      DIFEDX = ABEX - 1.
      EDY = EDY*(1. - (DIFEDX/(DIFEDX + ABEX)))
      EDX = (EDX/ABEX) * .999
      IF(EDY.GE.1.) GO TO 15
      GO TO 18
   14 SAVEDX = EDX
      SAVEDY = EDY
      DIFEDY = ABEY - 1.
      EDX = EDX * (1. - (DIFEDY/(DIFEDY + ABEY)))
      EDY = (EDY/ABEY) * .999
      GO TO 18
   15 EDX = SAVEDX
      EDY = SAVEDY
      IF(ABEX.GT.ABEY) GO TO 16
      IF(ABEY.GT.ABEX) GO TO 17
      EDX = (EDX/ABEX) * .999
      EDY = (EDY/ABEY) * .999
      GO TO 18
   16 DIFEXY = ABEX - ABEY
      EDY = (EDY/ABEY) * (1. - DIFEXY/ABEX)
      EDX = (EDX/ABEX) * .999
      GO TO 18
   17 DIFEYX = ABEY - ABEX
      EDX = (EDX/ABEX) * (1. - DIFEYX/ABEY)
      EDY = (EDY/ABEY) * .999
   18 CONTINUE
      ABEX = ABS(EDX)
      ABEY = ABS(EDY)
      WT = 0.
      IF(EDX.GE.0.) ABEX = (1.-ABEX)
      IF(EDY.GE.0.) ABEY = (1. - ABEY)
C
C FINDS THE REAL COORDINATES TO WHICH THE ICE WILL DRIFT AND THEN INTEGERIZES
C  THESE TO FIND THE GRID SQUARE COORDINATES TO WHICH THE ICE WILL DRIFT
C
  185 RI = I + EDX
      RJ = J + EDY
      IN(1) = RI
      JN(1) = RJ
      IN(2) = IN(1) + 1
      JN(2) = JN(1)
```

```
      IN(3) = IN(1)
      JN(3) = JN(1) + 1
      IN(4) = IN(2)
      JN(4) = JN(3)
C
C FINDS THE AMOUNT OF ICE DRIFT TO EACH SQUARE
C
      DO 20 N = 1,4
      K = IN(N)
      L = JN(N)
      GO TO (1,2,3,4),N
    1 W(1) = ABEX * ABEY
      IF(ITDM(K,L).GE.5) W(1) = 0.
      GO TO 19
    2 W(2) = (1.-ABEX) * ABEY
      IF(ITDM(K,L).GE.5) W(2) = 0.
      GO TO 19
    3 W(3) = ABEX * (1. - ABEY)
      IF(ITDM(K,L).GE.5) W(3) = 0.
      GO TO 19
    4 W(4) = (1.-ABEX) * (1. - ABEY)
      IF(ITDM(K,L).GE.5) W(4) = 0.
   19 WT = WT + W(N)
   20 CONTINUE
      IF(WT.LE..0001)     GO TO 28
C
C APORTIONS THE DRIFTED ICE TO ITS DESTINATION SQUARES AND ALSO FINDS THE
C  WEIGHTED ALBEDO AND SNOW COVER FOR THE NEW AREAS
C
      EVIJ = AEIS(I,J) * EIS(I,J)
      SVIJ = AEIS(I,J) * SSN(I,J)
      AIJ = AEIS(I,J)
      DO 21 N = 1,4
      K = IN(N)
      L = JN(N)
      EVD(K,L) = (W(N) * EVIJ)/WT + EVD(K,L)
      SVD(K,L) = (W(N) * SVIJ)/WT + SVD(K,L)
      AED(K,L) = (W(N) * AIJ)/ WT + AED(K,L)
      STWT(K,L) = STWT(K,L) + W(N)
      TEMALB(K,L) = TEMALB(K,L) + (W(N) * ALBEDO(I,J))
   21 CONTINUE
   28 CONTINUE
   29 CONTINUE
   30 CONTINUE
      DO 35 J = 2,22
      DO 34 I = 2,21
      AEIS(I,J) = 0.
      EIS(I,J) = 0.
      ALBEDO(I,J) = .08
      IF(ITDM(I,J).EQ.1.OR.ITDM(I,J).EQ.2) GO TO 37
      GO TO 34
   37 AEIS(I,J) = AED(I,J)
      IF(AEIS(I,J).GT.1.) AEIS(I,J) = 1.
      IF(AEIS(I,J).LT.0.) GO TO 31
      IF(AEIS(I,J).EQ.0.) GO TO 36
      GO TO 33
   31 AREAI = AEIS(I,J)
      WRITE(6,32) AREAI
      AEIS(I,J) = 0.
      GO TO 36
   32 FORMAT('0','NEGATIVE ICE AREA HAS BEEN CALCULATED =',F12.8)
   33 EIS(I,J) = EVD(I,J)/AEIS(I,J)
      SSN(I,J) = SVD(I,J)/AEIS(I,J)
      IF(STWT(I,J).LT..0001)     GO TO 38
      ALBEDO(I,J) = TEMALB(I,J)/STWT(I,J)
   38 IF(AEIS(I,J).EQ.0.) GO TO 36
      ITDM(I,J) = 2
      GO TO 34
   36 ITDM(I,J) = 1
   34 CONTINUE
   35 CONTINUE
      RETURN
      END
```